Airframe Beam Structural Test (ABST) Fixture Development

Reewanshu Chadha, John G. Bakuckas, Jr., Gregory Korkosz, Michael Fleming and John Lin

December 2019

DOT/FAA/TC-TN19/7

U.S. Department of Transportation
Federal Aviation Administration

NOTICE

Technical Report Documentation Page

1. Report No.	2. Government Accession No.	3. Recipient's Catalog No.
DOT/FAA/TC-TN19/7		

4. Title and Subtitle	5. Report Date
AIRFRAME BEAM STRUCTURAL TEST (ABST) FIXTURE DEVELOPMENT	December 2019
	6. Performing Organization Code
7. Author(s)	8. Performing Organization Report No.
Reewanshu Chadha[1], John G. Bakuckas, Jr.[2], Gregory Korkosz[3], Michael Fleming[4] and John Lin[4] [1]FAA William J. Hughes Technical Center (Diakon Solutions LLC) [2]FAA William J. Hughes Technical Center [3]Legacy Engineering [4]Boeing Research & Technology	ANG-E281
9. Performing Organization Name and Address	10. Work Unit No. (TRAIS)
Federal Aviation Administration William J. Hughes Technical Center Atlantic city, NJ 08405	11. Contract or Grant No.
12. Sponsoring Agency Name and Address	13. Type of Report and Period Covered
U.S. Department of Transportation Federal Aviation Administration William J. Hughes Technical Center Aviation Research Division Atlantic City International Airport, NJ 08405	14. Sponsoring Agency Code ANG-E2

15. Supplementary Notes

The FAA William J. Hughes Technical Center Aviation Research Division COR was Dr. John Bakuckas, Jr.

16. Abstract

This technical note describes the Airframe Beam Structural Test (ABST) fixture located in the Structures and Materials Laboratory in Building 245 at the FAA William J. Hughes Technical Center. The ABST fixture integrates mechanical, hydraulic, control, and data-acquisition systems enclosed by a portable barrier wall. This new structural test capability was developed in collaboration with The Boeing Company and is capable of applying major modes of loading to a beam structure representative of a typical wing or stabilizer components. Individual loading modes include constant moment, torsion, cantilever shear, and horizontal bending, which can be combined to yield complex loading configurations. Loads are applied using four hydraulic actuators (50 kip capacity and 12-inch stroke) powered by a 60-GPM hydraulic power unit controlled by a MTS Flex Test™ 100 system. A MTS FlexDAC™ 20 data-acquisition system provides 64 channels to collect strain gauges and displacement sensors data and a ARAMIS digital image correlation system is used to capture full-field strain and displacement distribution. Several non-destructive inspection capabilities are used to monitor damage, including Flash Thermography, Phased Array, Pulse Echo, Bondmaster, and Eddy Current. The ABST fixture is also equipped with several surveillance cameras to monitor real-time testing.

17. Key Words	18. Distribution Statement
Full-Scale Testing, Structural Integrity, Wing Panels	This document is available to the U.S. public through the National Technical Information Service (NTIS), Springfield, Virginia 22161. This document is also available from the Federal Aviation Administration William J. Hughes Technical Center at actlibrary.tc.faa.gov.

19. Security Classif. (of this report)	20. Security Classif. (of this page)	21. No. of Pages	22. Price
Unclassified	Unclassified		

Form DOT F 1700.7 (8-72) Reproduction of completed page authorized

ACKNOWLEDGEMENTS

The authors would like to acknowledge Diakon Solutions technicians Thuan Nguyen, Pat Ray (former employee), and Kelsey Warfle for their diligent efforts during the assembly of the ABST fixture and supporting infrastructure; and to Pat Ray for generating the engineering drawings of the mechanical system. In addition, the contributions of FAA ANG-E3 personnel, Hank Weber and Kimberly Weber, should be noted for their expert feedback throughout the fixture development process and efforts welding the major fixture subassemblies. In addition, special thanks goes to Kelly Greene, Russell Keller, and Ching Hsu from The Boeing Company for their support and contributions throughout the fixture development. The authors would also like to acknowledge FAA-Drexel fellow Ryan J. Neel for his contribution with the acceptance test. Last but not least, many thanks to Drexel senior design teams and their advisors Jonathan Awerbuch and Tein-Min Tan for their efforts in preliminary fixture design.

TABLE OF CONTENTS

LIST OF FIGURES

LIST OF TABLES

LIST OF ACRONYMS

ABST	Airframe Beam Structural Test
DAQ	Data acquisition
DIC	Digital image correlation
HPU	Hydraulic power unit
HSM	Hydraulic Service Manifold
P	Part
SA	Subassembly
SML	Structures and Materials Lab

EXECUTIVE SUMMARY

This technical note describes the Airframe Beam Structural Test (ABST) fixture located in the Structures and Materials Laboratory in Building 245 at the FAA William J. Hughes Technical Center. The ABST fixture integrates mechanical, hydraulic, control and data-acquisition systems enclosed by a portable barrier wall. This new structural test capability was developed in collaboration with The Boeing Company and is capable of applying major modes of loading to a beam structure representative of a typical wing or stabilizer components. Individual loading modes include constant moment, torsion, cantilever shear, and horizontal bending, which can be combined to yield complex loading configurations. Loads are applied using four hydraulic actuators (50 kip capacity and 12-inch stroke) powered by a 60-GPM hydraulic power unit controlled by a MTS Flex Test™ 100 system. A MTS FlexDAC 20 data-acquisition system provides 64 channels to collect strain gauges and displacement sensors data and a ARAMIS digital image correlation system is used to capture full-field strain and displacement distribution. Several non-destructive inspection capabilities are used to monitor damage including Flash Thermography, Phased Array, Pulse Echo, Bondmaster, and Eddy Current. The ABST fixture is also equipped with several surveillance cameras to monitor real time testing.

INTRODUCTION

Under a Cooperative Research and Development Agreement (07-CRDA-0236), the FAA and The Boeing Company have been investigating the safety and structural integrity issues of bonded repair technology through test and analysis. Initial focus has been the application of bonded repairs to metallic fuselage structure. Follow-on efforts were identified for bonded repairs of thicker structures, such as a primary beam structure representative of typical wing or stabilizer components that are subjected to much more complex loads.

To support this effort, a new structural test capability was recently commissioned, namely, the Aircraft Beam Structural Test (ABST) fixture. Acceptance testing to demonstrate the full functionality of the ABST fixture was completed on May 2017. The fixture is a self-reacting structure housed in the new Structures and Materials Lab in Building 245.

The design, fabrication, and integration of the ABST fixture was a collaborative team effort. The Boeing team provided funding, test equipment, and in-kind engineering support whereas the ABST fixture was designed by Greg Korkosz. The FAA metal shop team (ANG-E3)—Hank Weber, Kim Weber, and Bob Shea—assumed responsibility and took the lead in the mechanical fixture fabrication phase. The full system assembly and integration of the mechanical test fixture, the hydraulic system, and the control and data-acquisition (DAQ) system was accomplished by the Diakon support team: lead test engineers, Reewanshu Chadha and Yongzhe Tian, and technicians Thuan Nguyen, Pat Ray, Kelsey Warfle, and Jeff Panco, and Drexel graduate student, Ryan Neel.

The ABST fixture is currently being used to support a multi-year, multi-phased research program assessing bonded repairs to composite panels representative of transport airplane wing structure. The initial baseline testing of this program characterized the material response of composite panels in the unnotched pristine and open hole configurations under constant moment loading. This baseline information provided verification of the test fixture loading and validation of analysis models, and an initial reference point for non-destructive inspections (NDI) and structural health monitoring systems. Follow on phases of this program will support bonded repair size limit (BRSL) studies and methods used to predict the limit load residual strength for a failed scarfed repair in solid composite laminates and honeycomb panels.

DESCRIPTION OF AIRFRAME BEAM STRUCTURAL TEST (ABST) FIXTURE

Setup of the ABST fixture began in October 2016 and the functionality was demonstrated with an acceptance test in May 2017. Major upgrades were completed in August 2018 to the ABST fixture controller, DAQ, and hydraulic systems, which provided a more integrated test arrangement, efficient operation, and environmentally friendly environment. The ABST fixture consists of:

1. Mechanical system
2. Hydraulic system
3. Control and DAQ systems and monitoring center
4. Portable barriers surrounding the ABST support system

A summary of the major components of the control, DAQ, and hydraulic systems is provided in table 1. The complete floorplan of the ABST fixture is shown in figure 1. The figure shows all the sections of the ABST fixture with the personnel protective equipment and a portable gantry for lifting heavy items. All the major sections of the ABST fixture are shown in figure 2 and the details of these sections are described in this section.

Table 1. Equipment List for the ABST Fixture

Component	Description
Load Control and DAQ Systems	MTS FlexTest™ 100 MTS FlexDAC™ 20, 64 channel MOOG SmarTEST - CDS27634* VTI - EX1629, 48 channel*
Load Cells	Four, 50-KIP capacity
	One, 5-KIP capacity*
Servo Valves and Blocks	Four, 15-Gal/min capacity
Actuators	Four, 2–6-inch bore, 12-inch stroke capacity, 50-K capacity
	Two, 2–3 inch bore, 36-inch stroke capacity, 50-K capacity*
	One, 1–2-inch bore, 12-inch stroke capacity, 5K capacity*
Hydraulic Power Unit	MTS SILENTFLO™ 515 (320-gal reservoir, 60 gal/min, 3000 PSI capacity) Portable Hydraulic Pump (100-gal reservoir, 50 gal/min, 3000 PSI capacity)*
Digital Image Correlation (DIC) Camera system	ARAMIS System for full-field strain and displacement data acquisition.

*Equipment is currently not being used in the ABST fixture.

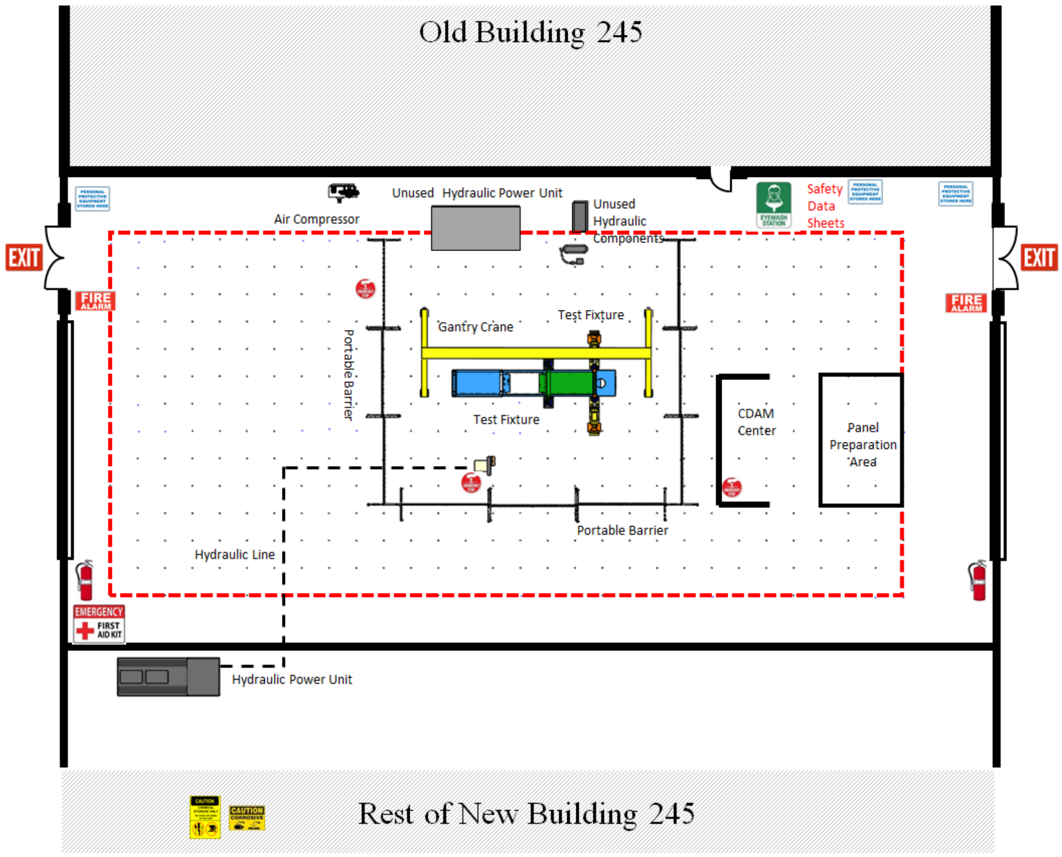

Number or Symbol	Equipment
FIRE ALARM	Fire Alarm
EMERGENCY STOP	Emergency Stop
EXIT	Exit
	Fire Extinguisher
EYEWASH STATION	Emergency Eye Wash
CAUTION CORROSIVE	Corrosive Material Storage Locker
EMERGENCY FIRST AID KIT	First Aid Kit
DANGER FLAMMABLE STORAGE	Flammable Material Storage
PERSONAL PROTECTIVE EQUIPMENT STORED HERE	Personal Protective Equipment (PPE) Storage or Dispenser
	Single Door
	Reinforced Concrete Slab Section

Figure 1. Layout of the ABST facility showing the ABST fixture, hydraulic components, control and DAQ systems and monitoring center, portable barriers, gantry crane, and all the safety equipment.

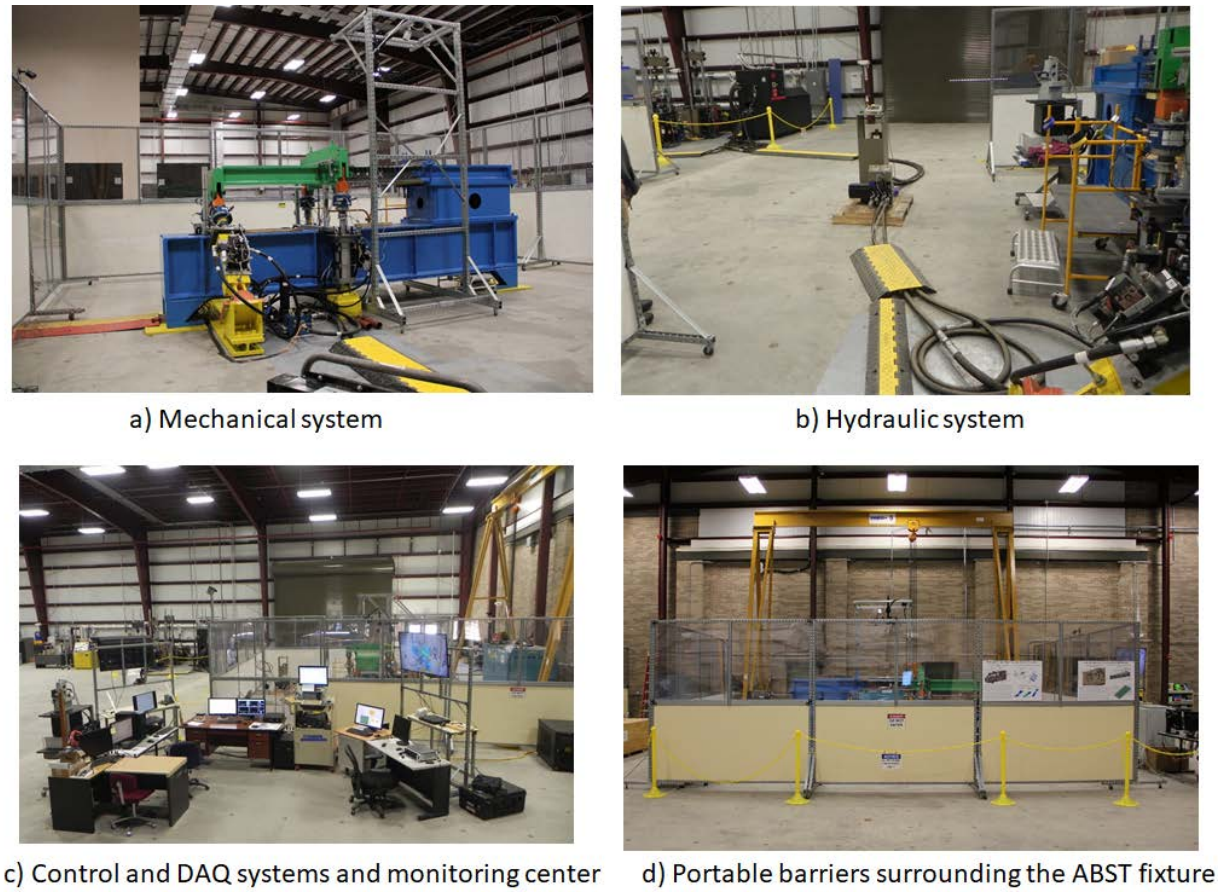

Figure 2. Major sections of ABST fixture: a) mechanical system, b) hydraulic system, c) control and DAQ systems and monitoring center, and d) portable barriers surrounding the ABST fixture

MECHANICAL SYSTEM

The ABST fixture is a self-reacting fixture used to test a primary beam structure representative of a typical wing or stabilizer components, subjected to complex loading scenarios. The development of the ABST mechanical system is described here.

MECHANICAL SYSTEM DEVELOPMENT

The fabrication and machining of all the parts of the ABST mechanical system was outsourced to an external vendor. The majority of these parts required size and position tolerance of 0.005 inch. The welding of the subassemblies and part of the machining work was conducted by the FAA machine shop and the system was assembled by laboratory personnel. The complete mechanical system is composed of several machined parts and welded subassemblies. The list of these subassemblies and parts are shown in figure 3. Overall, the ABST mechanical system can be divided into three major modules. These are:

1. Reaction Module
2. Loading Module
3. Wingbox

REACTION MODULE: The reaction module of the mechanical system is the section that reacts to the applied loads. It consists of several subassemblies (SA) and parts (P) such as base assembly (SA8), riser assembly (SA2), reaction head (SA3), and reactor clamp (P2). These subassemblies and parts are shown in figure 4. The detail drawings of all the parts of the subassemblies are provided in appendix A.

LOADING MODULE: The loading module of the ABST mechanical system is the section that applies load to the wingbox. It consists of loading head (SA5), four actuators (SA1), hoodoly (SA6), wedge mount assembly (SA7), jack support beams (P3 and P4), and hoodoly clamps (P1). These subassemblies and parts are shown in figure 5. The detail drawings of all the parts of the subassemblies are provided in appendix A. Each actuator has 50-kip capacity and 12-inch stroke and are mounted with a ± 50-kip capacity load cells. The two inside actuators are mounted vertically and attached to the hoodoly via pins. The two outside actuators are mounted at a 45˚ angle and attached to the loading head via pins.

Main Assembly		
Sub-Assembly	Sub-Assembly Name	Quantity
SA1	Actuator assembly	4
SA2	Riser assembly	1
SA3	Reaction head	1
SA4	Wingbox	1
SA5	Loading head	1
SA6	Hoodoly assembly	1
SA7	Wedge mount assembly	2
SA8	Base assembly	1
P1	Hoodoly clamp	2
P2	Reactor clamp	1
P3	Base I-beam 1	1
P4	Base I-beam 2	1

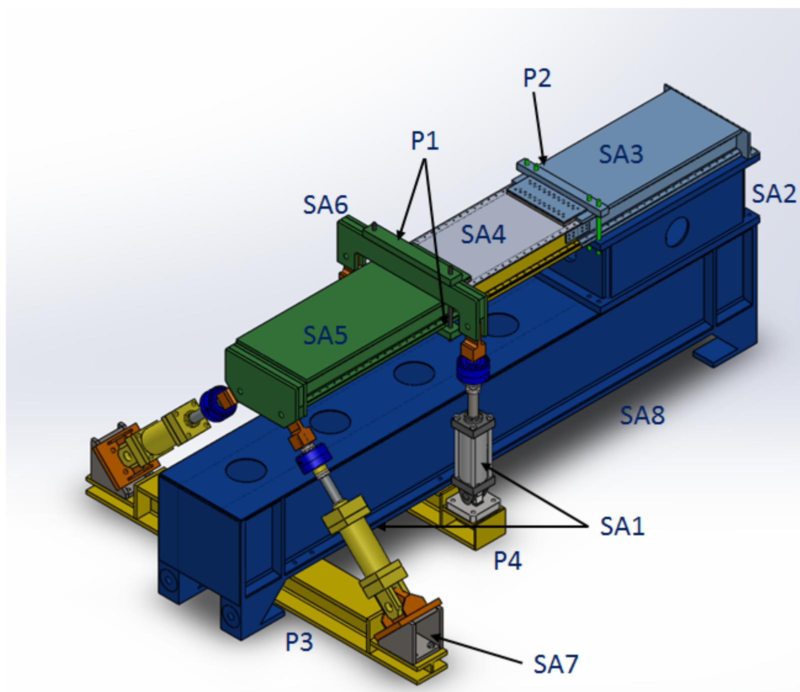

Figure 3. ABST mechanical system

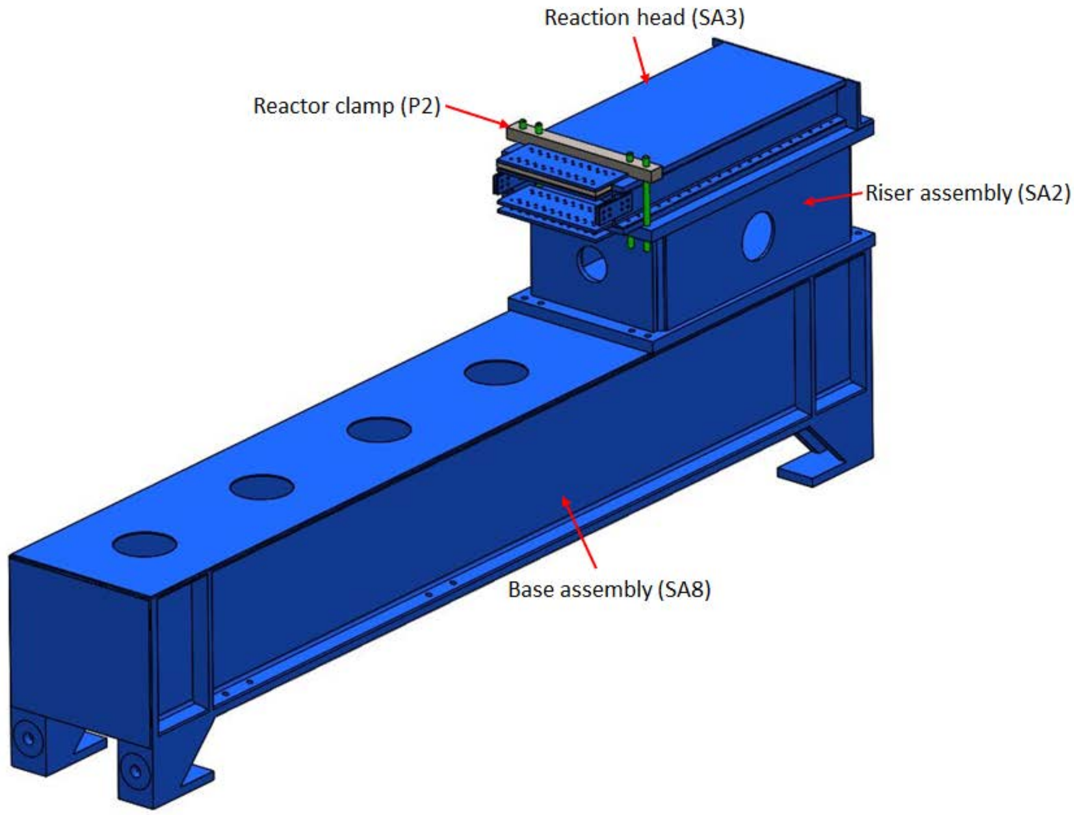

Figure 4. The subassemblies and parts that form the reaction module of the ABST mechanical system: a) base assembly (SA8), b) riser assembly (SA2), c) reaction head (SA3), and d) reactor clamp (P2)

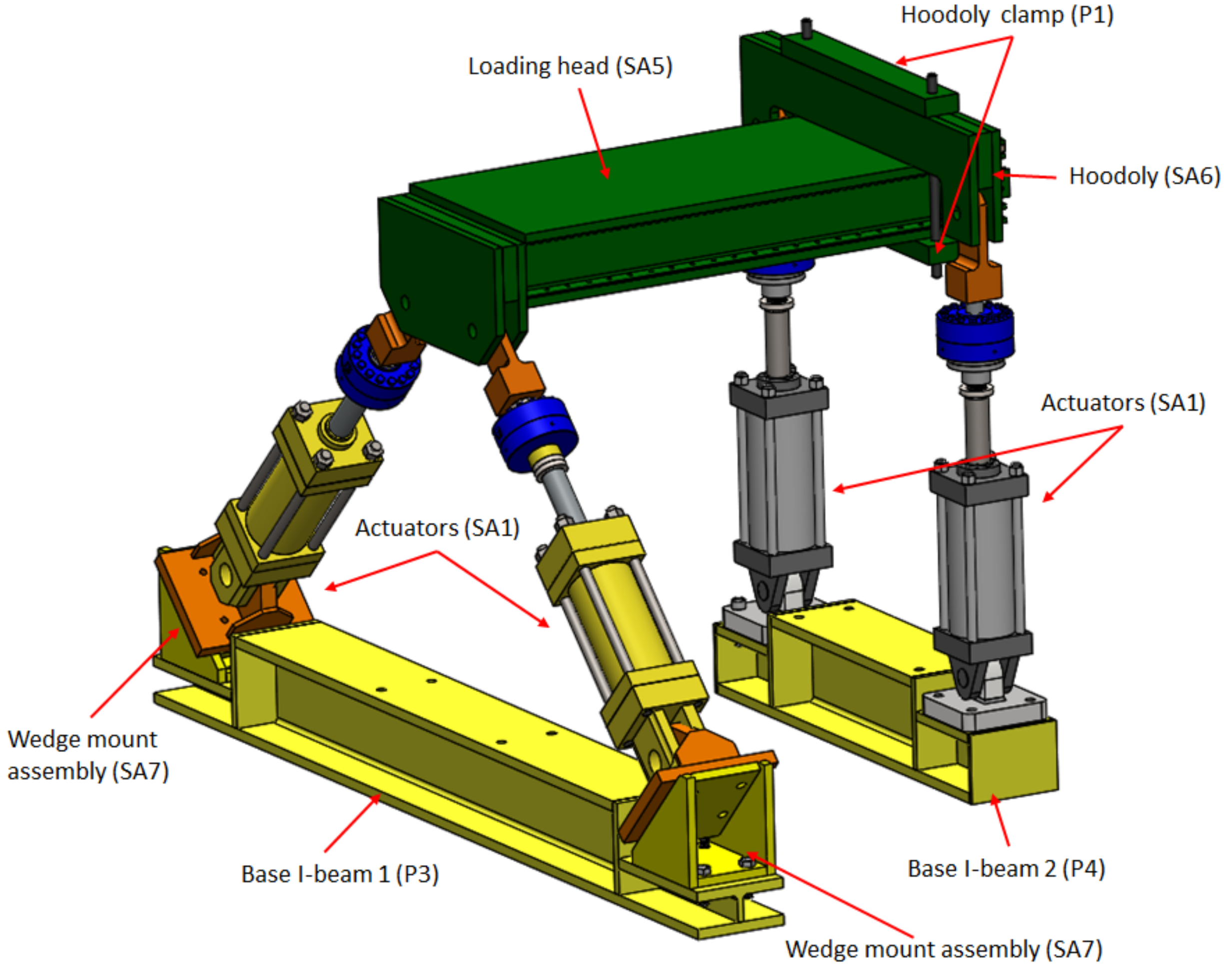

Figure 5. The subassemblies and parts that form the loading module of the ABST Fixture: a) loading head (SA5), b) actuators (SA1), c) hoodoly (SA6), d) wedge mount assembly (SA7), e) jack support beams (P3 and P4), and f) hoodoly clamps (P1)

WINGBOX: The third section is the wingbox (SA4), which is between the reaction head and loading head. The wingbox is the primary testing section of the ABST mechanical system and comprises the test panel, two pultrusion fiberglass side walls, and a steel bottom plate, as shown in figure 6. The pultrusion fiberglass side walls allow for efficient load transfer to the test panel. The bottom steel plate of the wingbox is attached to the reaction module and loading module via splice plates with 42 (0.5 inch diameter) bolts at both axial ends. On top of the transverse sides of the bottom plates, fiberglass channels are attached by 18 (3/8 inch diameter) bolts. A test panel of 40-by-24 inches with a maximum thickness of 1 inch can be fitted in the wingbox. Figure 7 shows the location of the test panel and engineering drawing of a test panel. Similar to the bottom steel plate, the test panel is attached to the reaction head and loading head via splice plates with 42 (0.5 inch diameter) bolts at each end and to the fiberglass channels on both transverse sides via 18 (3/8 inch diameter) bolts. The design of the wingbox allows reusing the wingbox with different test panels.

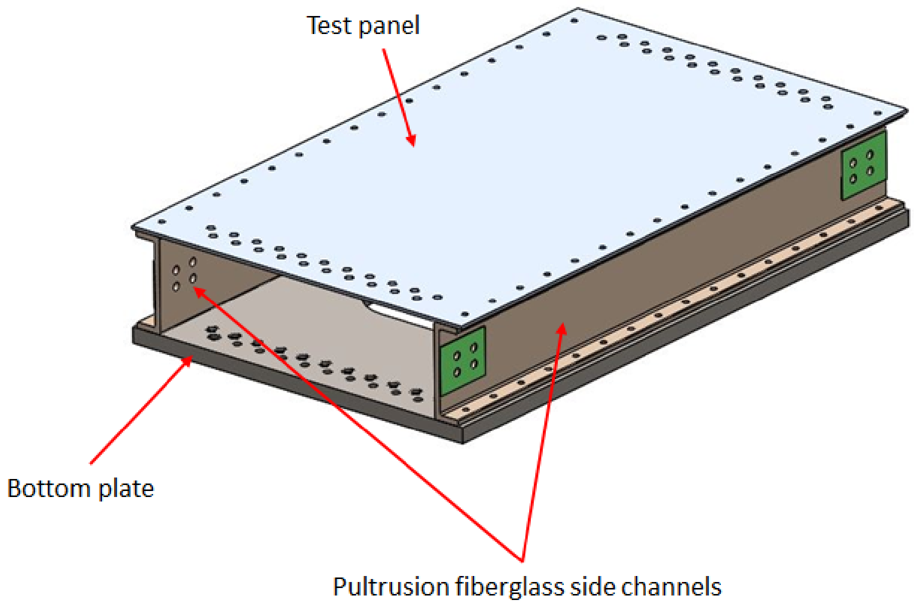

Figure 6. Parts of the wingbox

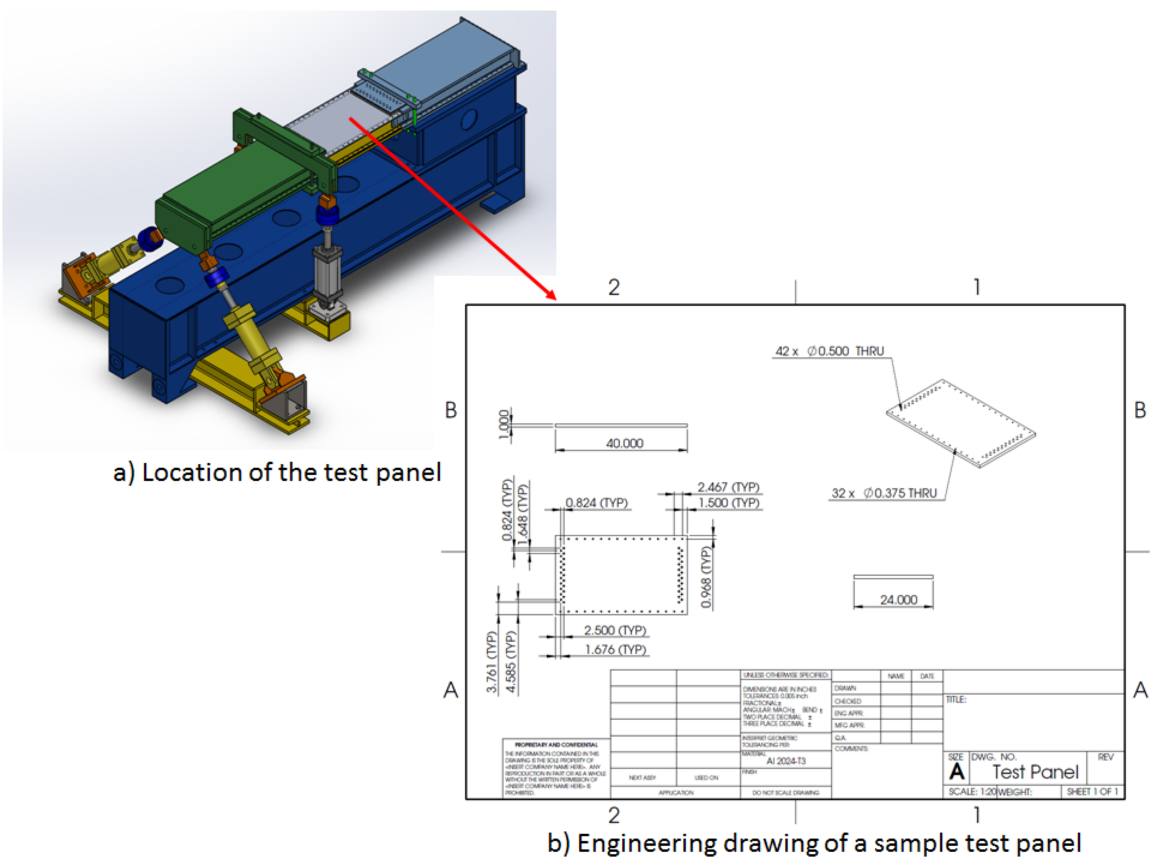

Figure 7. a) Location of test panel, and b) engineering drawing of the test panel

LOADING MECHANISM

The system of two central vertical actuators and two end actuators mounted at a 45˚ angle enable the ABST mechanical system to apply several complex loading configurations to a primary beam structure. The central actuators provide torsion loading and/or normal bending gradient from zero to constant moment and the end actuators apply forces through the center of the specimen beam and provide in-plane shear and normal bending forces, as shown in figure 8. Overall, the major loading conditions include constant moment, cantilever shear, bending, torsion, torsion with shear, and torsion with bending, as shown in figure 9. The red arrows in the figure show the direction of the movement of the actuators. The figure shows only the tensile loading configurations but the ABST mechanical system is capable of applying both tensile and compressive loads to a test panel.

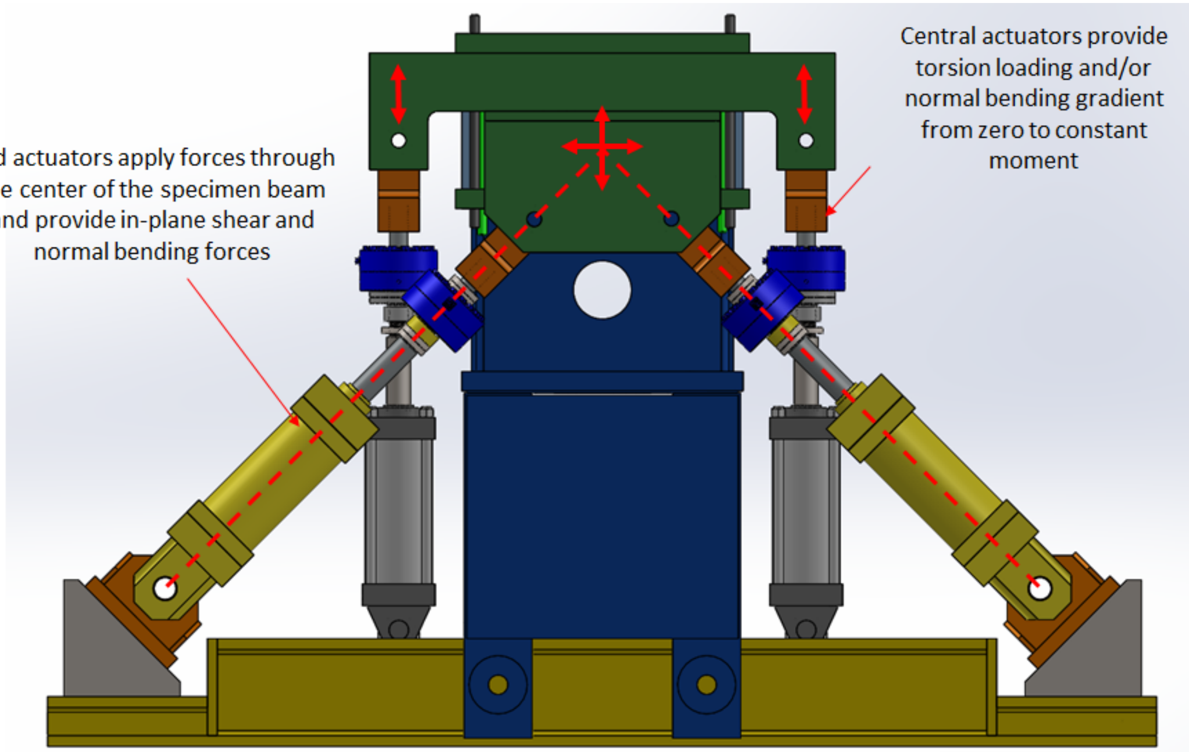

Figure 8. ABST fixture design concept

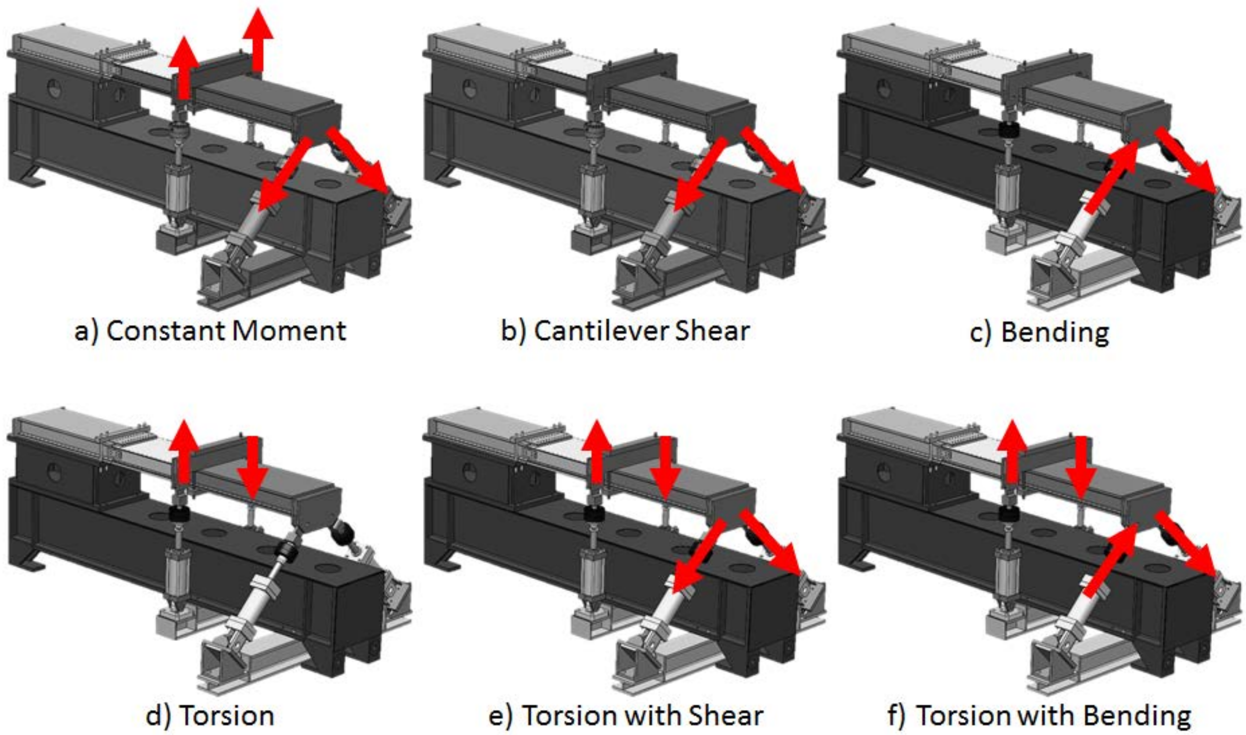

Figure 9. ABST fixture loading configurations

HYDRAULIC SYSTEM

The ABST fixture is powered by the hydraulic system. The schematic of this hydraulic system is shown in figure 10. In the figure, the hydraulic components that are exclusively used with the ABST fixture are highlighted in orange. The hydraulic power unit (HPU) and the chiller are shared by other mechanical systems in the Structures and Materials Lab (SML) laboratory. The details of the components are explained in the following section.

HYDRAULIC POWER UNIT (HPU)

MTS SilentFlo 515.60 HPU is used to power the ABST fixture, as shown in figure 11. It includes a pump that runs on 460V, 3-phase voltage. This pump has a flow rate of 60 GPM (expandable to 90 GPM) and working pressure of 3000 psi. Mobil DTE25 hydraulic oil is used in the HPU and is stored in a 320-gallon reservoir. The HPU supplies the power to the ABST fixture and three MTS load frames (not included in this document). Details of the HPU are provided in reference 1.

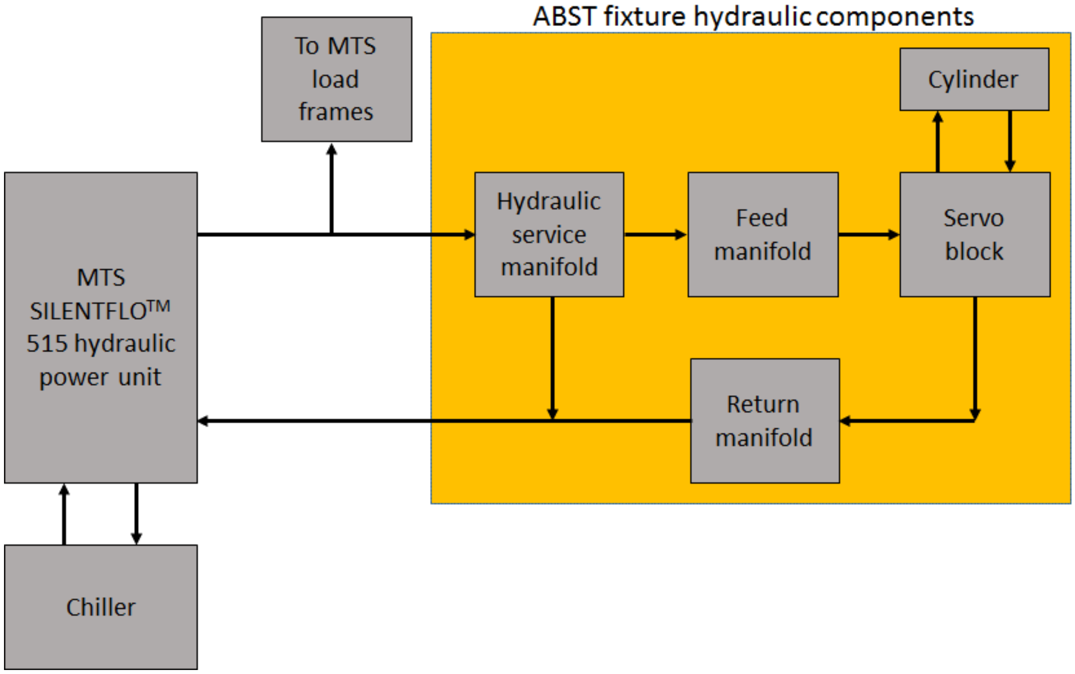

Figure 10. Schematic of the hydraulic system

Figure 11. Hydraulic Power Unit (HPU)

HYDRAULIC SERVICE MANIFOLD (HSM): The next component in the hydraulic system is the HSM, as shown in figure 12, which controls the low-pressure and high-pressure flow requirements of the system. The HSM is equipped with a filter, accumulators, and two independent output lines each with a high-pressure and a low-pressure line. Currently, only one output line is used. The operator of the MTS controller controls the HSM via MTS AeroPro™ software.

Figure 12. Hydraulic Service Manifold (HSM)

FEED AND RETURN MANIFOLDS: Feed and return manifolds (see figure 13) are mechanical lines that allow the fluid to flow into the four actuators and bleed out the fluid from the four actuators, respectively. The feedline to each actuator is fitted with a mechanical valve to switch on/off the supply of hydraulic fluid to the servo-block of the actuator.

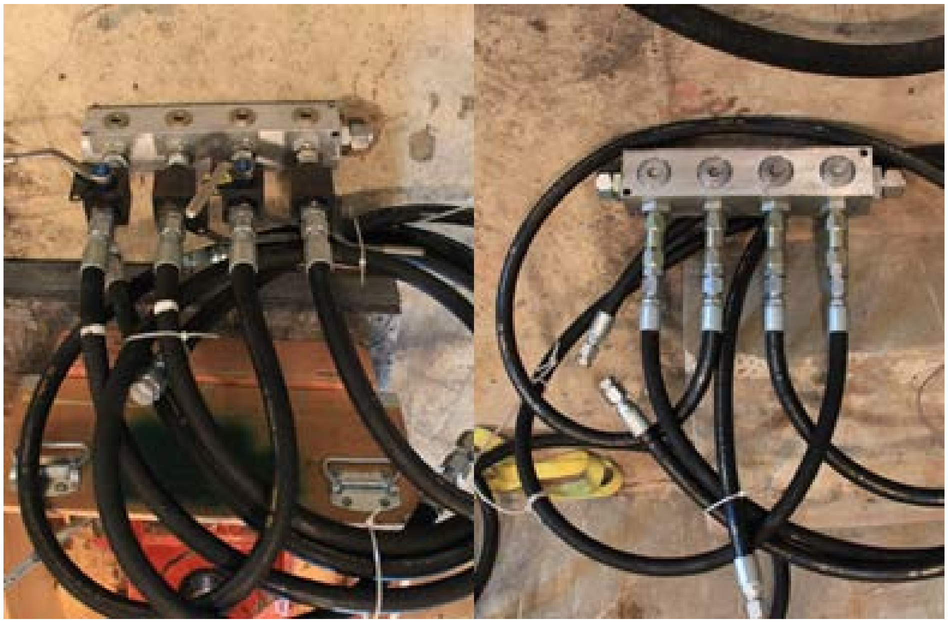

Figure 13. Feed and return manifolds

SERVO-BLOCK: Each actuator is equipped with a servo-block that controls the flow of the fluid to the actuator. A servo-valve (capacity: 15 gal/min), solenoid valve, and a filter is fitted on each servo-block. The servo-valve controls the flow of the fluid based on the error between the target value and the load cells reading. The solenoid is controlled by the test operator to switch on/off the fluid flow. One of the servo-blocks mounted on the actuator with its components is shown in figure 14.

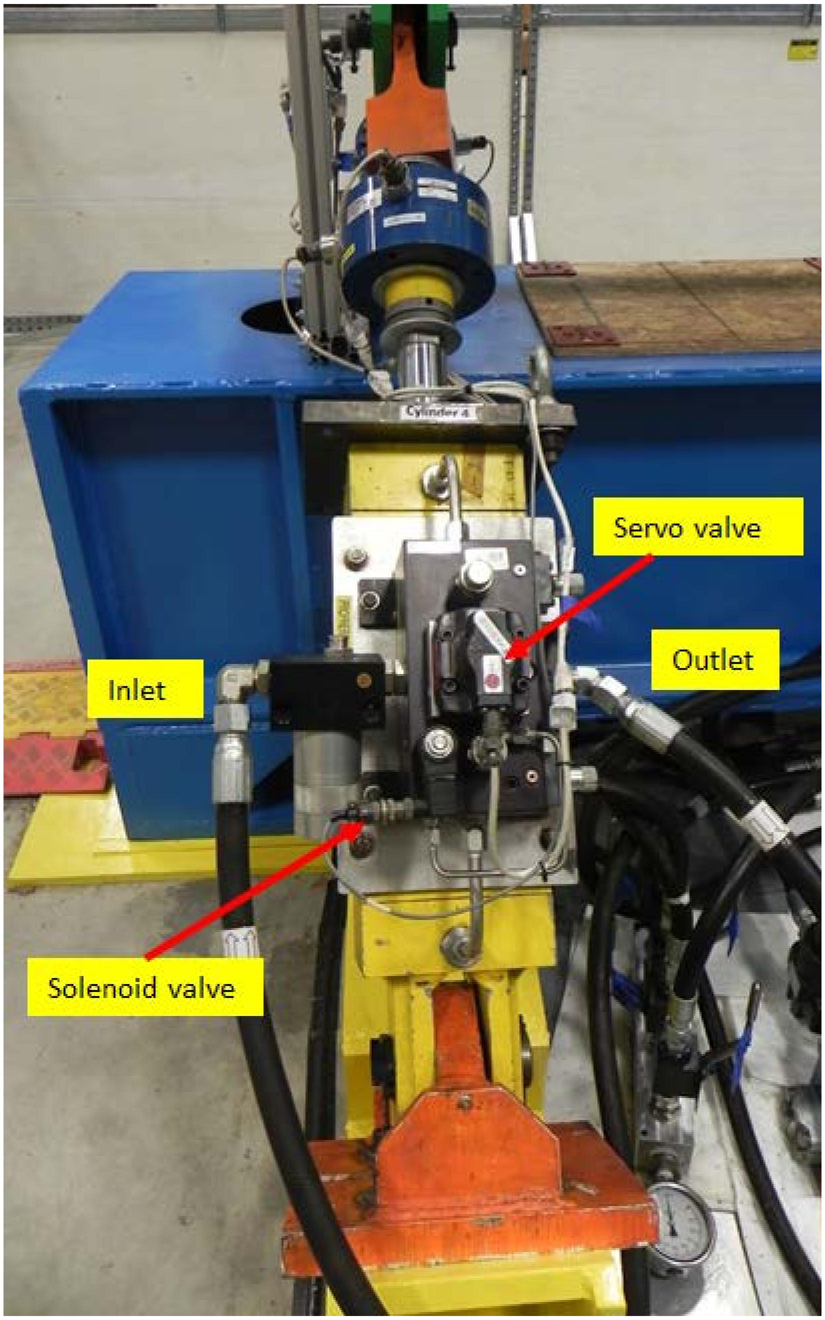

Figure 14. Servo-block mounted on an actuator

CHILLER: The final component in the hydraulic system is a chiller (see figure 15), which is common for the whole building. The manufacturer of the chiller is Thermal Care and it is located outside the building. The model number of the chiller is TSER 80D and it has a 78-ton capacity.

Figure 15. Chiller

CONTROL AND DAQ SYSTEMS AND MONITORING CENTER

The test is controlled using the MTS Flex Test 100 controller. A 64-channel MTS FlexDAC 20 data acquisition system is used to acquire the data from the strain gauges and displacement sensors. ARAMIS DIC system is used to capture full-field displacement and strain values and to monitor the progress of the test. LOREX^{TM} surveillance system is used. All the equipment in the monitoring center are shown in figure 16 and the details are provided in this section.

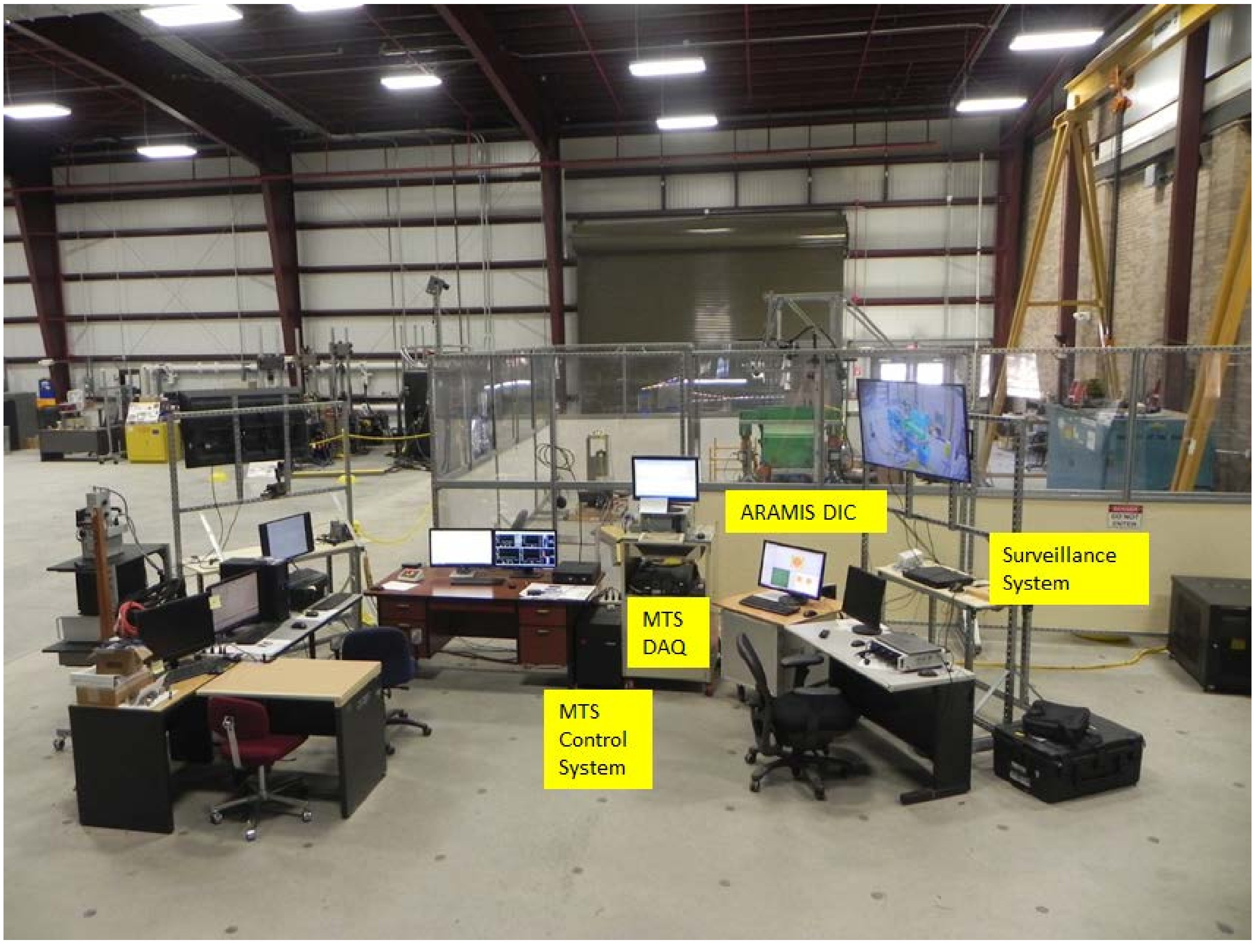

Figure 16. Control and DAQ systems and monitoring center

TEST CONTROLLER

MTS Flex Test 100 (model #494.10), shown in Figure 17, is used as the test controller of the ABST fixture. The FlexTest chassis has an eight-channel servo valve MUD driver (model #494.79) for servovalve control; 12 Dual Digital Universal Conditioners (model #494.26) for load cells and stroke; two eight-channel D/A output cards (model #494.46), and one eight-channel A/D input card (model # 494.465). The chassis also includes an HPU interface and two HSM interfaces to control the pump and HSM from the workstation. The controller is also connected to a 16-channel high-current DI/O breakout box to switch on/off the hydraulic flow to each actuators [2].

a) Front view of the MTS controller b) Rear view of the MTS controller

Figure 17. MTS controller

<u>DAQ SYSTEM</u>

MTS FlexDAC 20 is used for strain gauge and displacement sensors data acquisition. This system is comprised of 64 channels to synchronize data acquisition. Both the test controller and the DAQ system are compatible with AeroPro^{TM} software, which brings all the test data in one place for convenient post-test data reduction [3]. The MTS FlexDAC 20 DAQ system is shown in figure 18.

Figure 18. MTS DAQ system

TESTING SOFTWARE

MTS AeroPro is a user-friendly and powerful structural testing software developed by MTS [4]. AeroPro is used to interface test controller and DAQ systems; define tests loads and test spectrum; calibrate load cell, strain gauges, displacement sensors; amd control HPU and HSM and interface the controller with other DAQ to capture reliable test data. Figure 19 shows the graphical user interface of the AeroPro software.

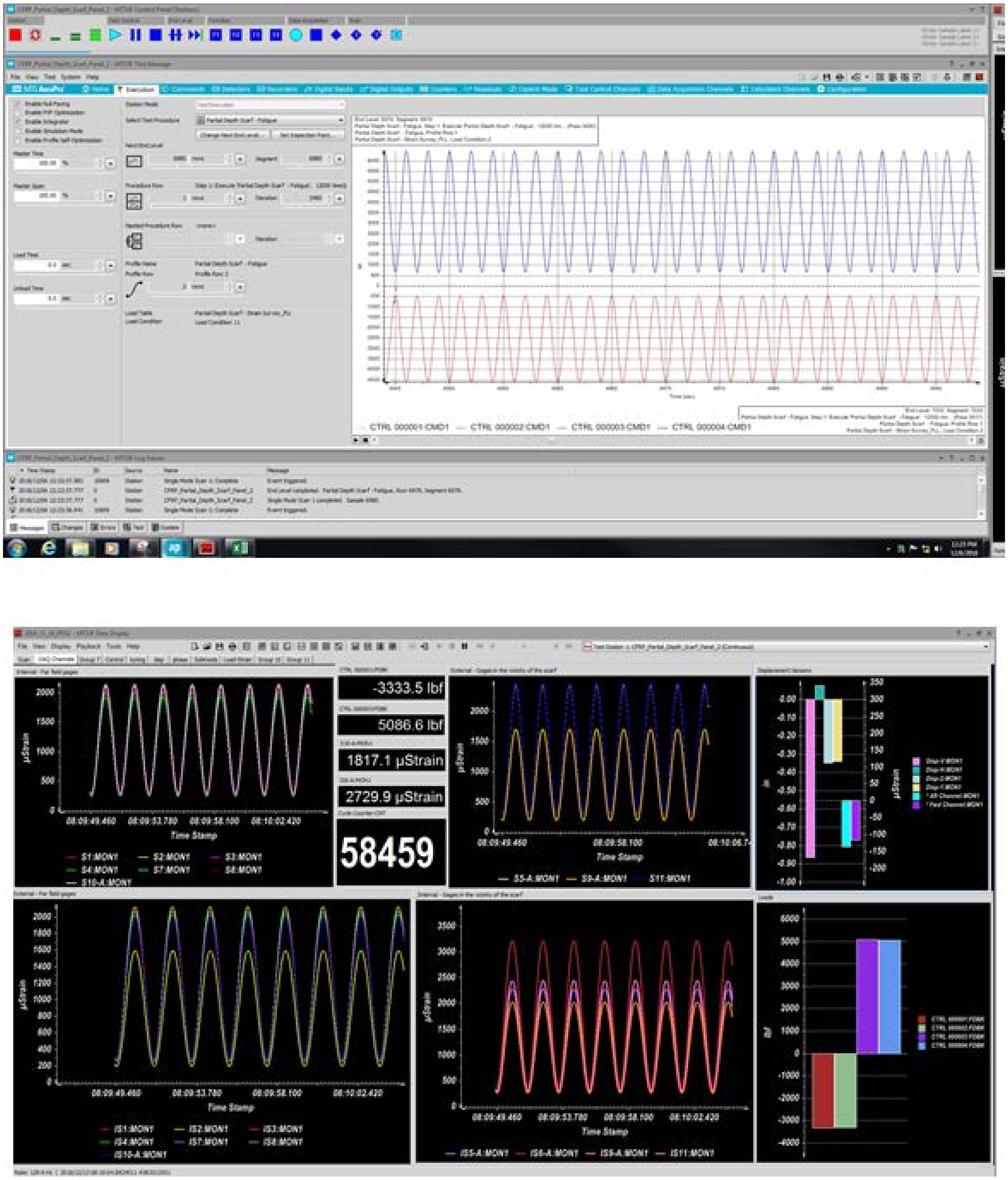

Figure 19. Graphical user interface of the MTS AeroPro software

ARAMIS DIC SYSTEM

Full-field deformation and strain data are recorded during the loading of the test panels using the ARAMIS three-dimensional deformation and strain DIC system. The system, using two 5-megapixel cameras, is capable of accurately measuring full-field strain within 50 με. Figure 20 shows the DIC camera setup, strain distribution calculated via DIC system, and comparison of DIC results and strain gauge. Prior to testing, the area to be monitored by the DIC system is coated with a high-contrast stochastic speckle pattern. Flat black spray paint is used to create a random pattern over the top of a flat white layer. The coarseness of the pattern directly affects the resolution of the measured strain field. Baseline images are taken using both cameras at zero loads. Deformed images are recorded using both cameras while under an applied load. The baseline and deformed images are then used to determine the full-field deformation and strain field.

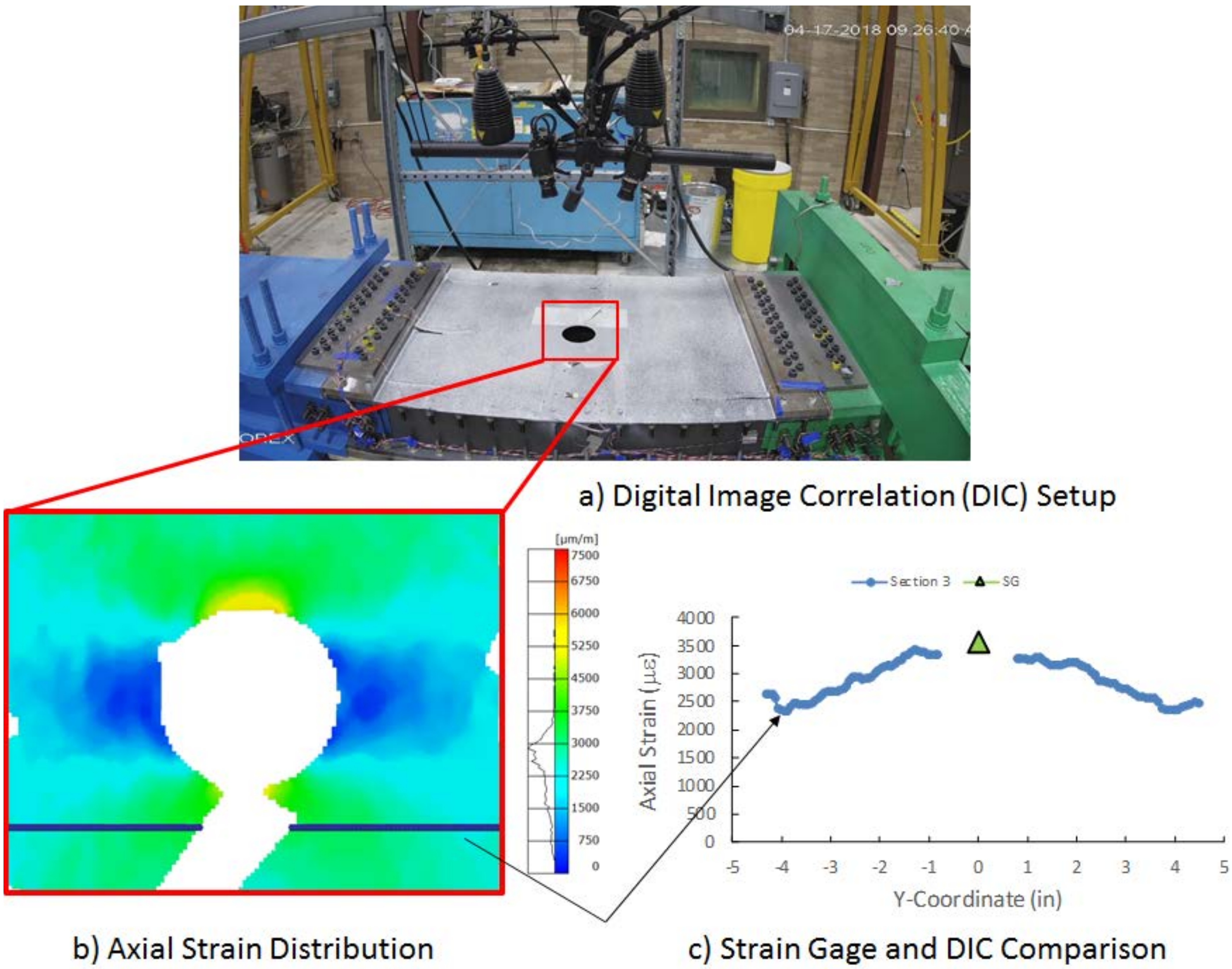

Figure 20. DIC system used for deformation and strain measurements

PORTABLE BARRIERS SURROUNDING THE ABST FIXTURE

The ABST mechanical system and the hydraulics system are surrounded by a wall on one side and nine portable barriers covering the other three sides. These barriers are 8 feet high and 8 feet wide. The frame of the barriers is constructed using struts with 8-inch by 4-inch by 0.75-inch plywood fastened at the bottom and two 8-inch by 4-inch by 0.25-inch polycarbonate sheets on top of the plywood. The portable barrier works as a physical barrier that keeps the personnel out of the testing area during the testing. Figure 21 shows the portable barrier surrounding the fixture.

Figure 21. Portable barrier surrounding the ABST fixture

DEVELOPMENT OF ABST MECHANICAL SYSTEM

The development of the ABST mechanical system was undertaken in three steps. The first step was the machining of the individual parts. The parts were machined by an external vendor and delivered to the SML laboratory. The next step was to weld the individual parts to assemble individual subassemblies. The last step was to assemble the individual subassemblies to build the complete mechanical system. Figure 22 shows some of the parts of the ABST mechanical system after machining. Welding setup and some of the welded subassemblies are shown in figure 23.

a) Riser assembly plates (SA2)

b) Actuator base beams (P3 & P4)

c) Hoodoly assembly parts (SA6)

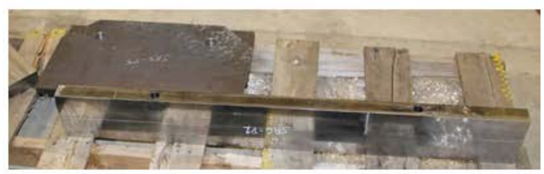

d) Parts of loading head (SA5)

e) Hoodoly and reactor clamp (P1 & P2

f) Parts of the reactor head (SA3)

Figure 22. Machined parts of the ABST mechanical system

a) Welding of the sub-assemblies

b) Base assembly (SA8)

c) Welding of the loading head (SA5)

d) Riser assembly (SA2)

e) Welding of the reactor head (SA3)

f) Actuator wedge assembly (SA7)

Figure 23. Welding setup and welded subassemblies of the ABST mechanical system

Assembly of the ABST mechanical system was achieved in a systematic manner. At first, the reaction head (SA3), wingbox (SA4) and loading head (SA5) were placed on a flat surface (base assembly), as shown in figure 24. Then the three subassemblies were aligned and bolted together. The parts of the reaction head and, similarly, the parts of the loading head were then welded, as shown in figure 24. When the reaction head (SA3), wingbox (SA4), and loading head (SA5) was assembled, the assembled parts were removed from the base assembly and the riser assembly (SA2) was placed on the base assembly (SA8) and bolted, as shown in figure 25. Next, the assembled section of reaction head (SA3), wingbox (SA4), and loading head (SA5) was placed on the riser assembly and bolted, as shown in figure 26. Finally, the actuators were attached to the mechanical system, as shown in figure 27. The final assembled and painted system is shown in figure 28.

a) Reaction head (SA3), wingbox (SA4) and loading head (SA5) are bolted and placed on the base assembly

b) Welded reaction head (SA3)

c) Welded loading head (SA5)

Figure 24. Reaction head, wingbox, and loading head are bolted together on a flat surface

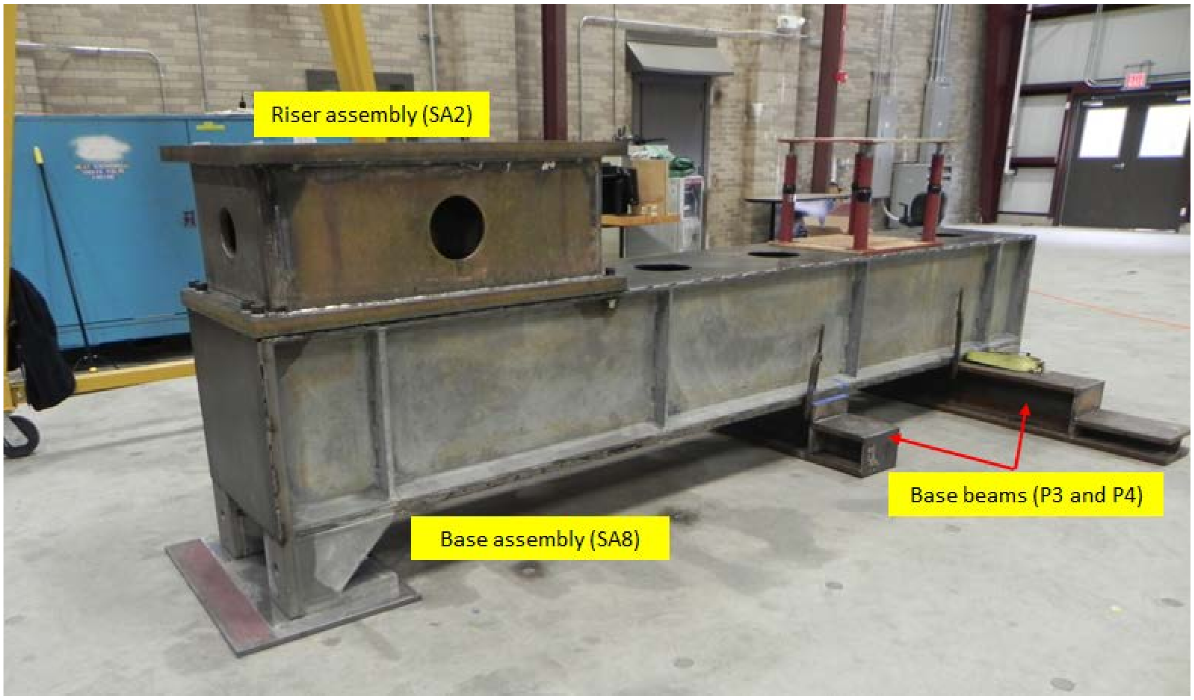

Figure 25. Riser assembly (SA2) is bolted on top of the base assembly (SA8)

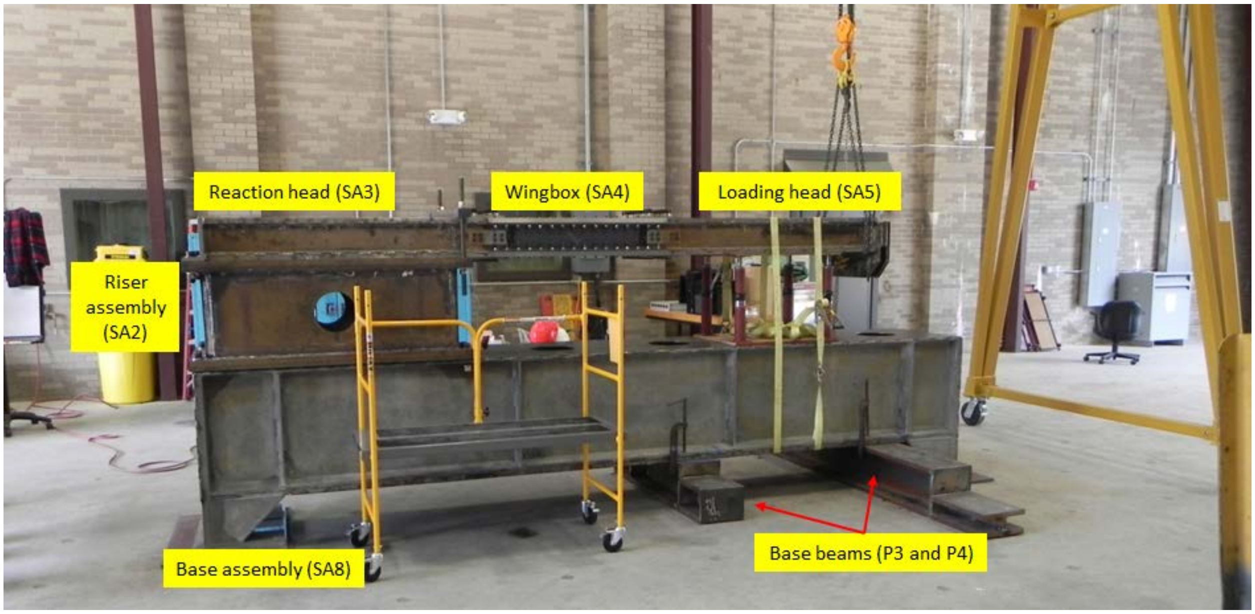

Figure 26. The assembled reaction head (SA3), wingbox (SA4), and loading head (SA5) are bolted on top of the riser assembly (SA2)

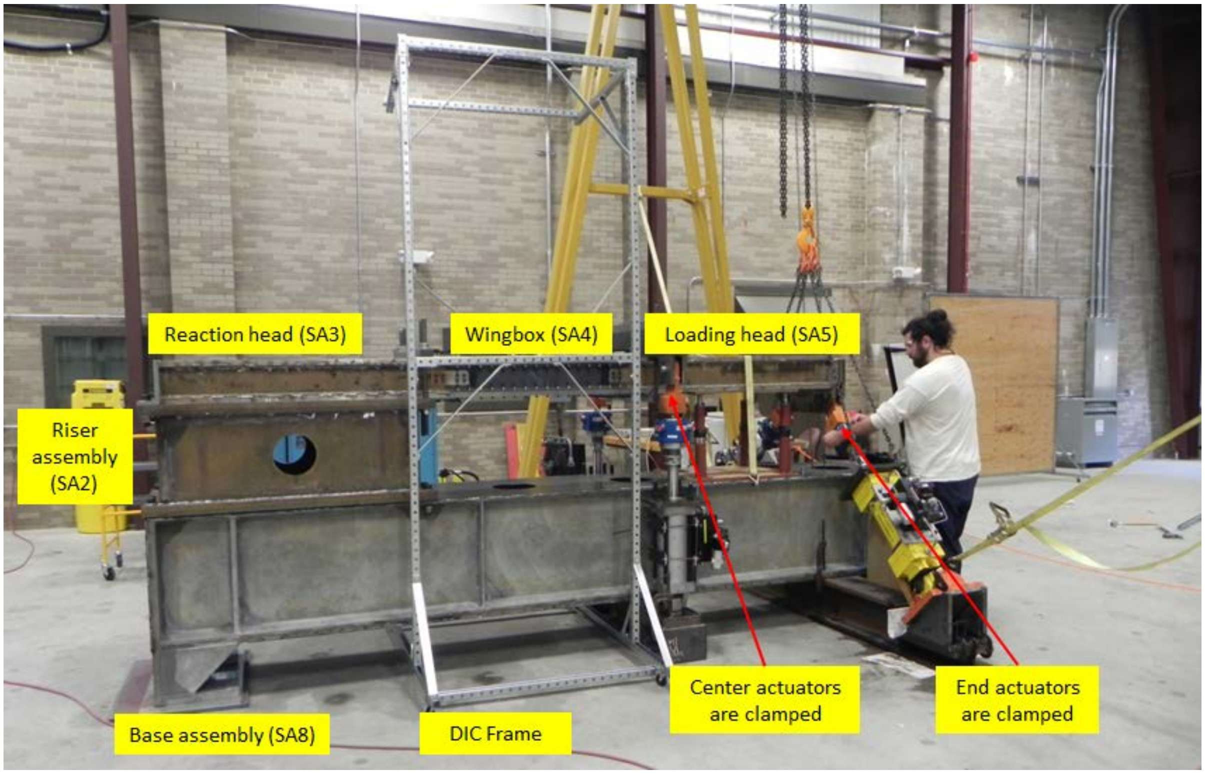

Figure 27. Attaching the actuators to the ABST mechanical system

Figure 28. Assembled ABST mechanical system

ACCEPTANCE TEST

Prior to the commencement of the test program, an acceptance test was conducted to verify the capability of the fixture. During the acceptance test, a 40-by-24-by-1-inch aluminum 6061 panel was installed on the fixture. The panel was instrumented with strain gauges and the black/white speckle pattern for DIC, as shown in figures 29–30. In addition to the panel, the wingbox side channels were also instrumented with strain gauges, as shown in figure 29. The test panel was subjected to three types of loading configuration constant moment (both tension and compression), torsion (both clockwise and counter-clockwise) and cantilever shear (only tension). The target load values and the actual load values for each loading configuration are provided in table 2. The tests were conducted by quasi-statically loading the panel up to the target loads at an increment of 10%.

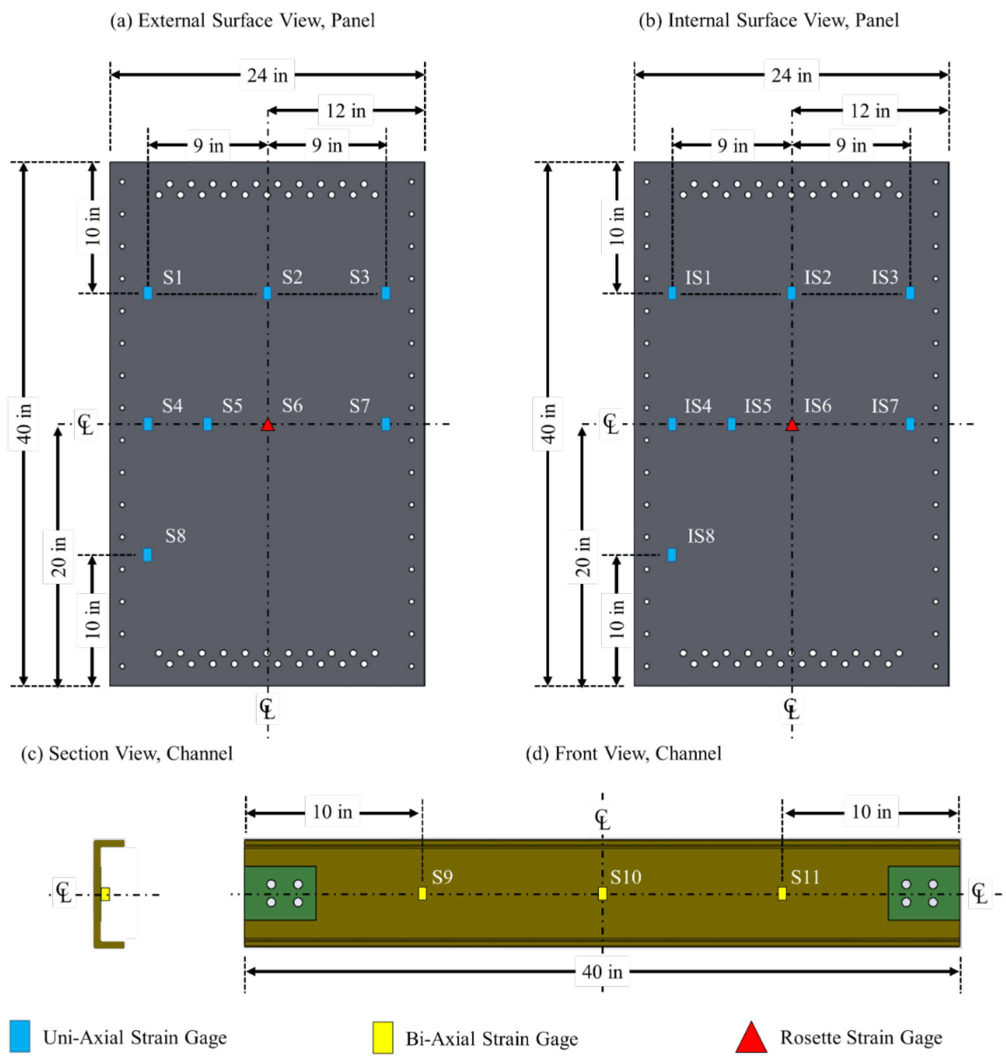

Figure 29. Strain gauge layout for acceptance test panel and wingbox side channels

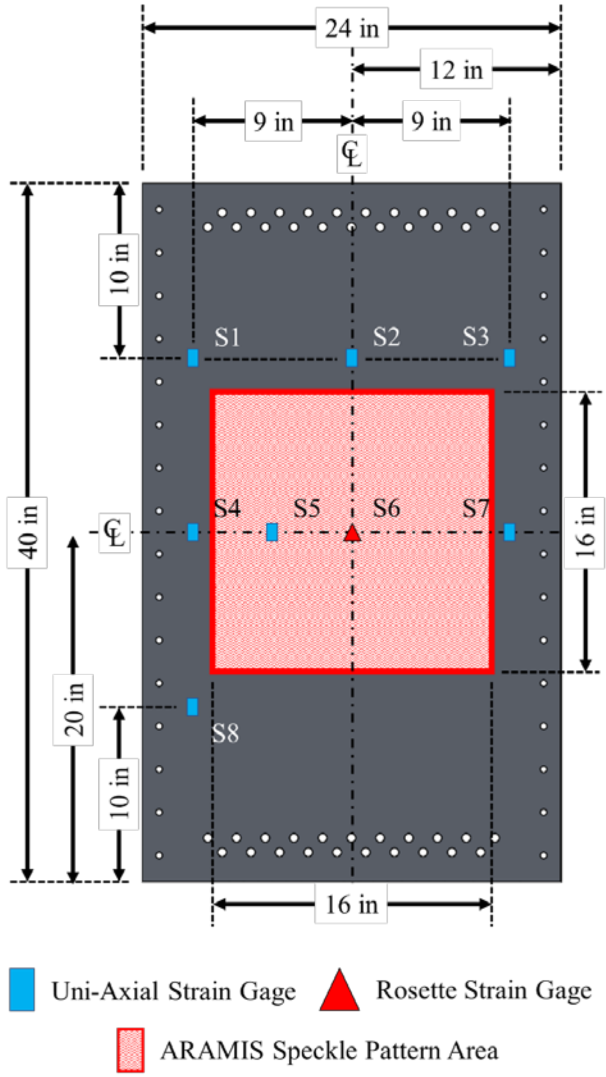

Figure 30. Location of DIC speckle pattern area with respect to the test panel

During the acceptance tests, the strain data were collected using the strain gauges and DIC equipment. Representative results for the constant moment, torsion, and cantilever shear loading configurations are shown in figures 31–33, respectively. In all three figures, section (a) shows the DIC sections, strain gauge location, and maximum load levels; section (b) shows the DIC results at 0 load and maximum load level; and section (c) shows the strains along the DIC sections and strain gauge results (red squares). As seen in these figures, the DIC results correlated very well with the strain gauge results. For the constant moment and torsion loading configurations, the test was able to reach the target load values. In the case of cantilever shear, the side channels failed at approximately 93.5% of the target load levels. The acceptance test provided the upper bounds of the fixture for each type of loading configuration.

Table 2. Target and actual load values for each configuration during the acceptance test

Load Configuration	Loading Type	Test Status	Maximum Load			
			Actuator 1 (lb)	Actuator 2 (lb)	Actuator 3 (lb)	Actuator 4 (lb)
Constant Moment	Compression	Target	25,093	25,093	-35,493	-35,493
		Actual	25,993	25,993	-36,754	-36,754
	Tension	Target	-30,112	-30,112	42,591	42,591
		Actual	-31,192	-31,192	44,105	44,105
Cantilever Shear	Tension	Target	0	0	27,825	27,825
		Actual	0	0	26,000	26,000
Torsion	Clockwise	Target	-20,293	20,293	0	0
		Actual	-20,293	20,293	0	0
	Counter-Clockwise	Target	20,293	-20,293	0	0
		Actual	20,293	-20,293	0	0

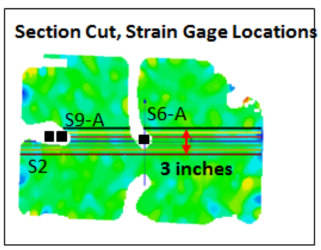

Actuator #	100 % Load Level
Actuator 1	-31192 lbs
Actuator 2	-31192 lbs
Actuator 3	44105 lbs
Actuator 4	44105 lbs

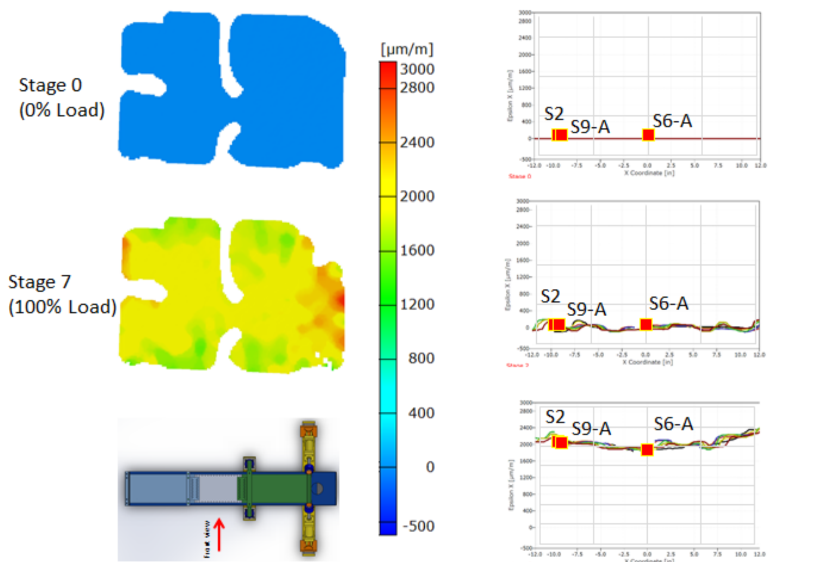

a) DIC sections, strain gage locations and maximum load level

b) Axial strains measured by DIC at no load and maximum load level

c) Axial strains along the DIC sections and comparison with corresponding strain gages

Figure 31. Comparison of axial strains measured using DIC and strain gauges during constant moment (tension) loading configuration

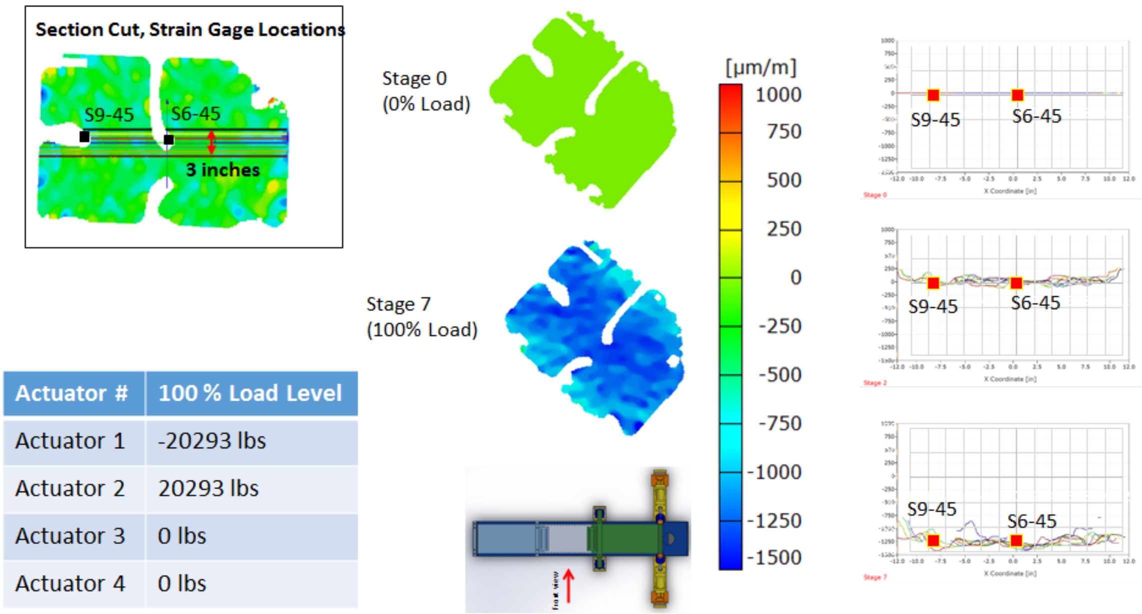

Actuator #	100 % Load Level
Actuator 1	-20293 lbs
Actuator 2	20293 lbs
Actuator 3	0 lbs
Actuator 4	0 lbs

a) DIC sections, strain gage locations and maximum load level

b) Strains at 45˚ angle measured by DIC at no load and maximum load level

c) Strains at 45˚ angle along the DIC sections and comparison with corresponding strain gages

Figure 32. Comparison of strains at 45˚ angle measured using DIC and strain gauges during torsion (clockwise) loading configuration

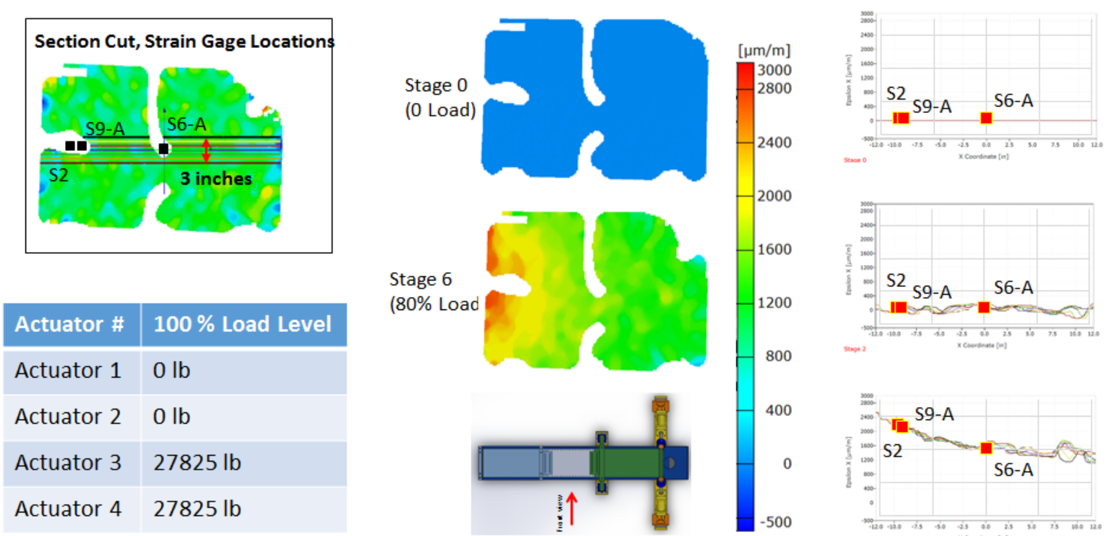

Actuator #	100 % Load Level
Actuator 1	0 lb
Actuator 2	0 lb
Actuator 3	27825 lb
Actuator 4	27825 lb

a) DIC sections, strain gage locations and maximum load level

b) Axial strains measured by DIC at no load and maximum load level

c) Axial strains along the DIC sections and comparison with corresponding strain gages

Figure 33. Comparison of axial strains measured using DIC and strain gauges during cantilever shear (tension) loading configuration

REFERENCES

1. MTS Systems Corporation (2017). *MTS SilentFlo^{TM} 515 Hydraulic Power Units user's manual*. Eden Prairie, MN: MTS.

2. MTS Systems Corporation (2014). *FlexTest® Models 40/60/100/200 Controller Hardware user's manual*. Eden Prairie, MN: MTS.

3. MTS Systems Corporation (2018). *MTS FlexDAC^{TM} 20 Data Acquisition System user's manual*. Eden Prairie, MN: MTS.

4. MTS Systems Corporation (2014). AeroPro™ Control and Data Acquisition Software user's manual. Eden Prairie, MN: MTS.

APPENDIX A—ENGINEERING DRAWINGS OF THE ABST MECHANICAL SYSTEM

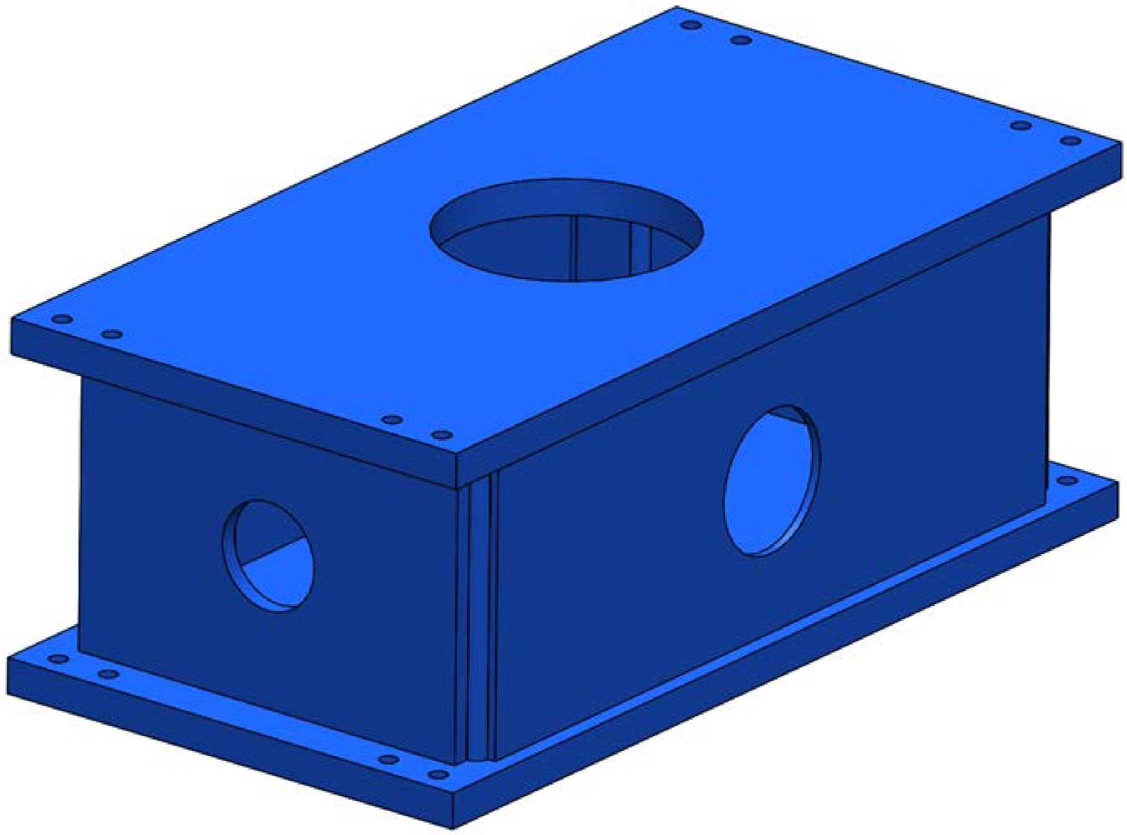

Figure A-1. 3-D model of the riser assembly (SA2)

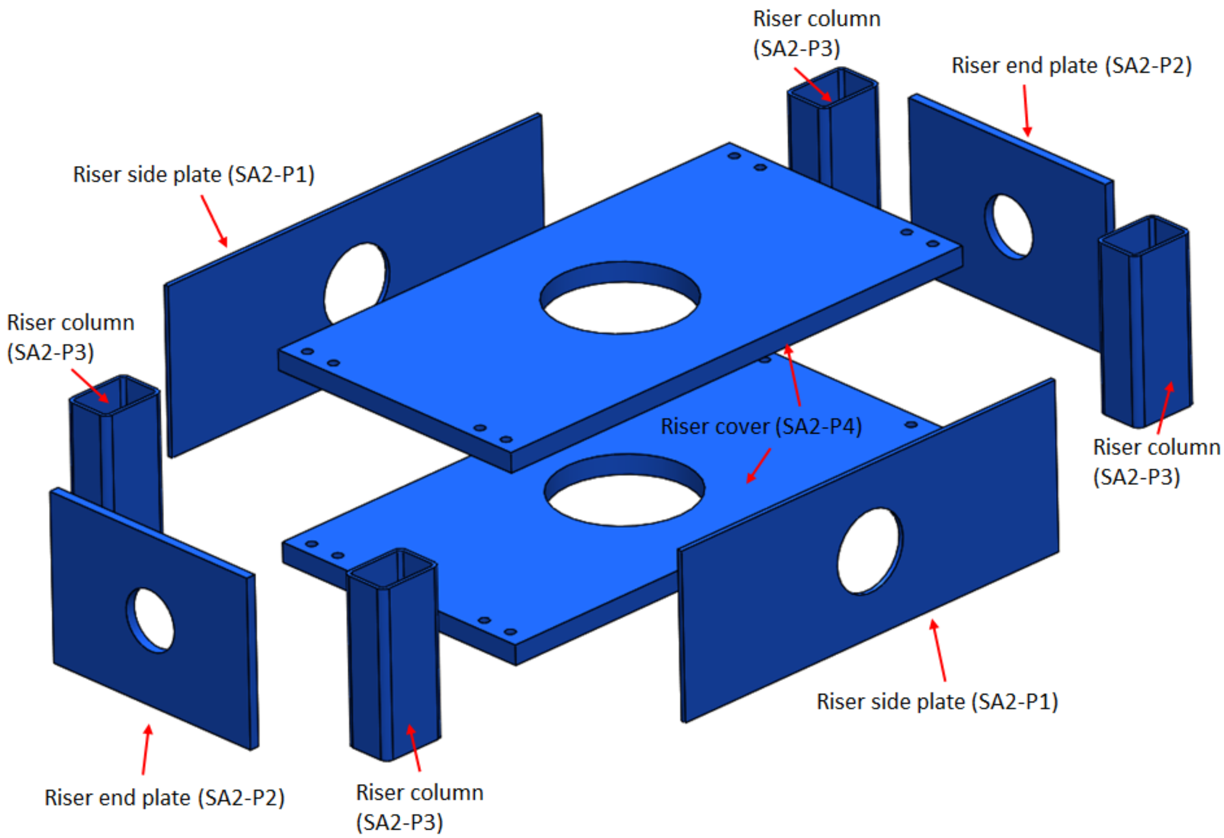

Figure A-2. Exploded view of the riser assembly (SA2)

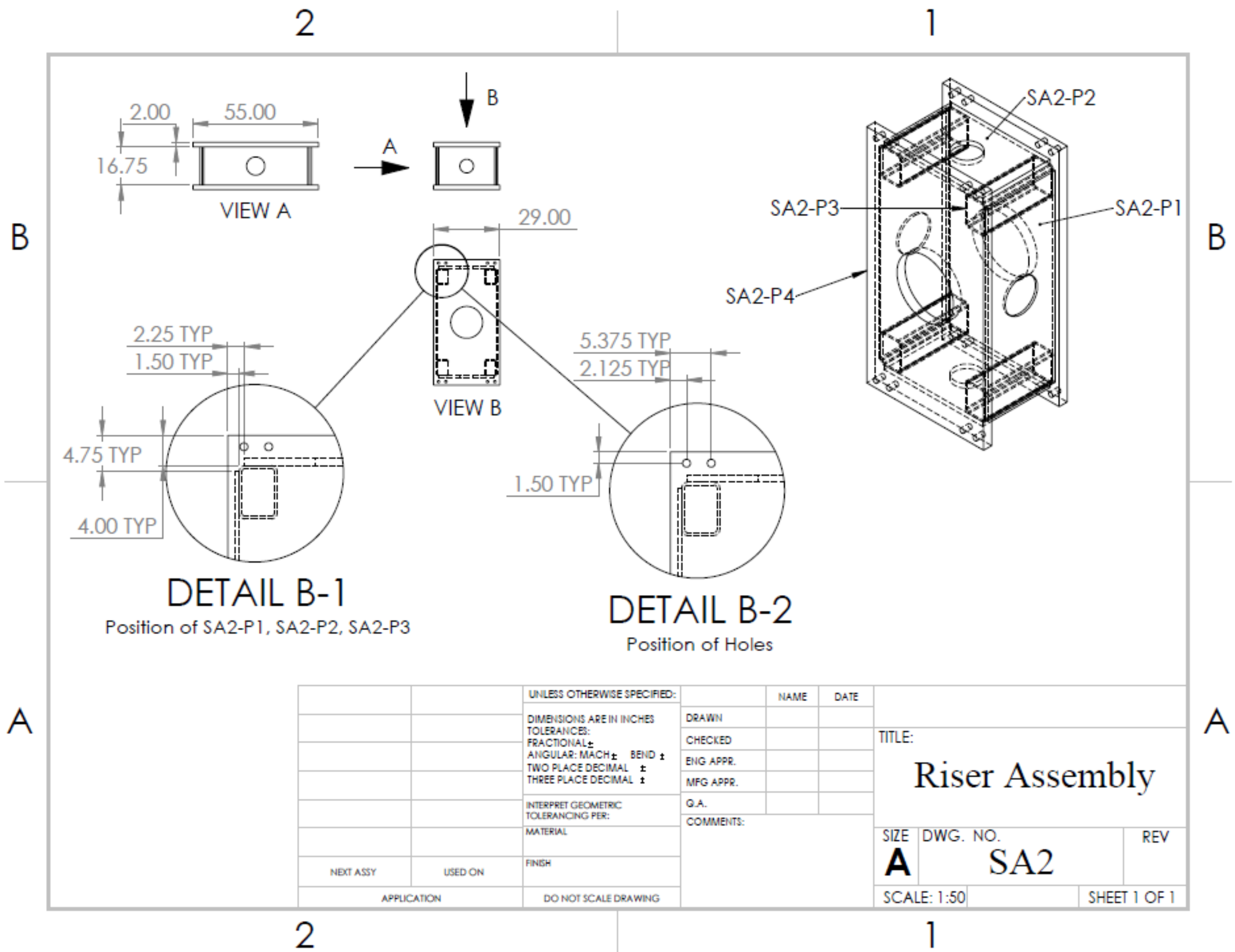

Figure A-3. Drawing of the riser assembly (SA2)

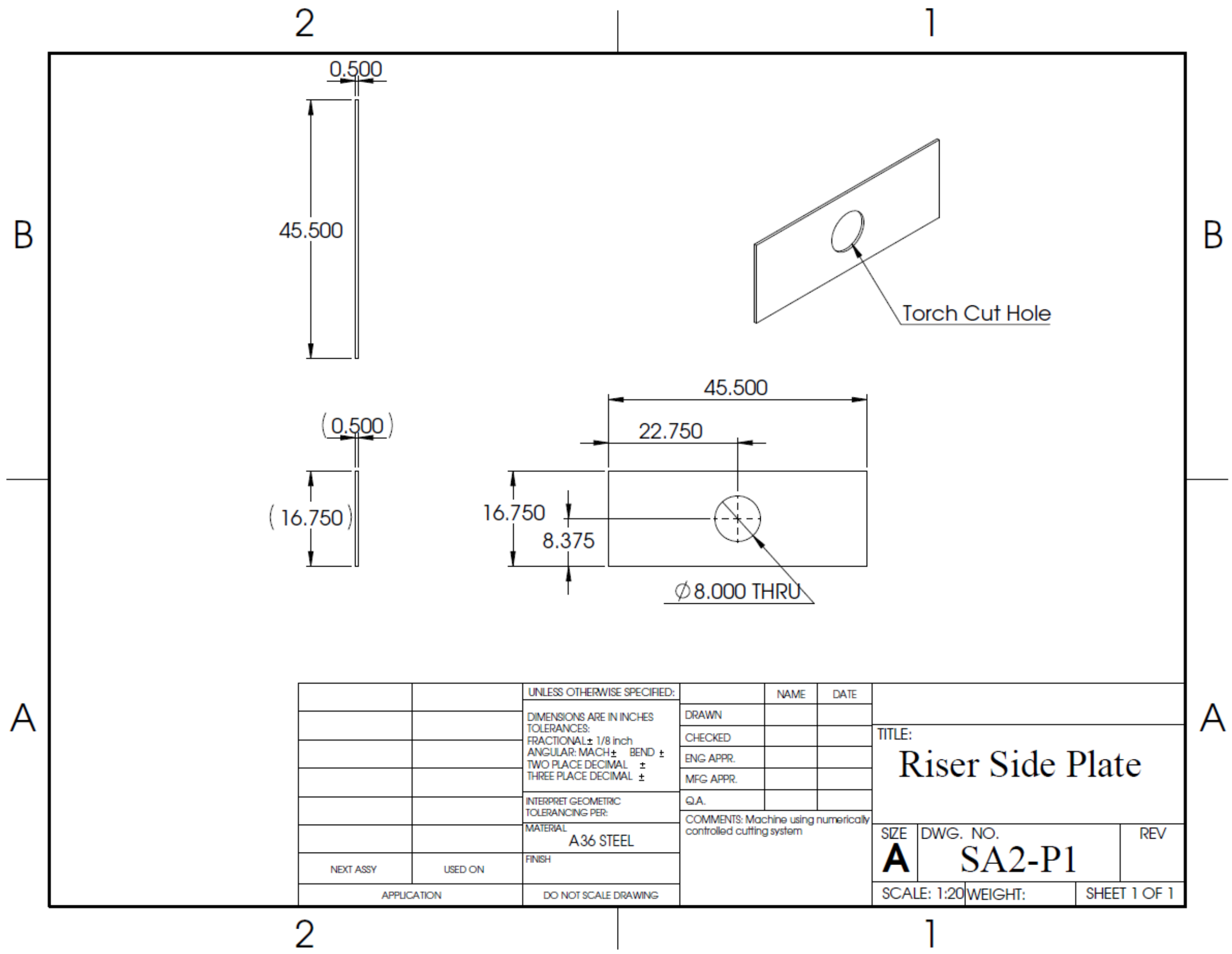

Figure A-4. Drawing of the riser—side plate (SA2-P1)

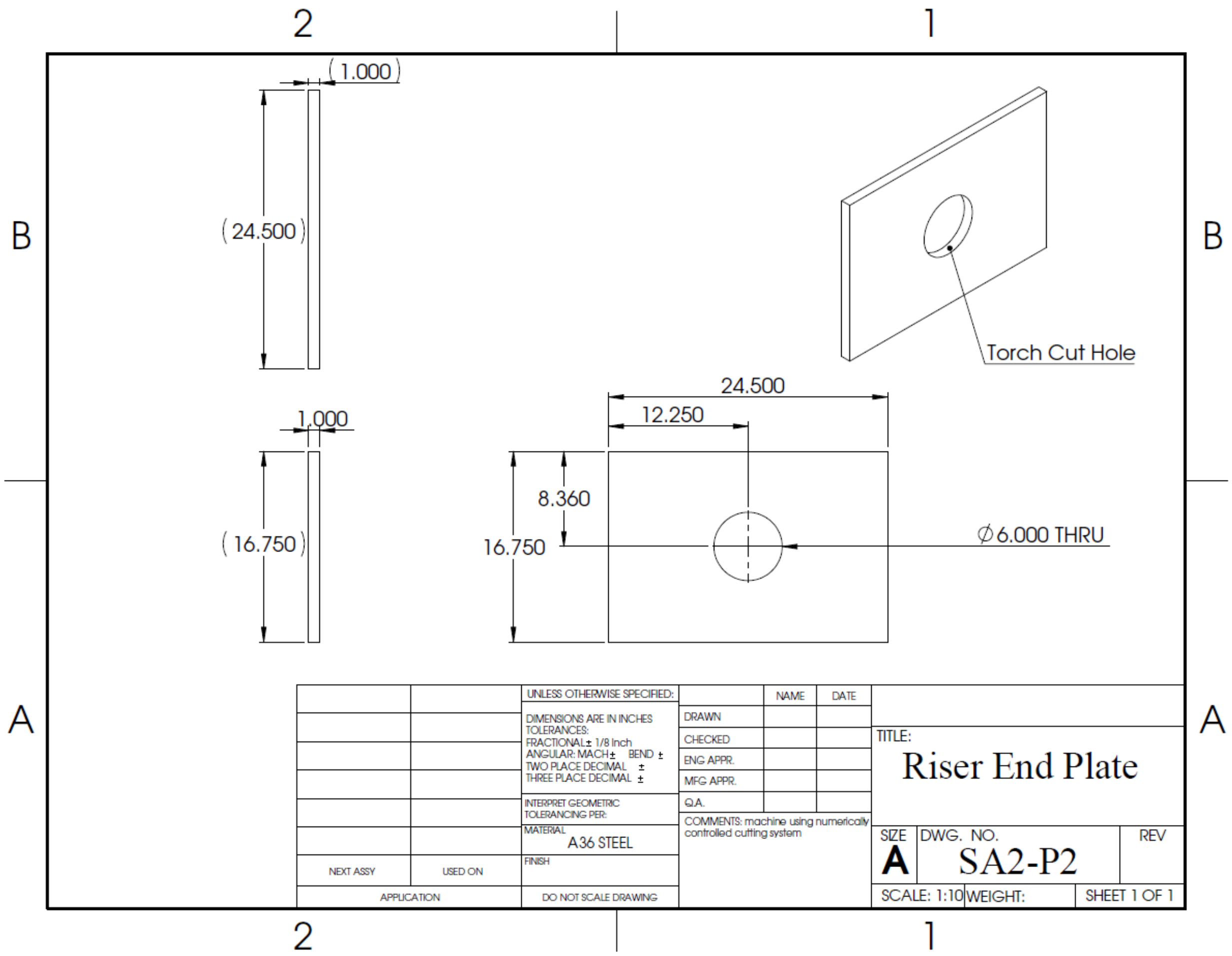

Figure A-5. Drawing of the riser—end plate (SA2-P2)

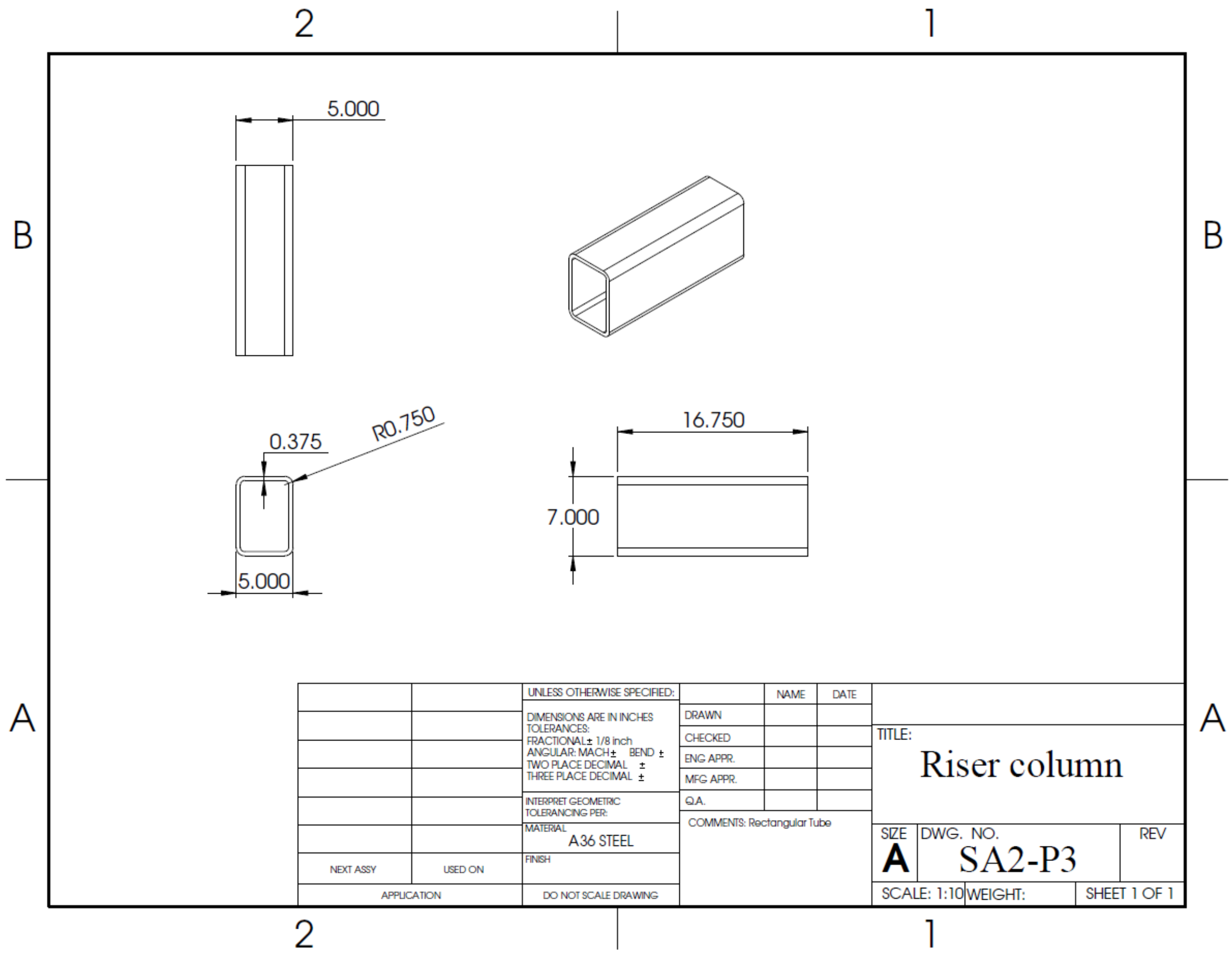

Figure A-6. Drawing of the riser—column (SA2-P3)

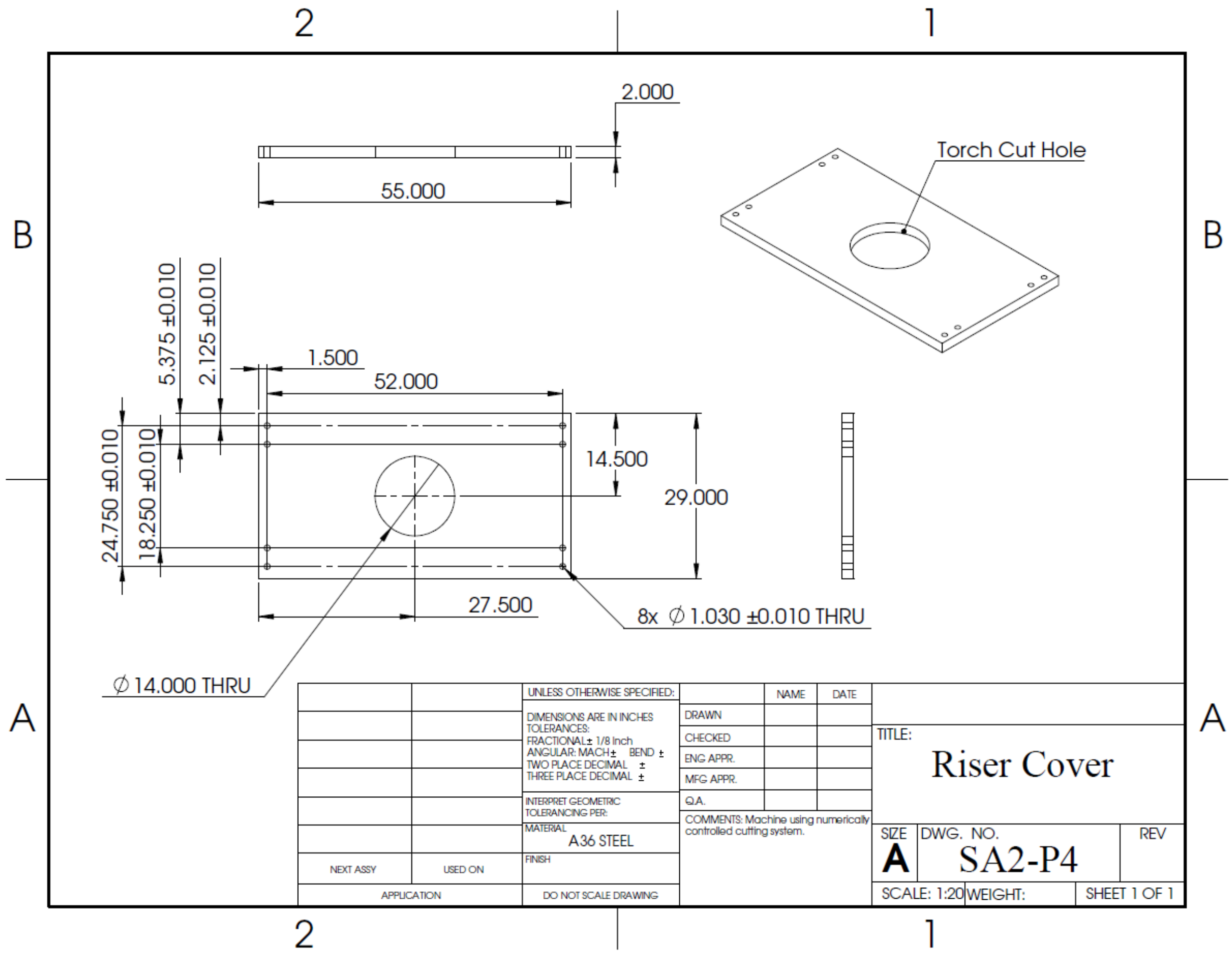

Figure A-7. Drawing of the riser—cover (SA2-P4)

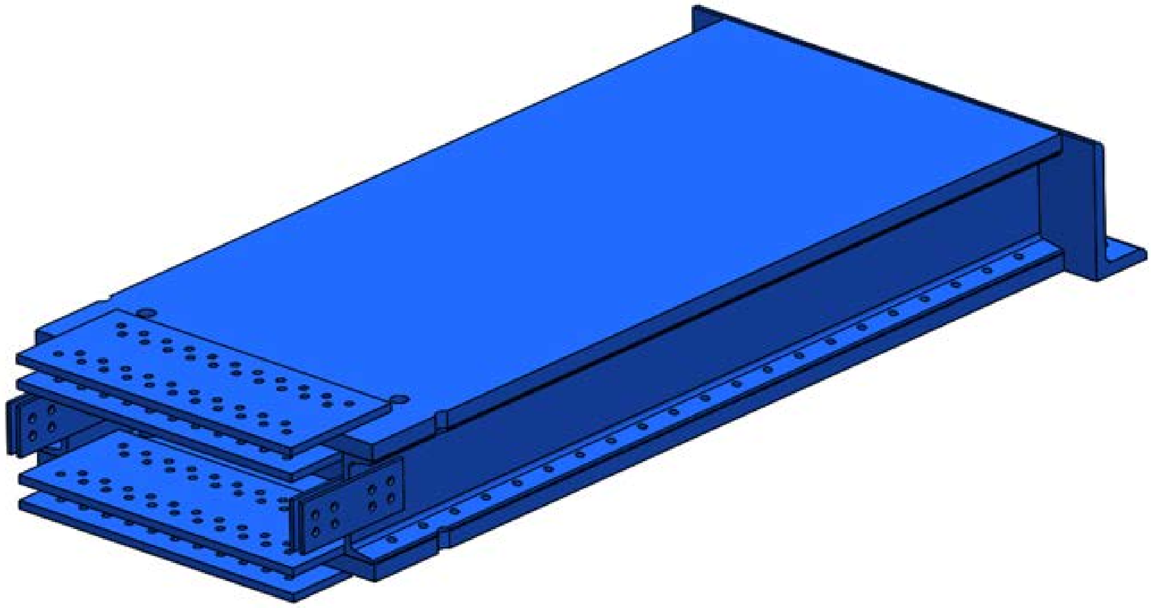

Figure A-8. 3-D model of the reaction head (SA3)

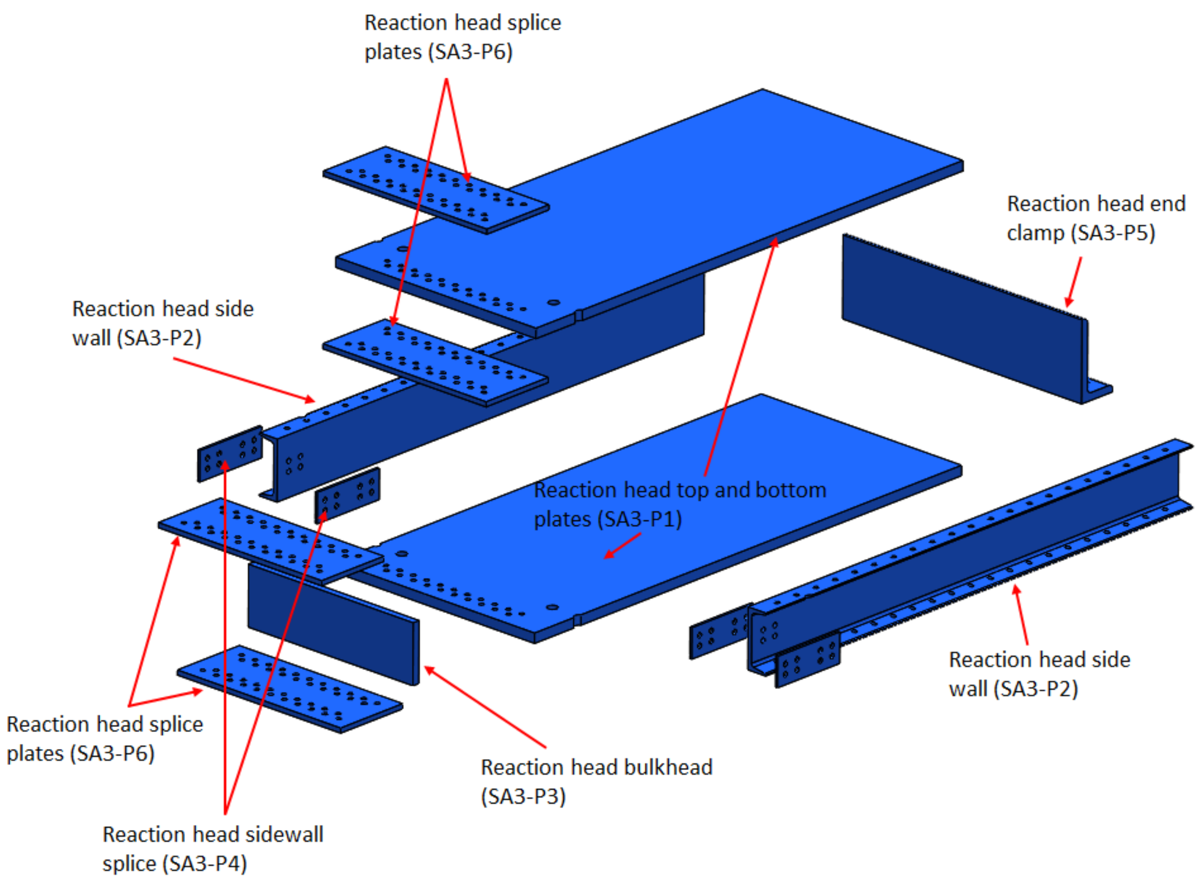

Figure A-9. Exploded view of the reaction head (SA3)

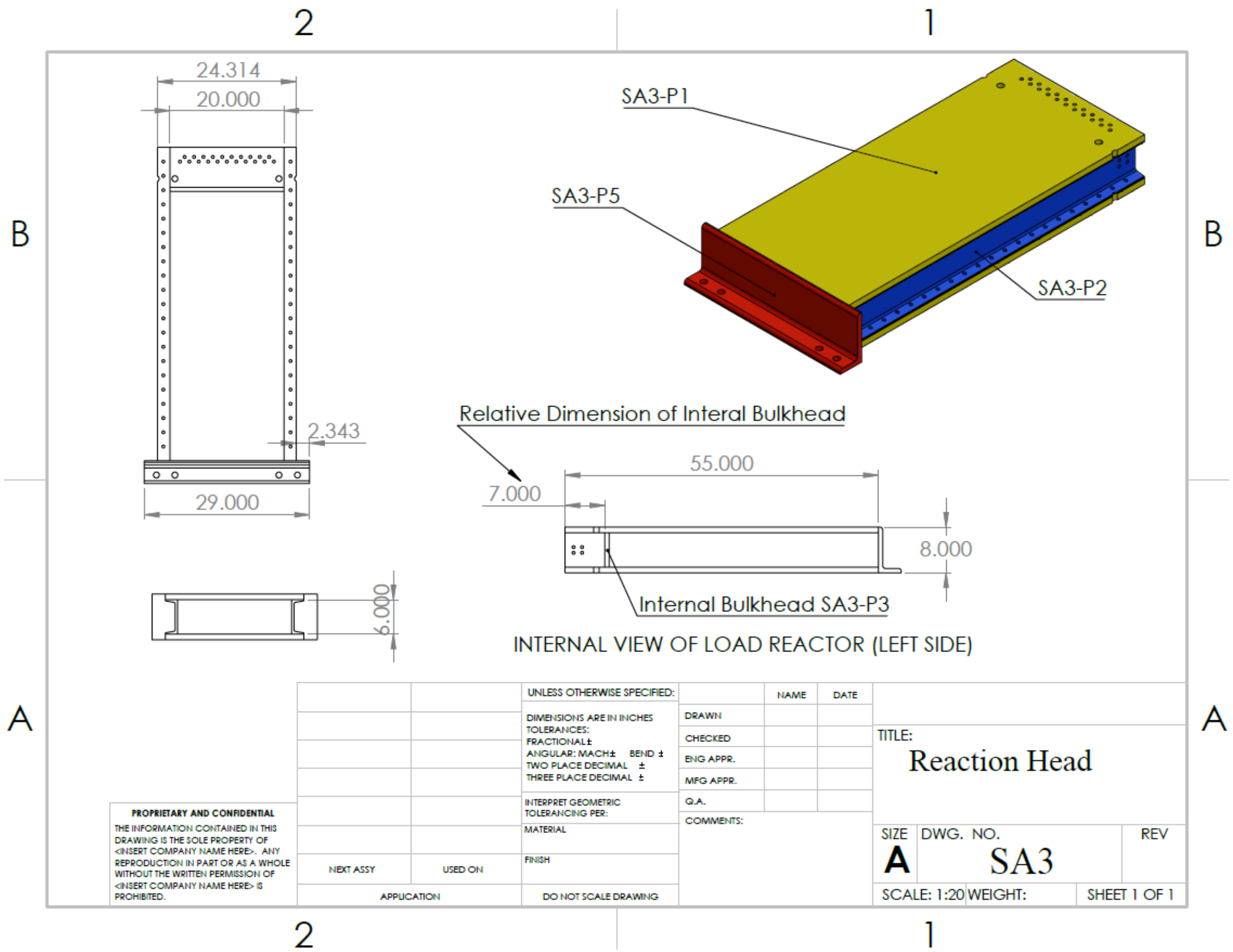

Figure A-10. Drawing of the reaction head (SA3)

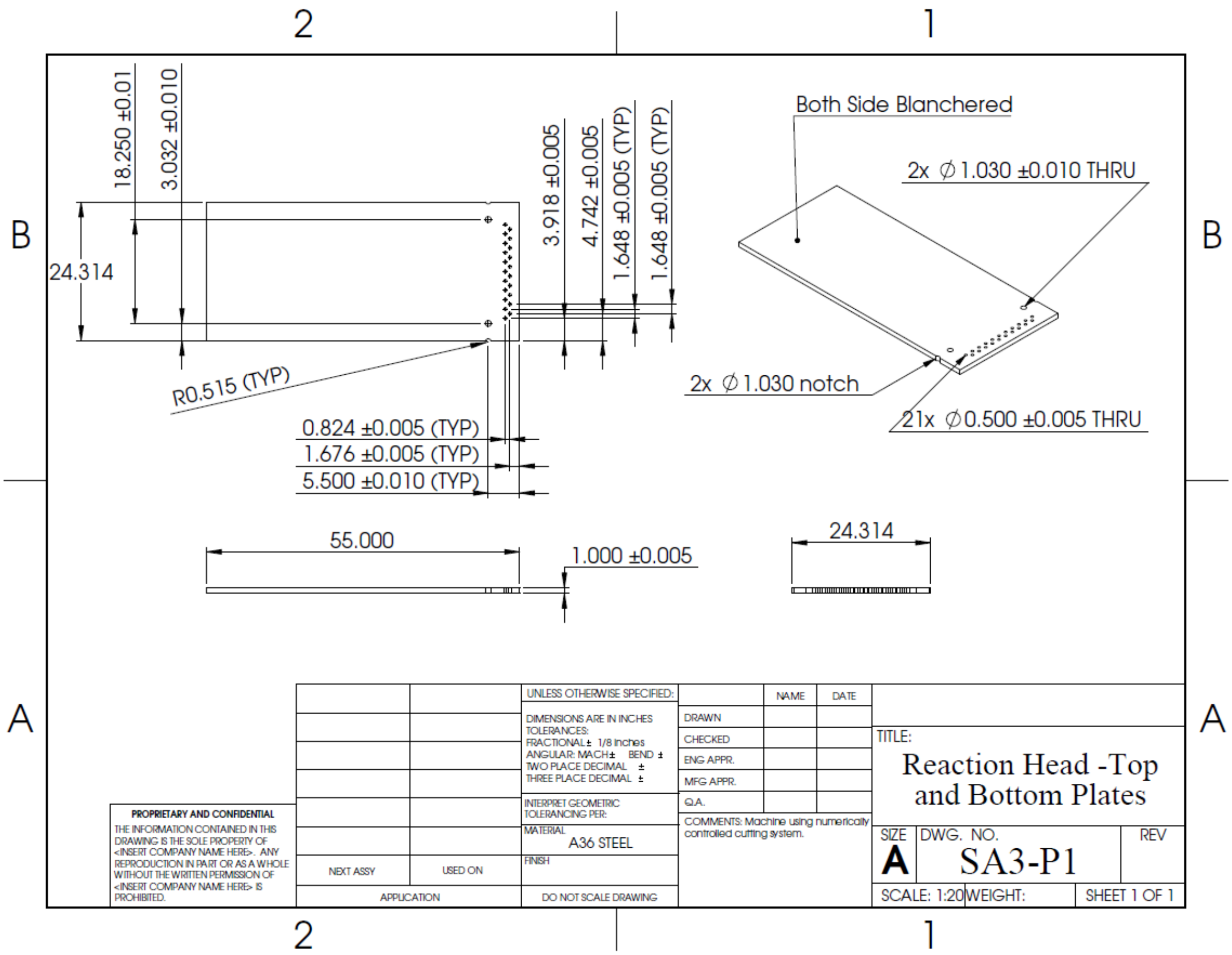

Figure A-11. Drawing of the reaction head—bottom plate (SA3-P1)

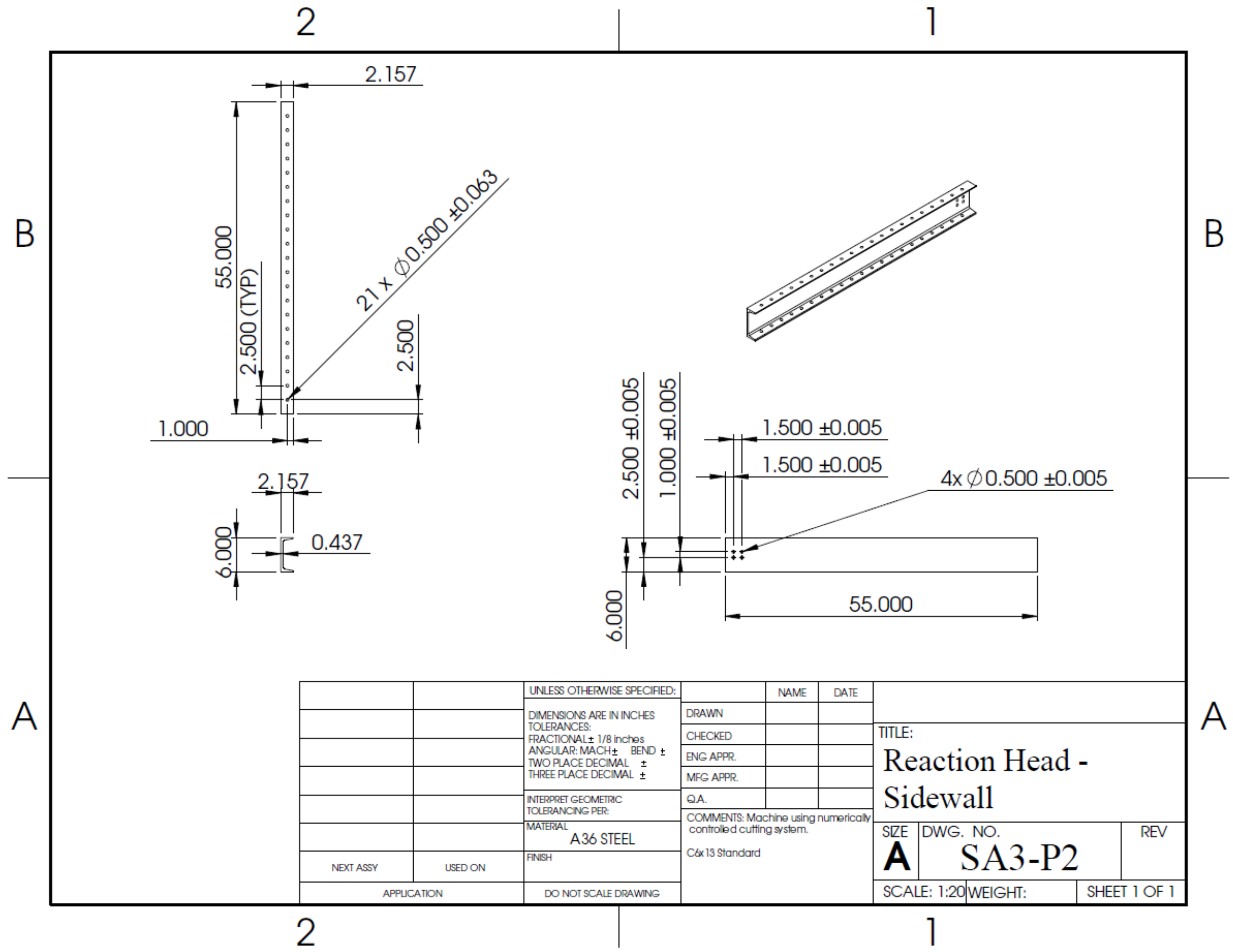

Figure A-12. Drawing of the reaction head—sidewall (SA3-P2)

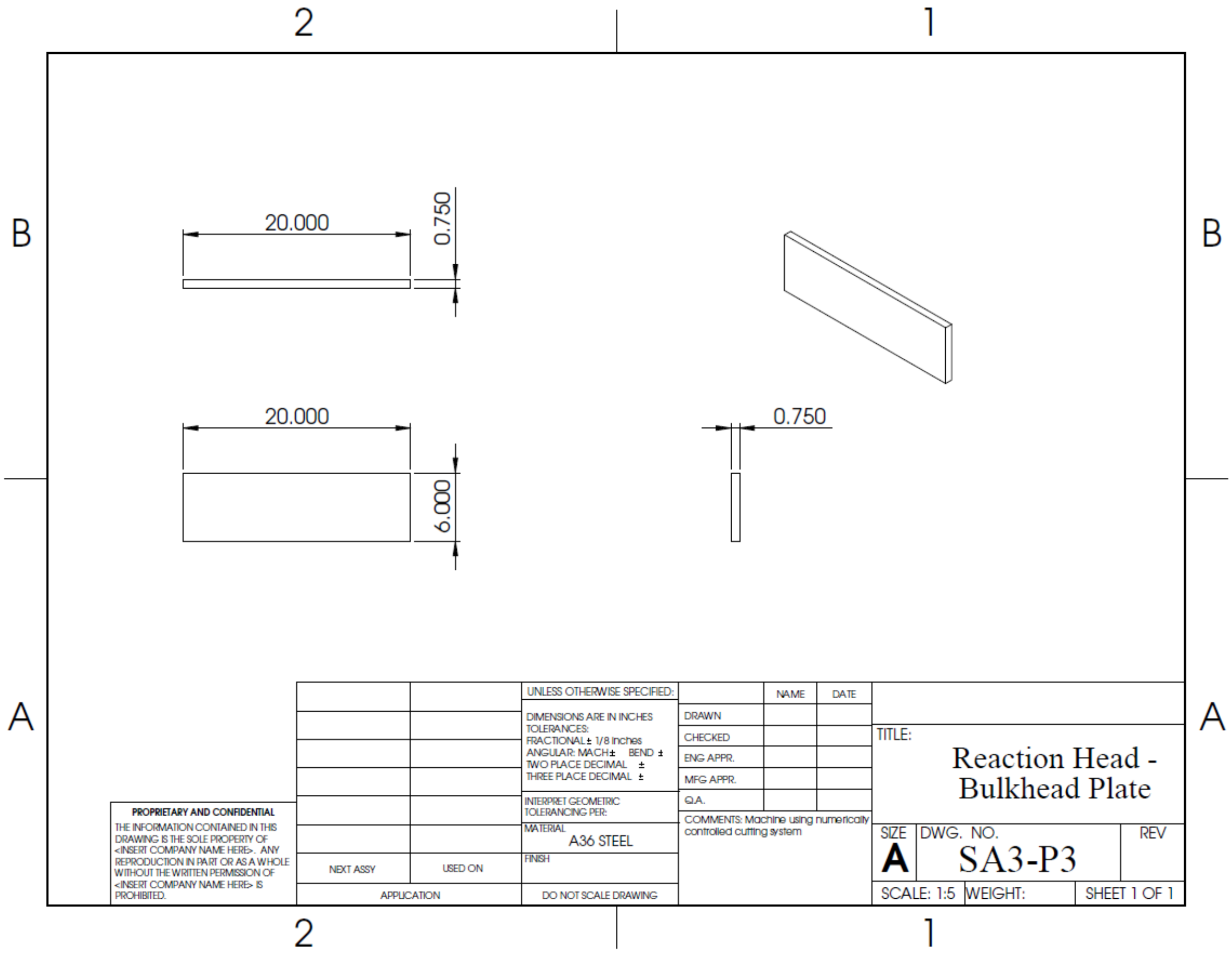

Figure A-13. Drawing of the reaction head—bulkhead plate (SA3-P3)

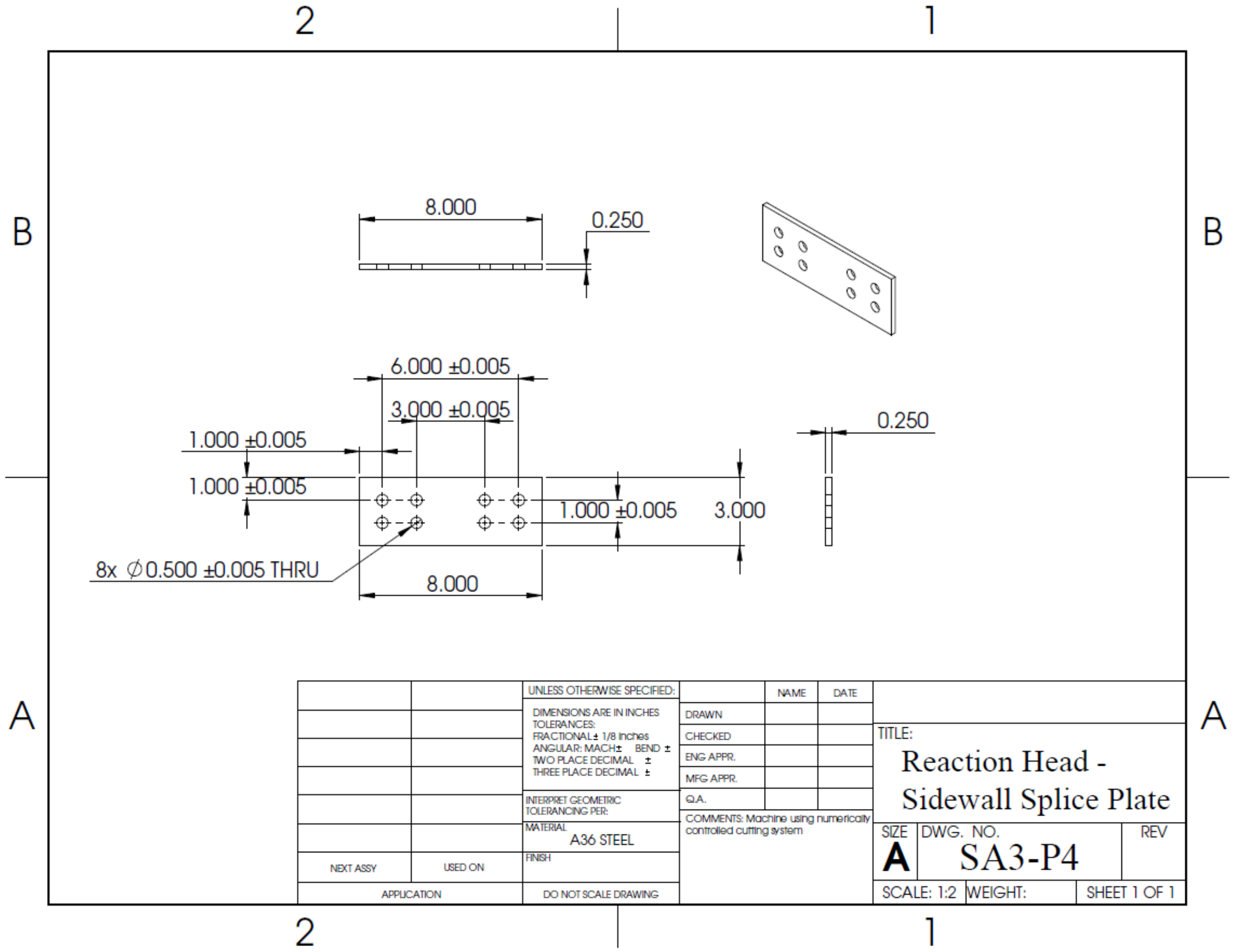

Figure A-14. Drawing of the reaction head—sidewall splice plate (SA3-P4)

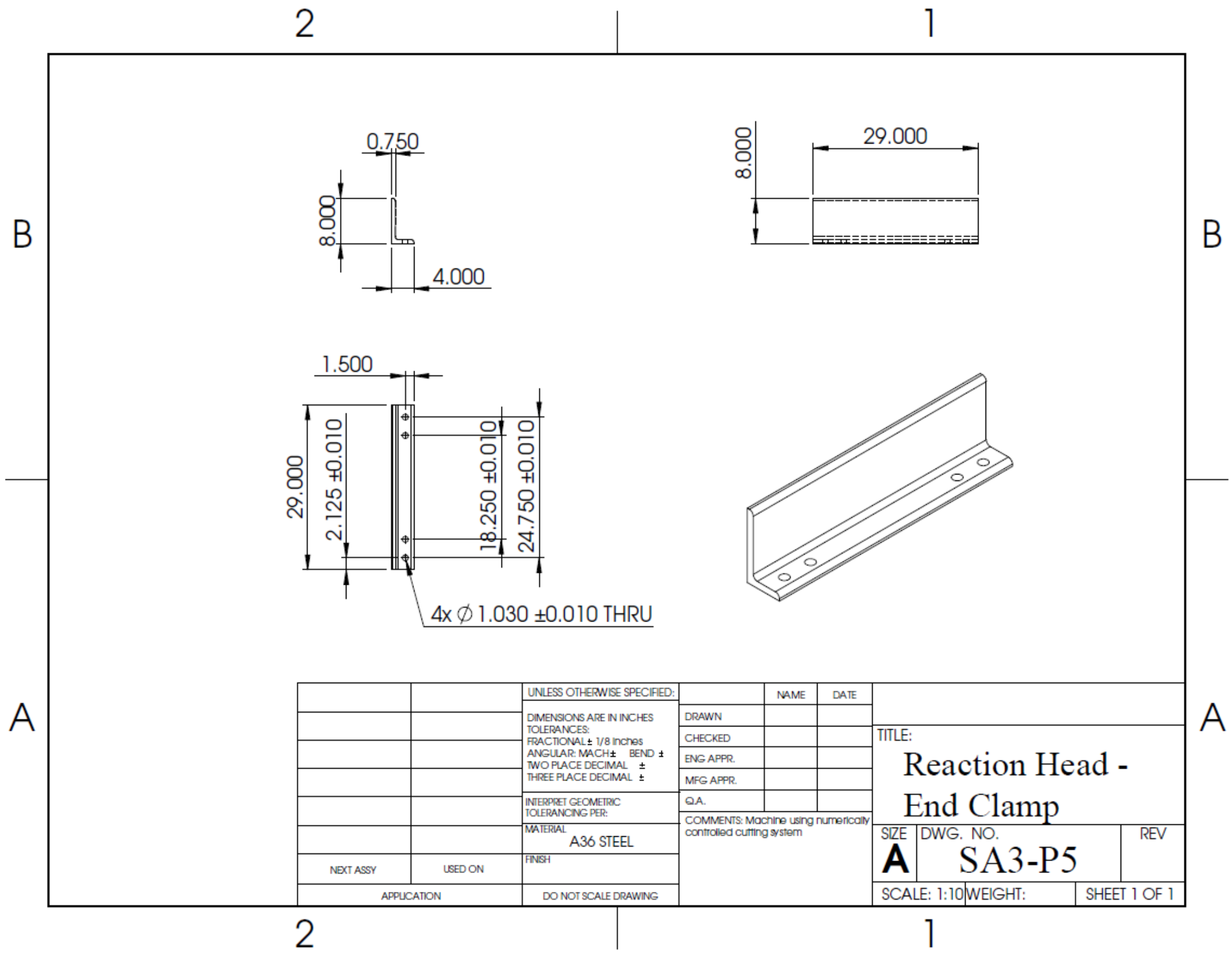

Figure A-15. Drawing of the reaction head—end clamp (SA3-P5)

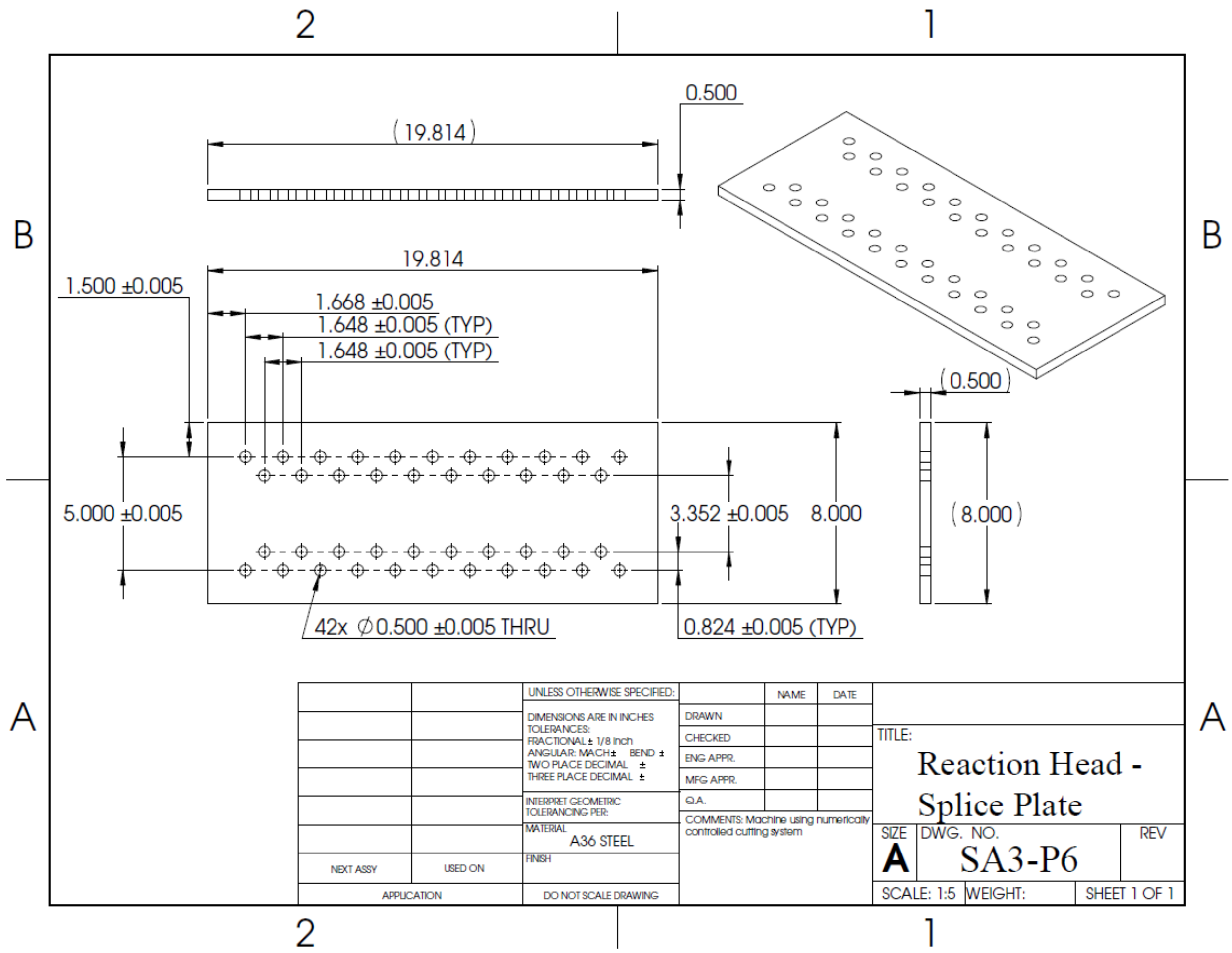

Figure A-16. Drawing of the reaction head—splice plates (SA3-P6)

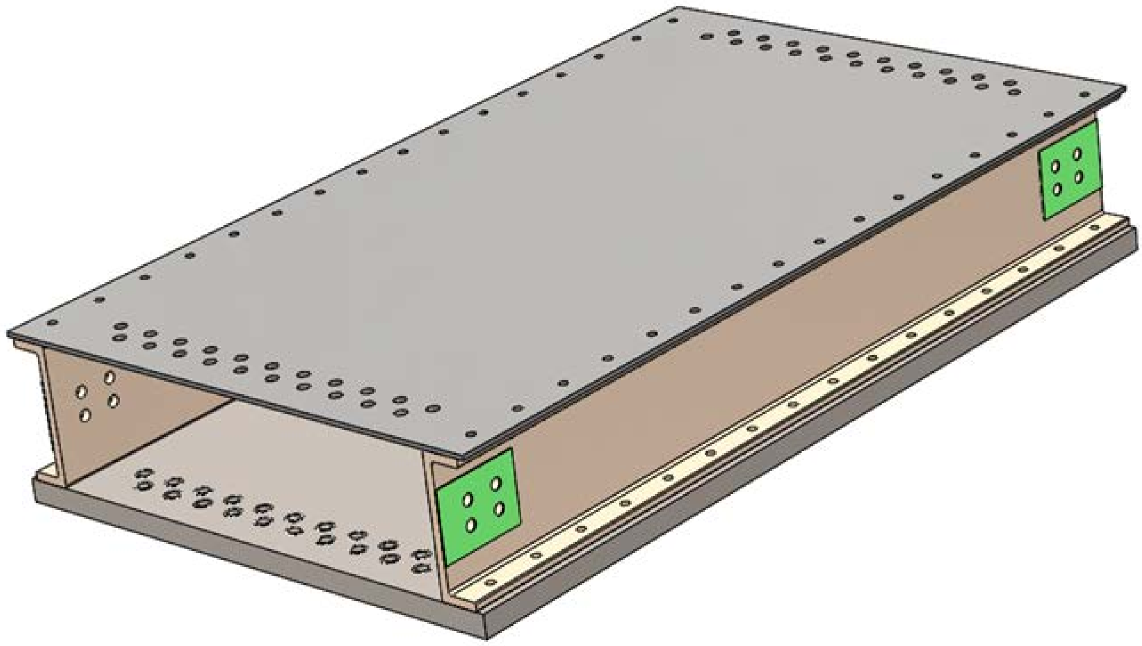

Figure A-17. 3-D model of the wingbox (SA4)

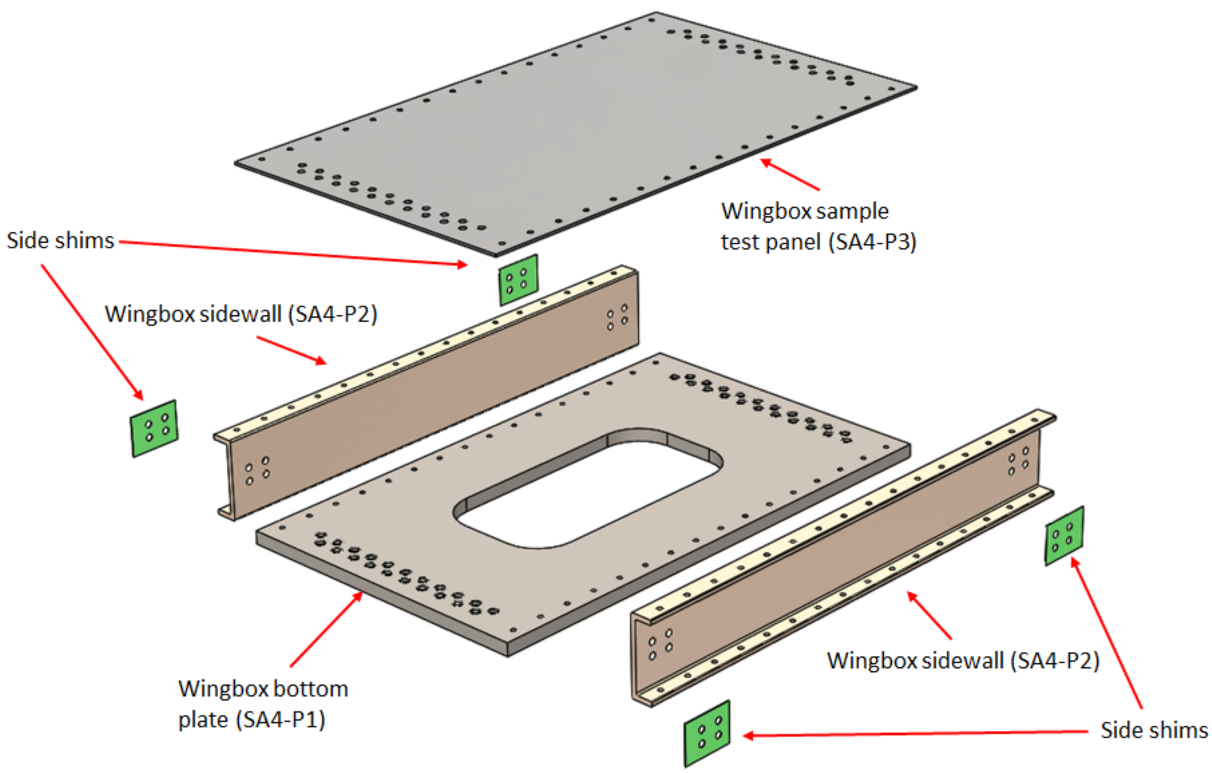

Figure A-18. Exploded view of the wingbox (SA4)

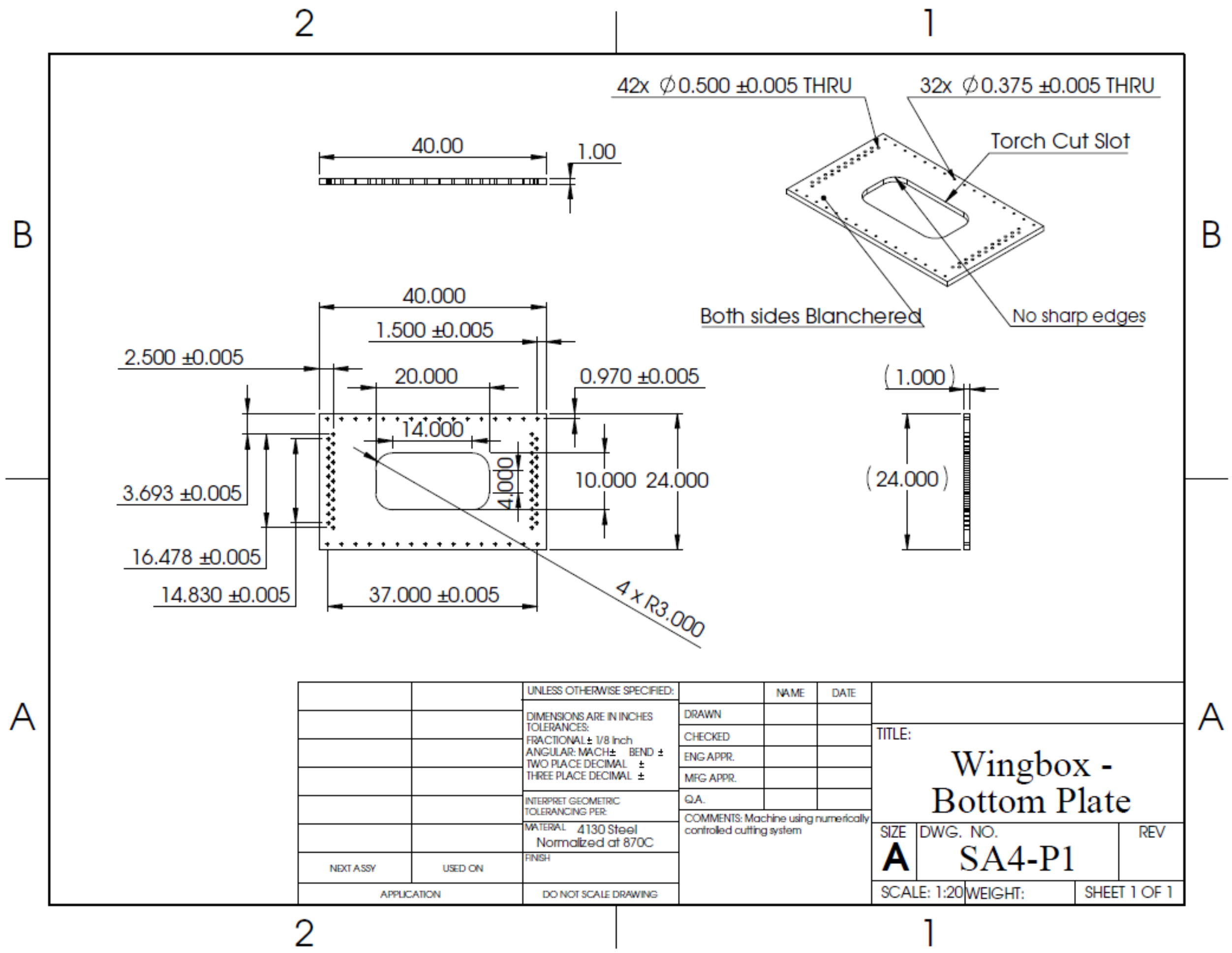

Figure A-19. Drawing of the wingbox—bottom plate (SA4-P1)

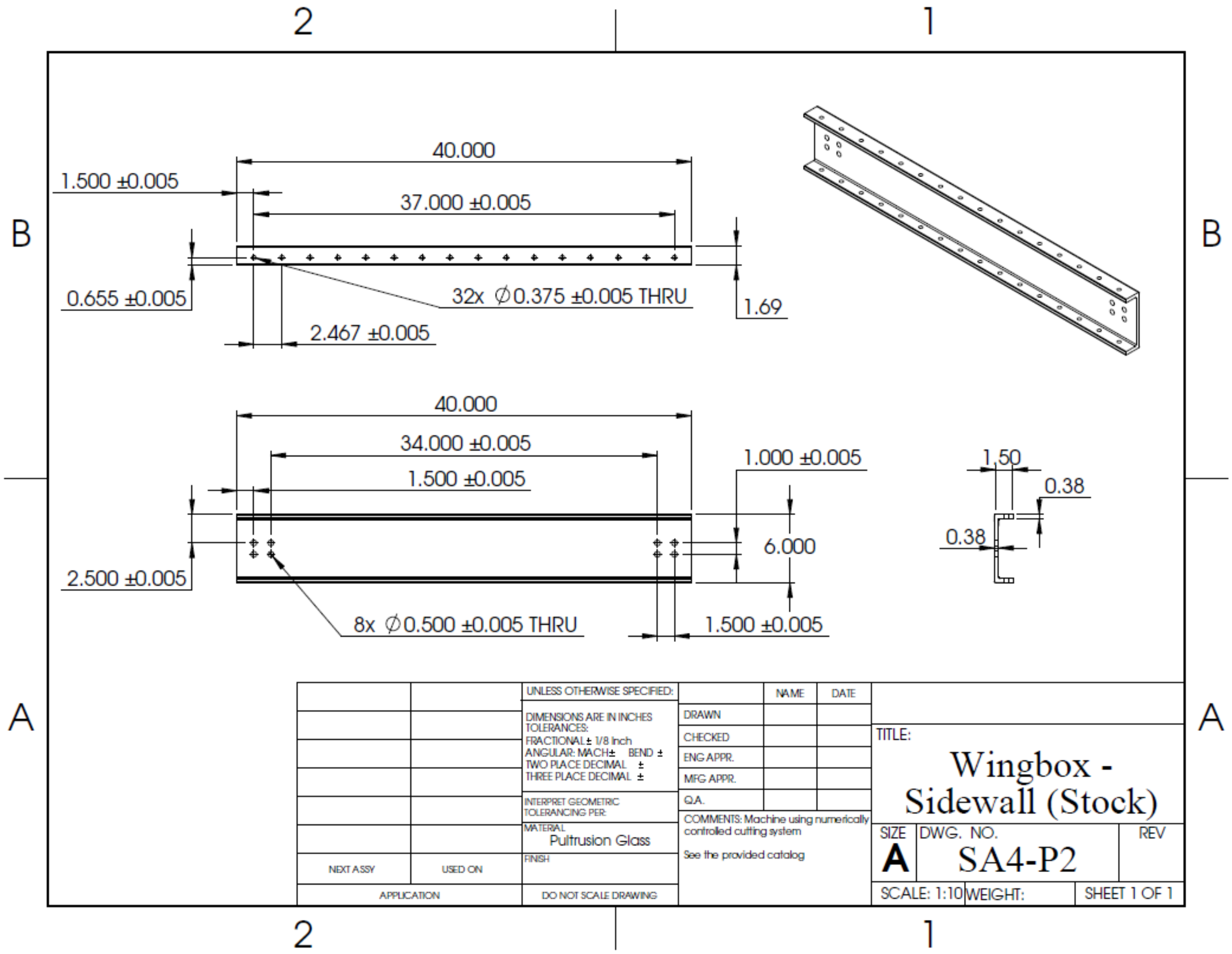

Figure A-20. Drawing of the wingbox—sidewalls (SA4-P2)

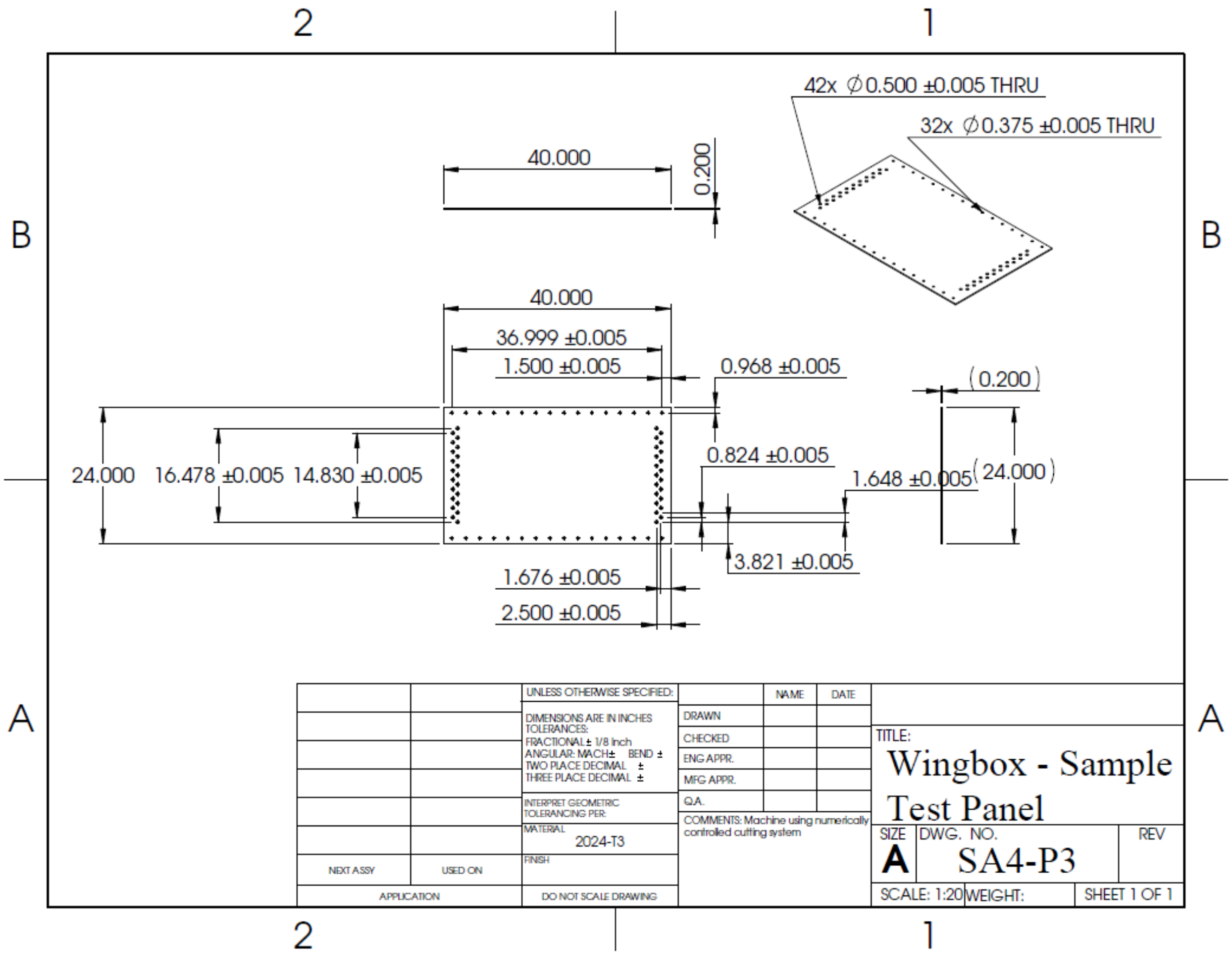

Figure A-21. Drawing of the wingbox—sample test panel (SA4-P3)

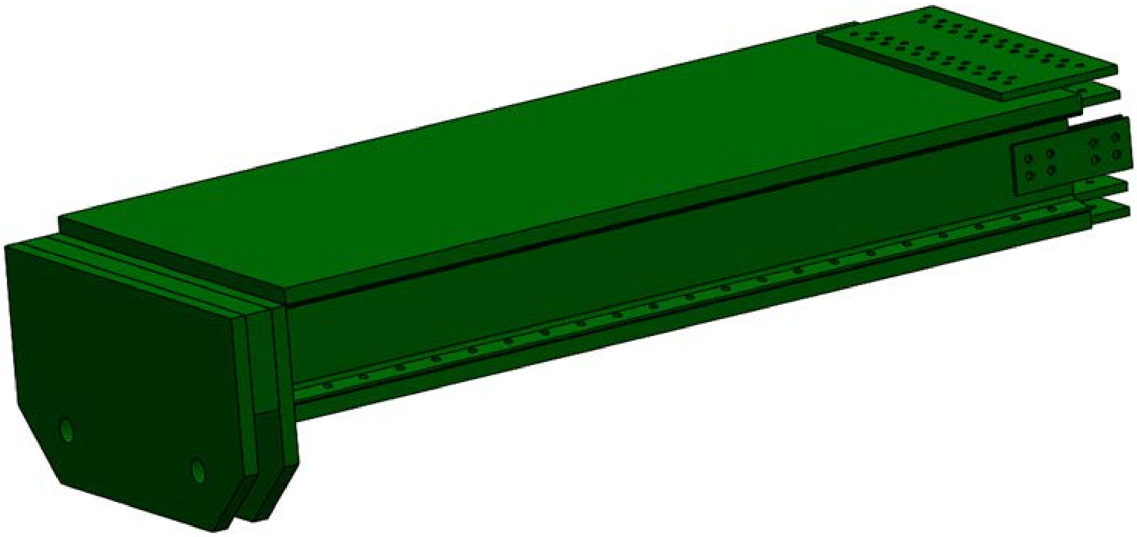

Figure A-22. 3-D model of the loading head (SA5)

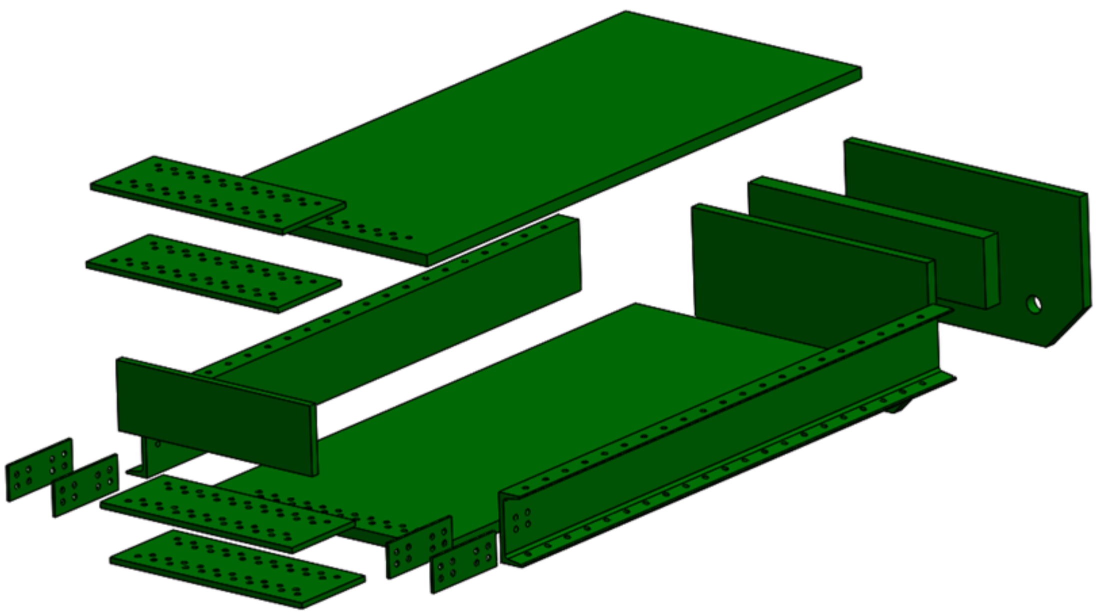

Figure A-23. Exploded view of the loading head (SA5)

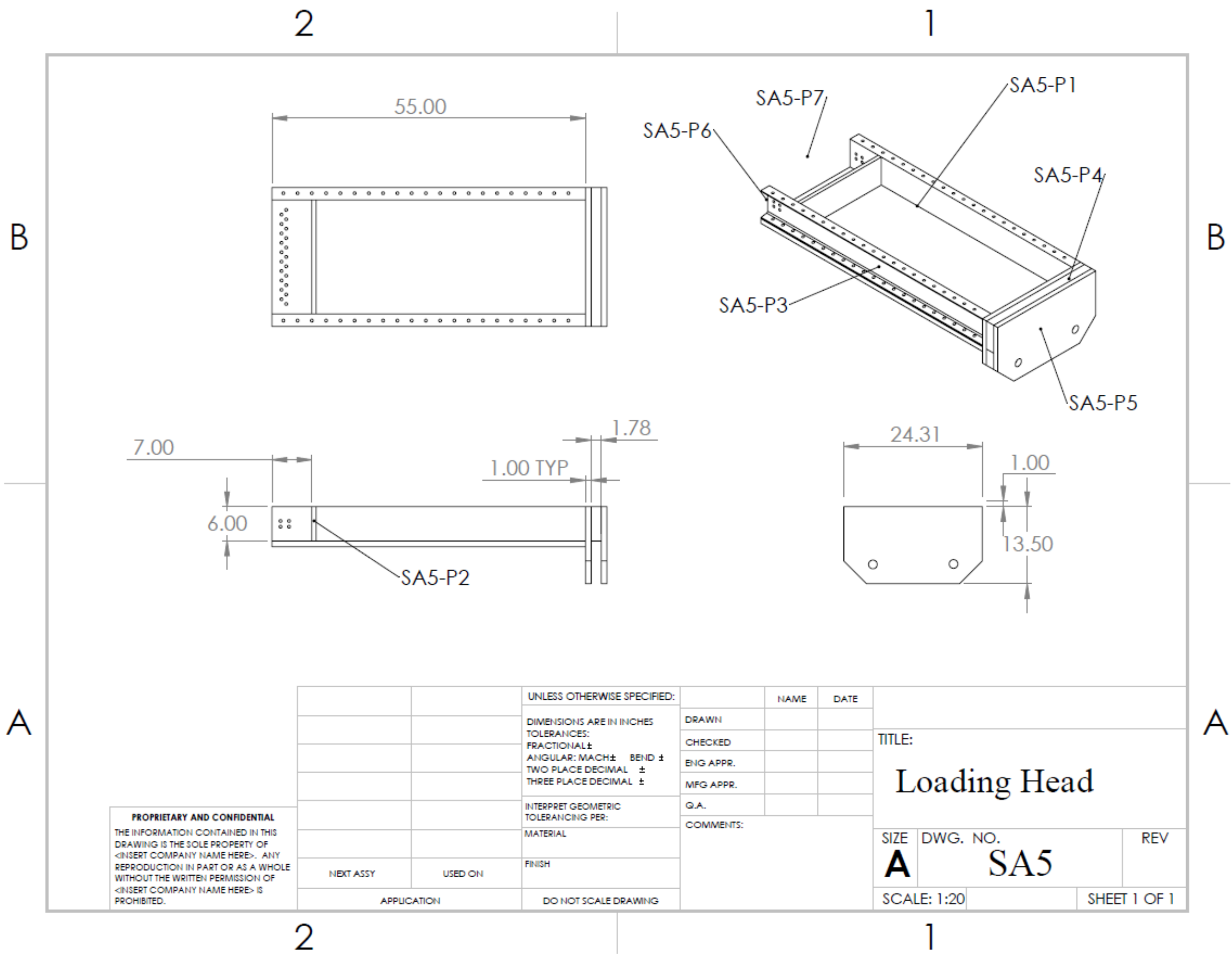

Figure A-24. Drawing of the loading head (SA5)

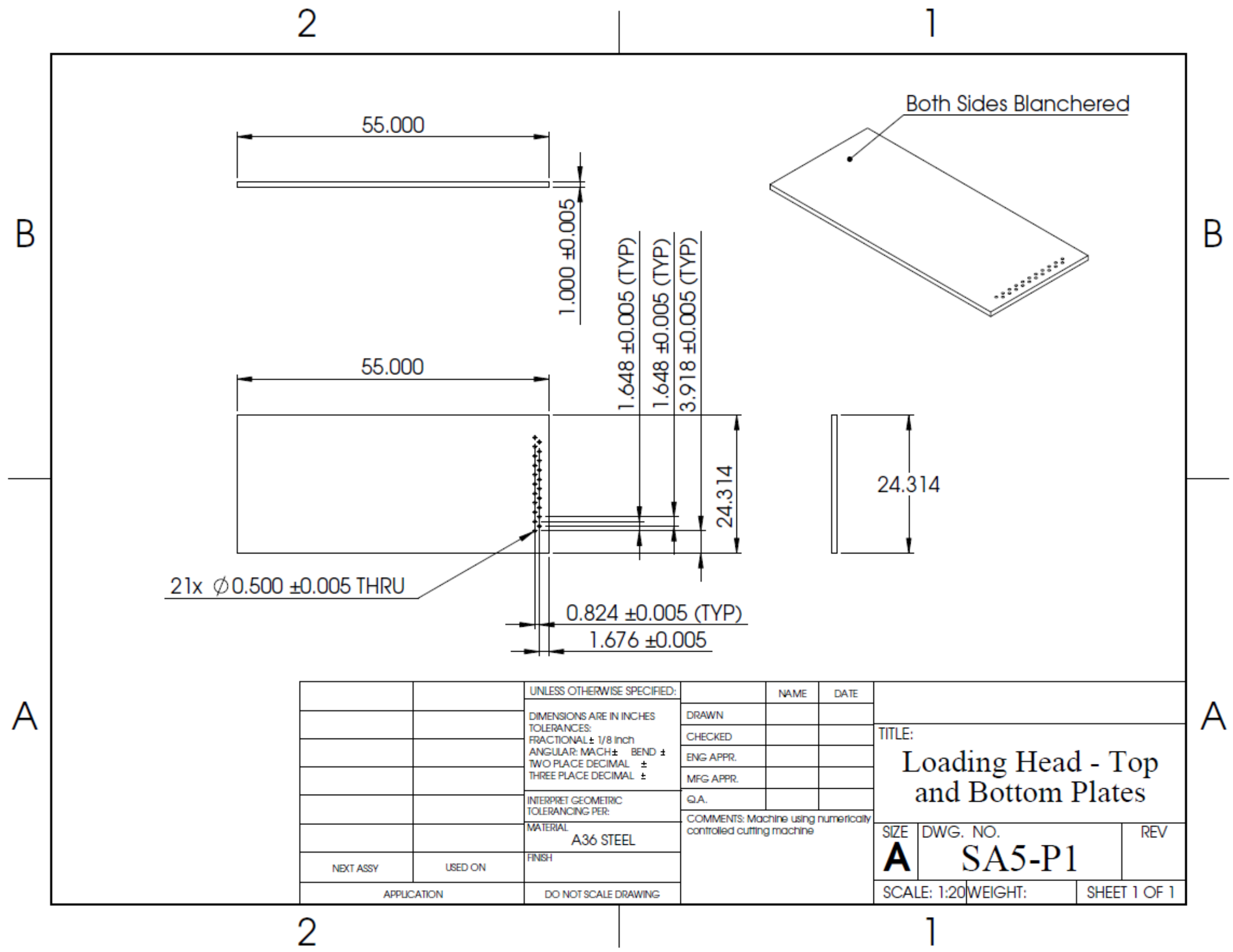

Figure A-25. Drawing of the loading head—top and bottom plates (SA5-P1)

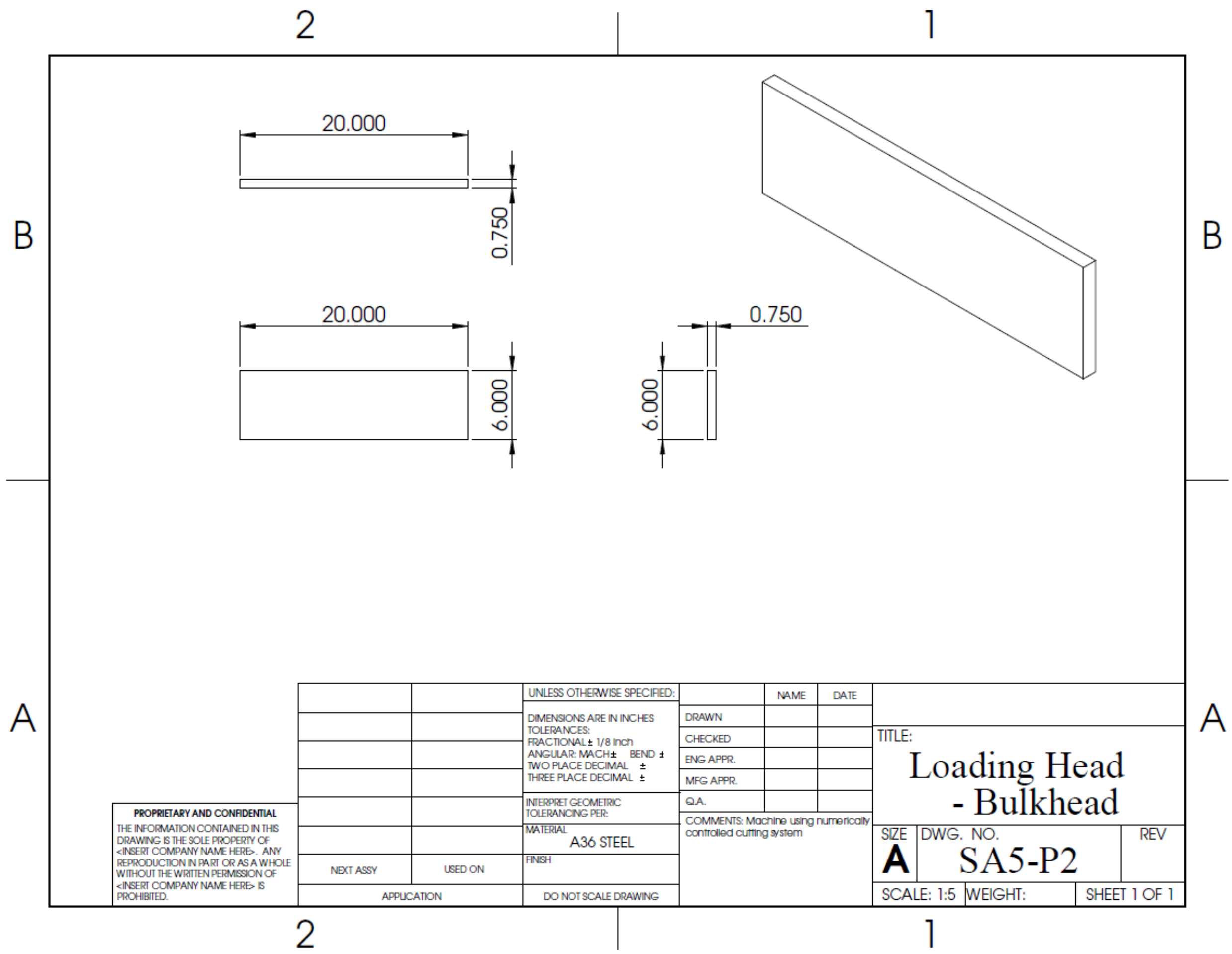

Figure A-26. Drawing of the loading head—bulkhead (SA5-P2)

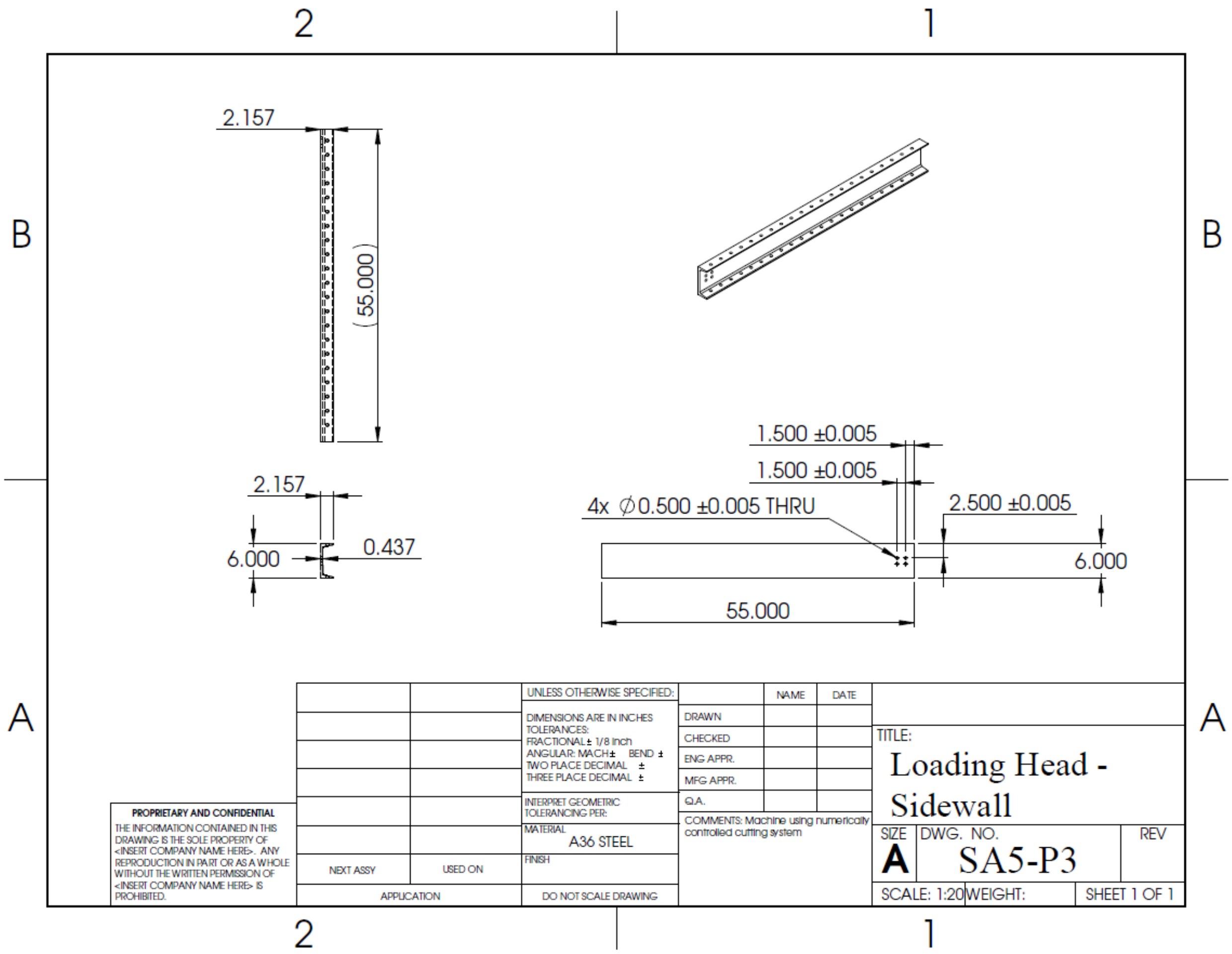

Figure A-27. Drawing of the loading head—sidewall (SA5-P3)

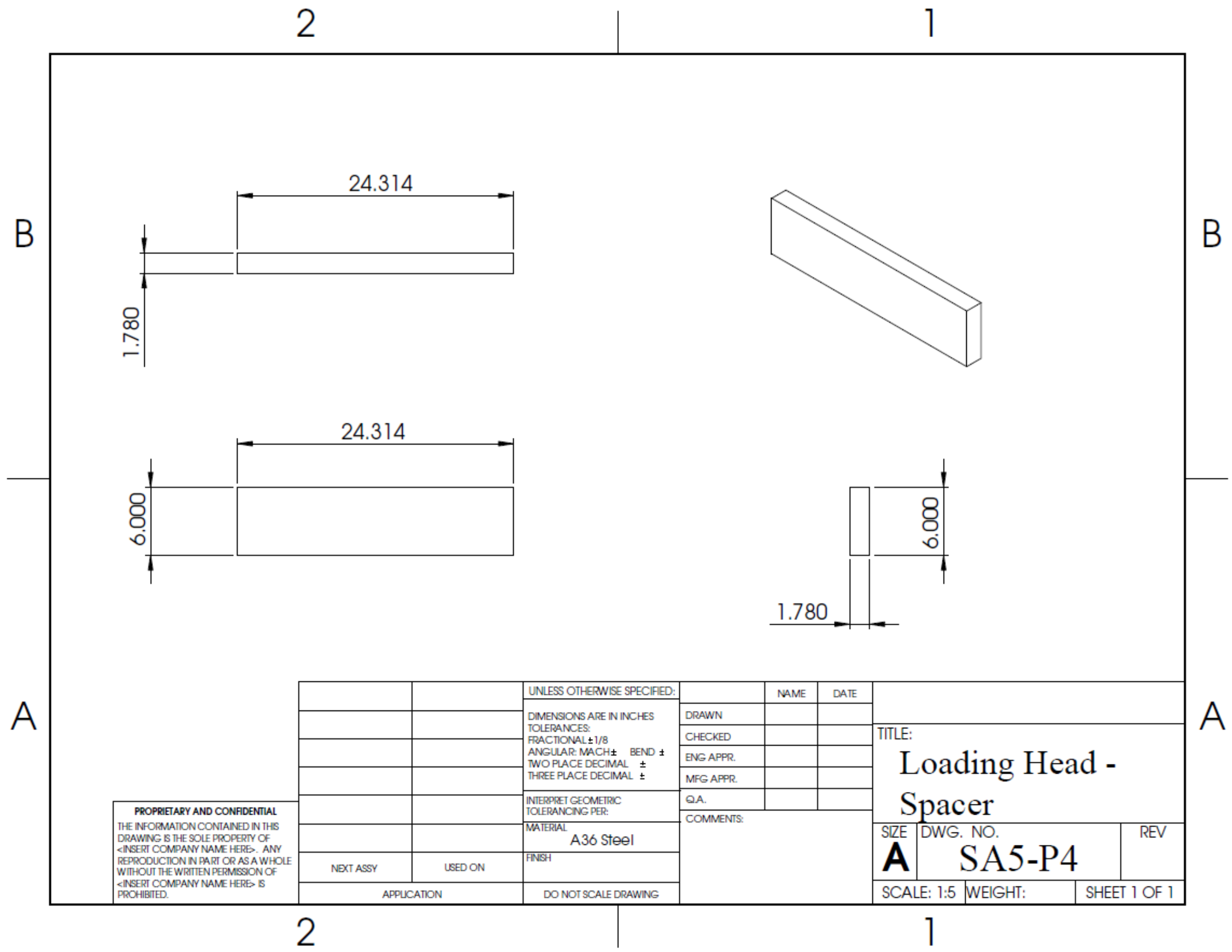

Figure A-28. Drawing of the loading head—spacer (SA5-P4)

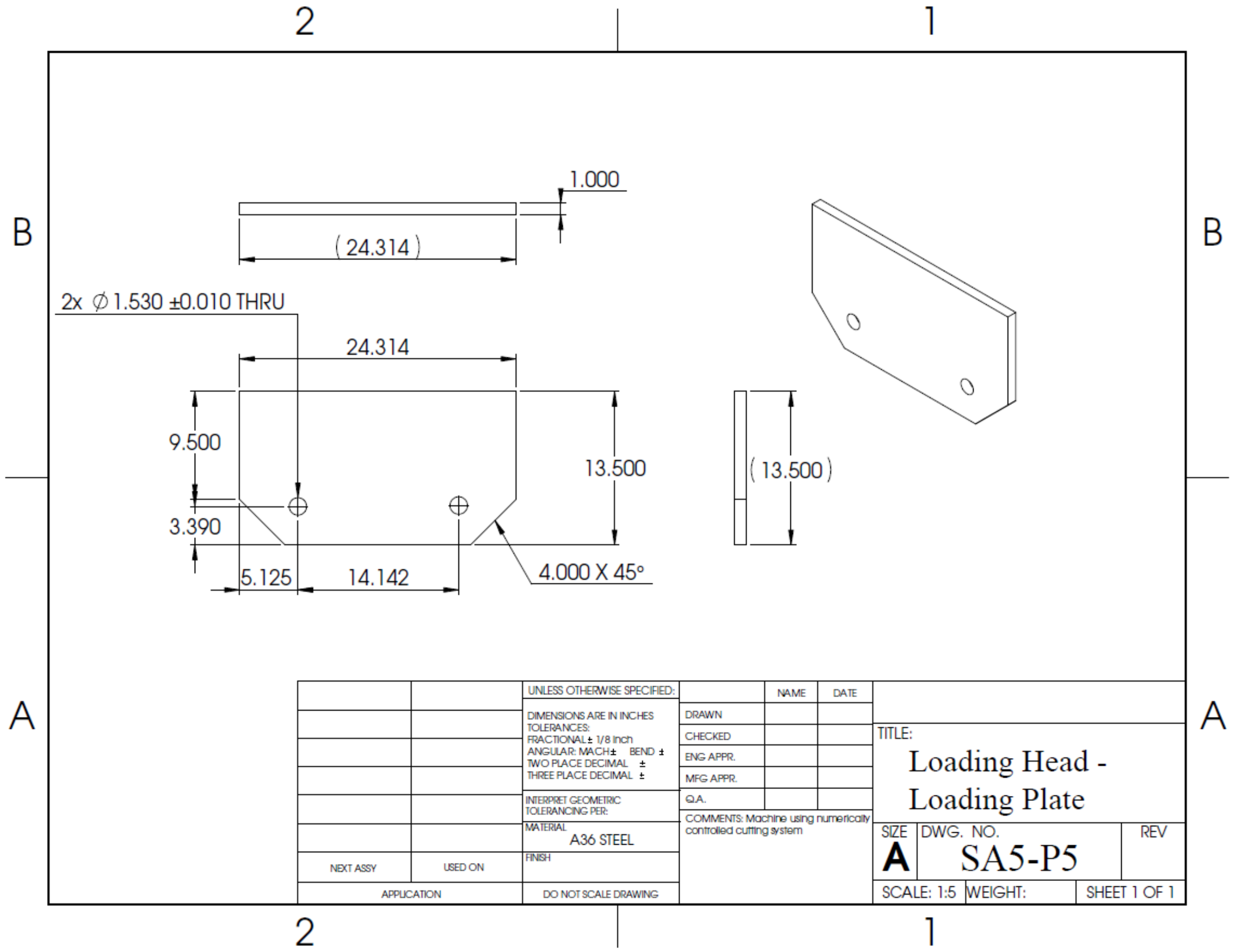

Figure A-29. Drawing of the loading head—loading plate (SA5-P5)

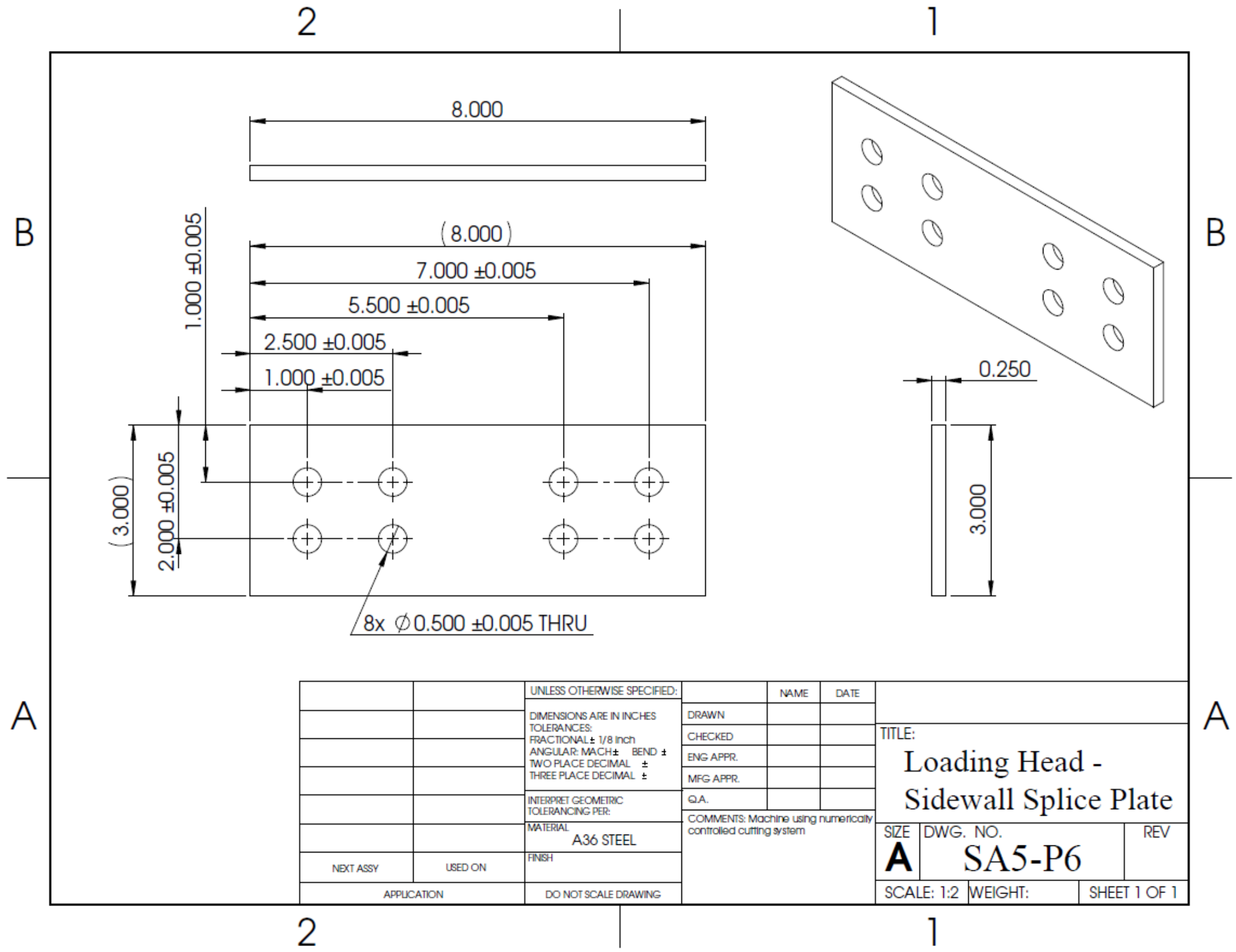

Figure A-30. Drawing of the loading head—sidewall splice plate (SA5-P6)

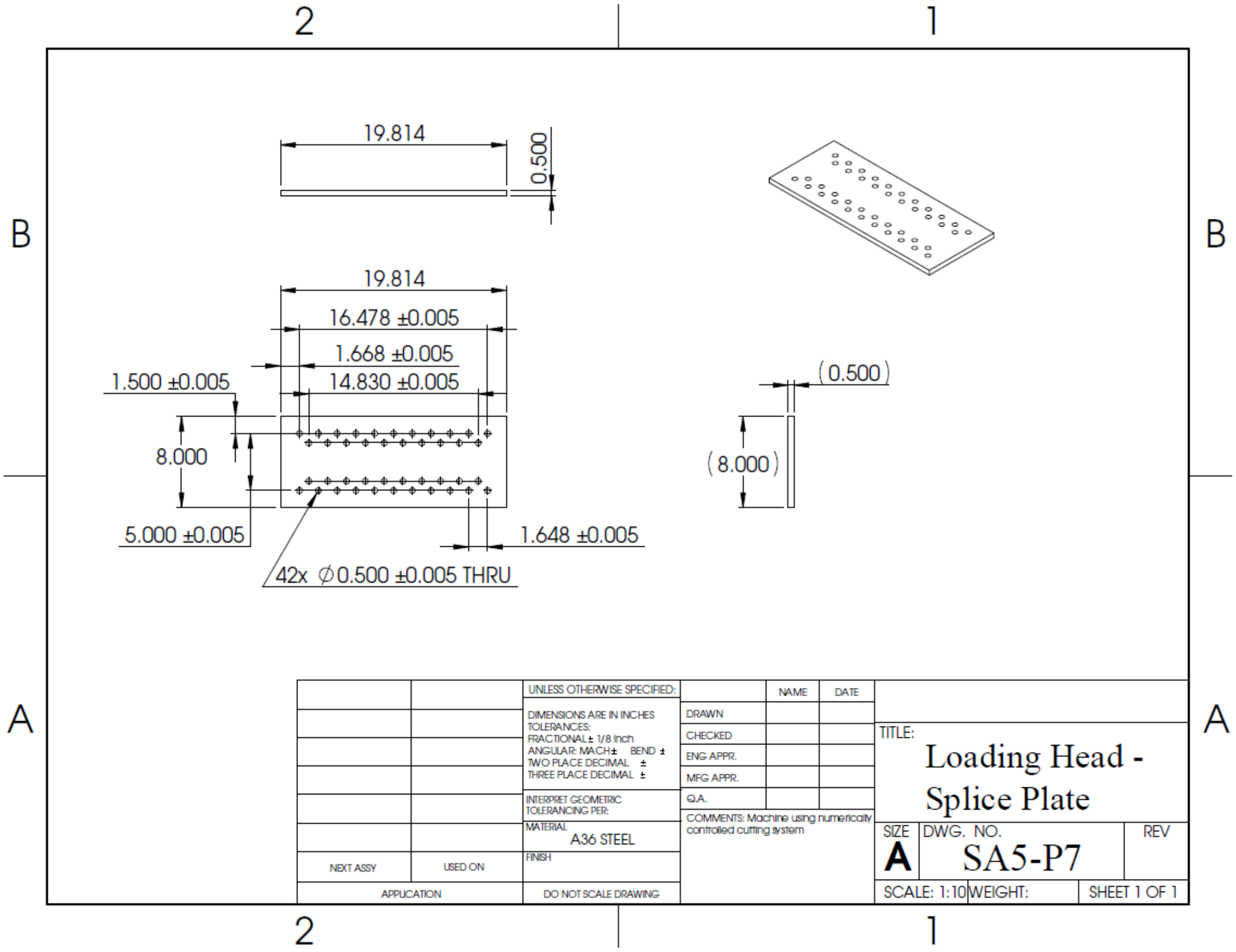

Figure A-31. Drawing of the loading head—splice plate (SA5-P7)

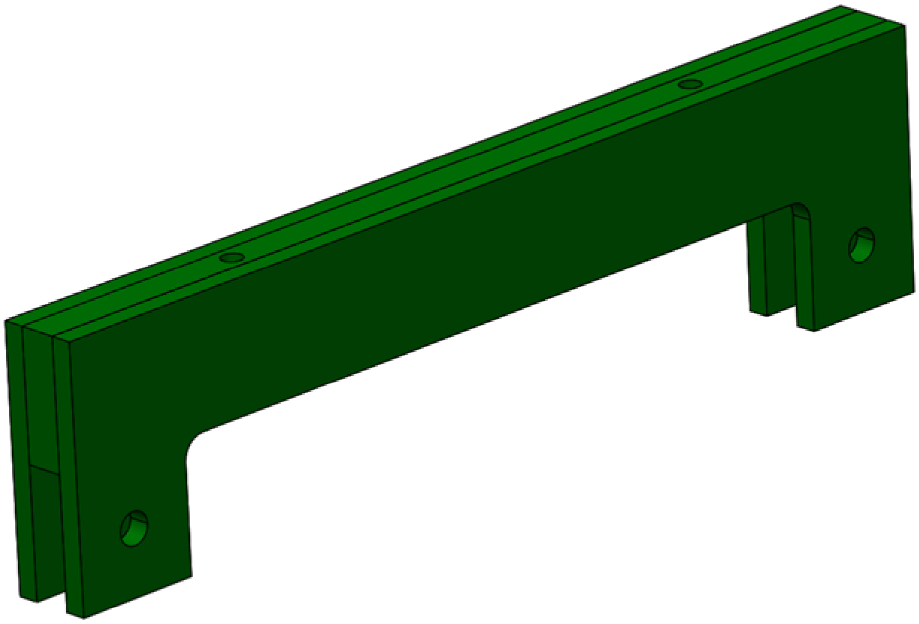

Figure A-32. 3-D model of the hoodoly assembly (SA6)

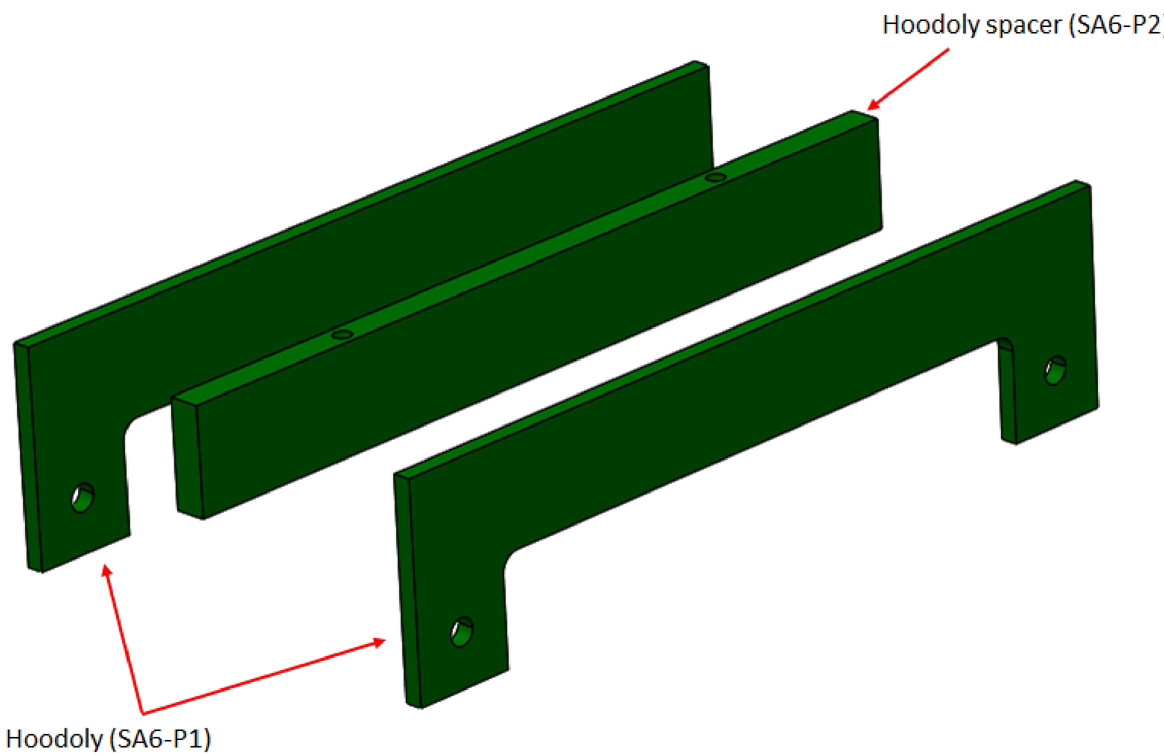

Figure A-33. Exploded view of the hoodoly assembly (SA6)

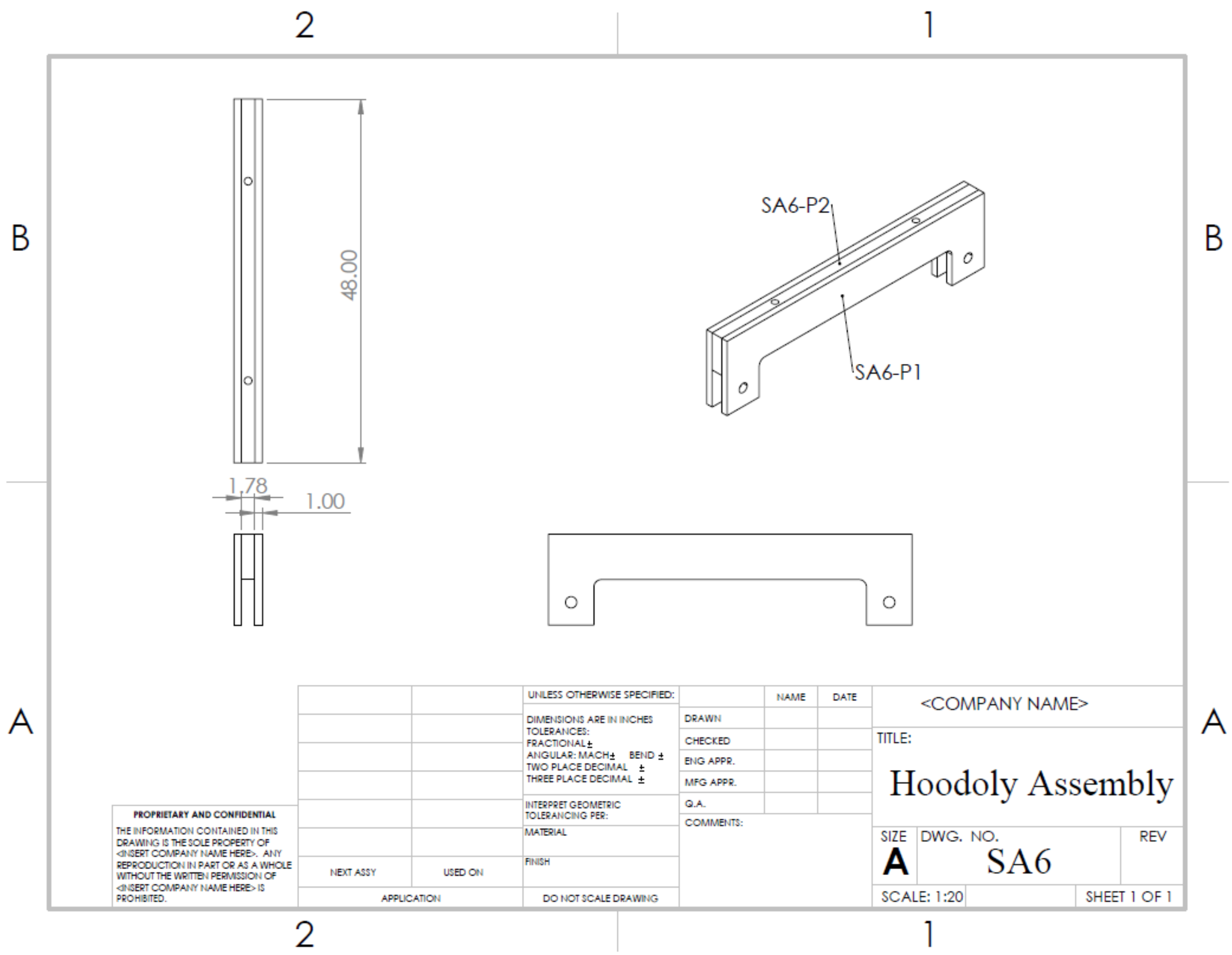

Figure A-34. Drawing of the hoodoly assembly (SA6)

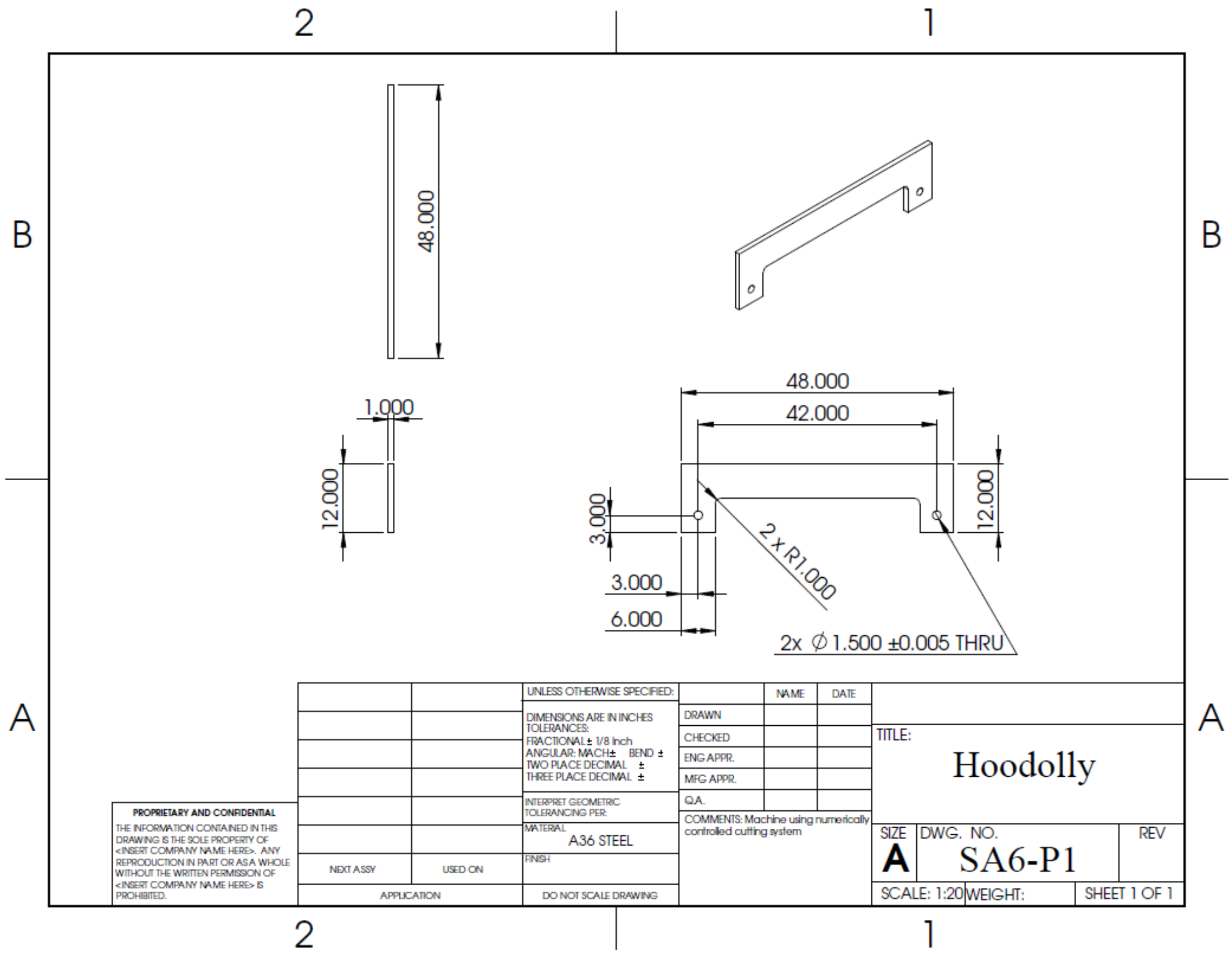

Figure A-35. Drawing of the hoodoly (SA6-P1)

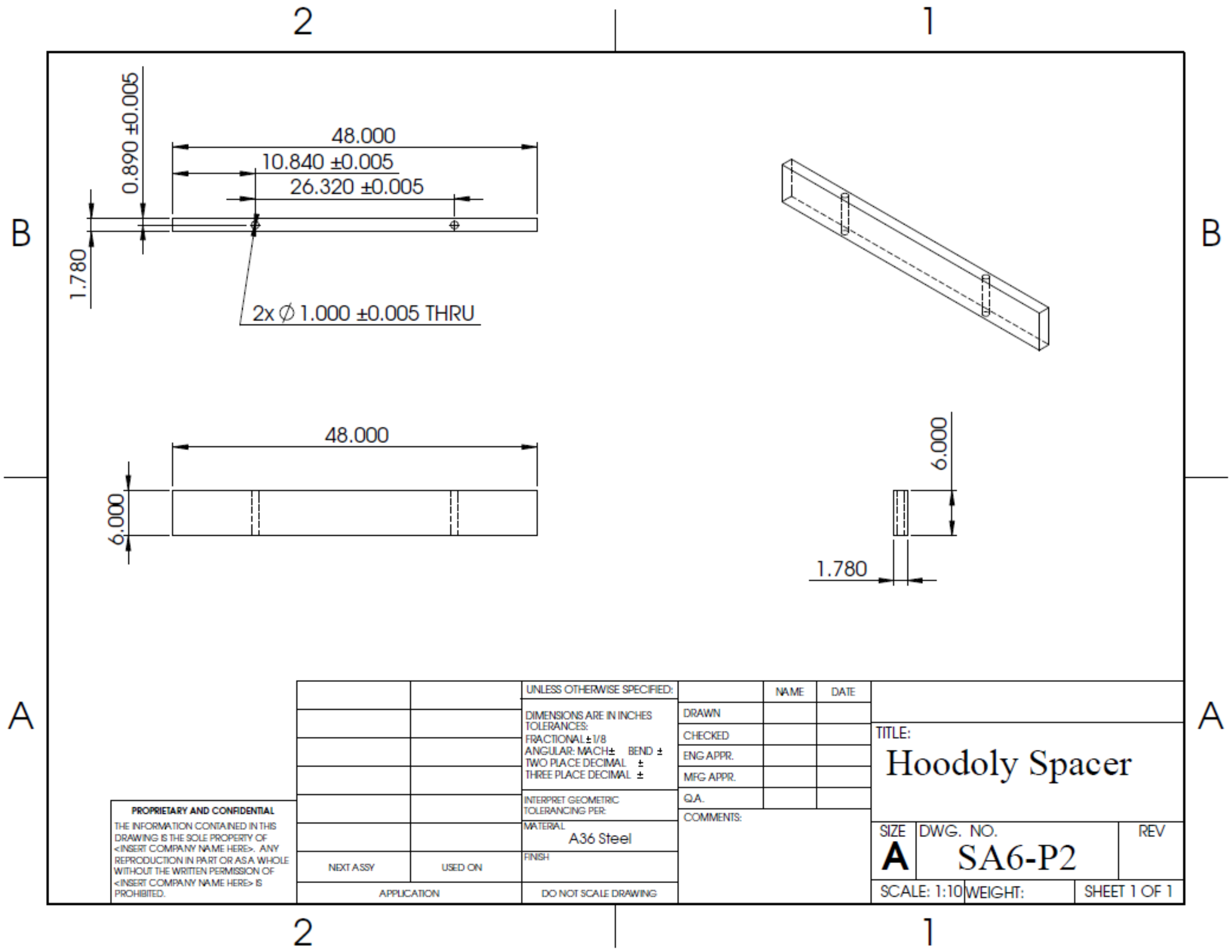

Figure A-36. Drawing of the hoodoly—spacer (SA6-P2)

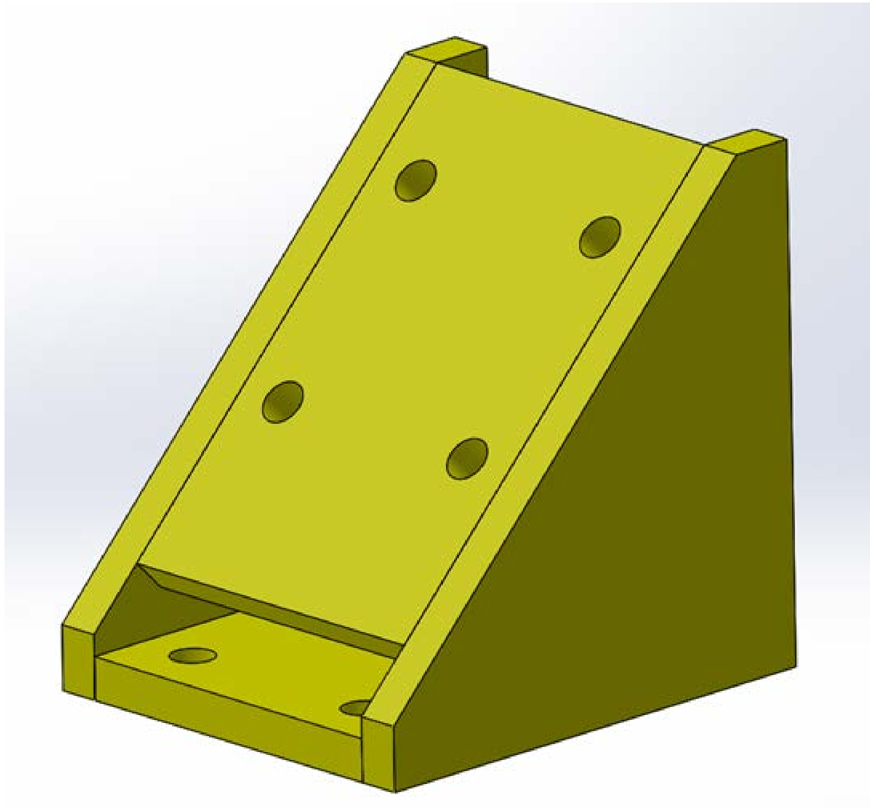

Figure A-37. 3-D model of the wedge mount (SA7)

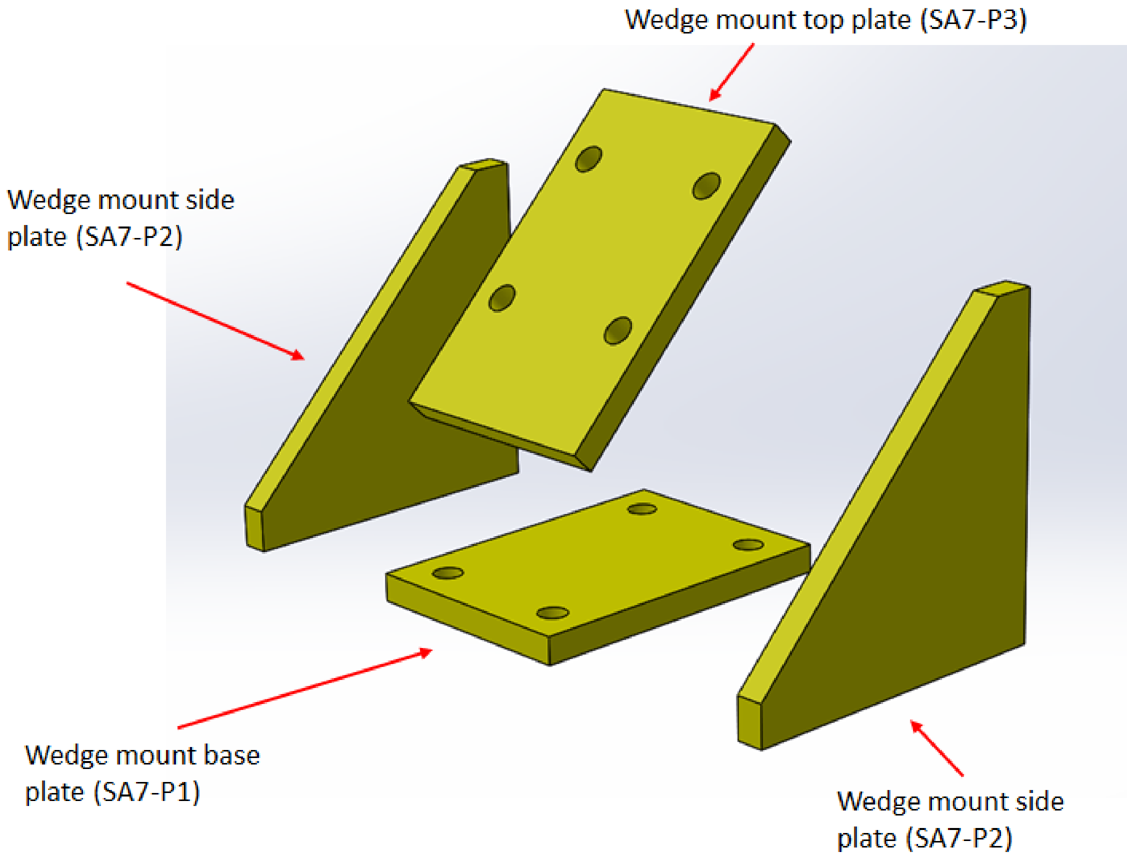

Figure A-38. Exploded view of the wedge mount (SA7)

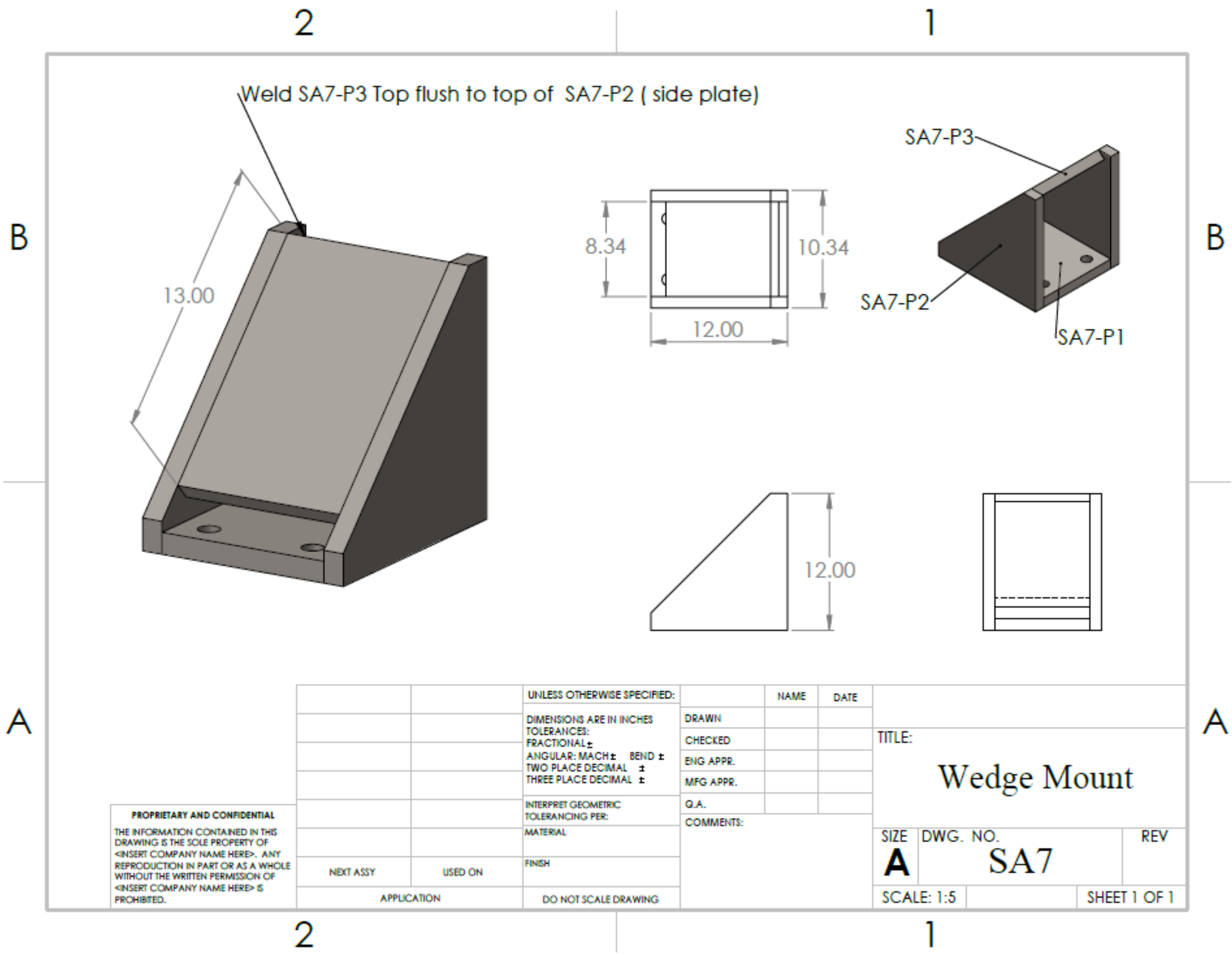

Figure A-39. Drawing of the wedge mount (SA7)

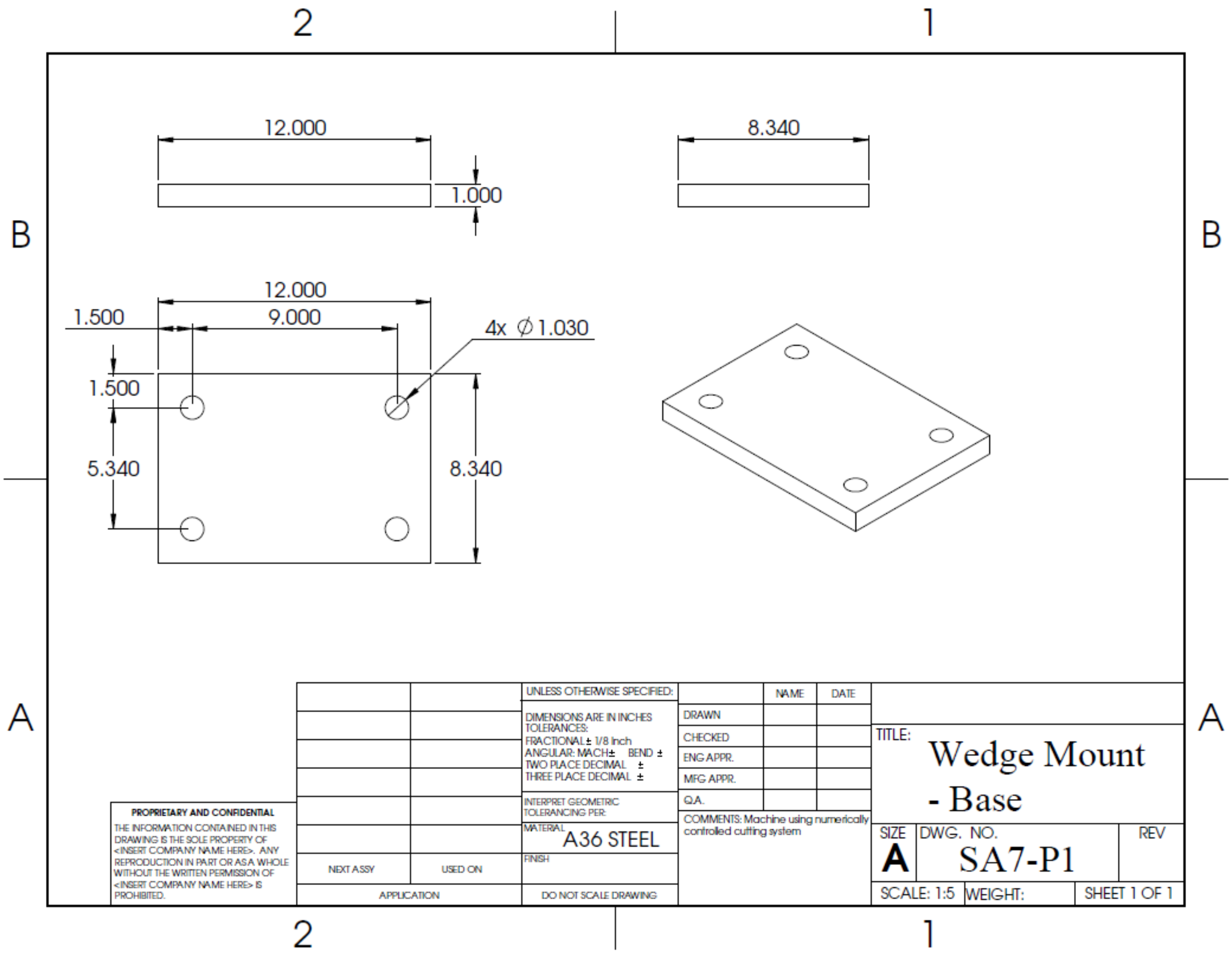

Figure A-40. Drawing of the wedge mount—base (SA7-P1)

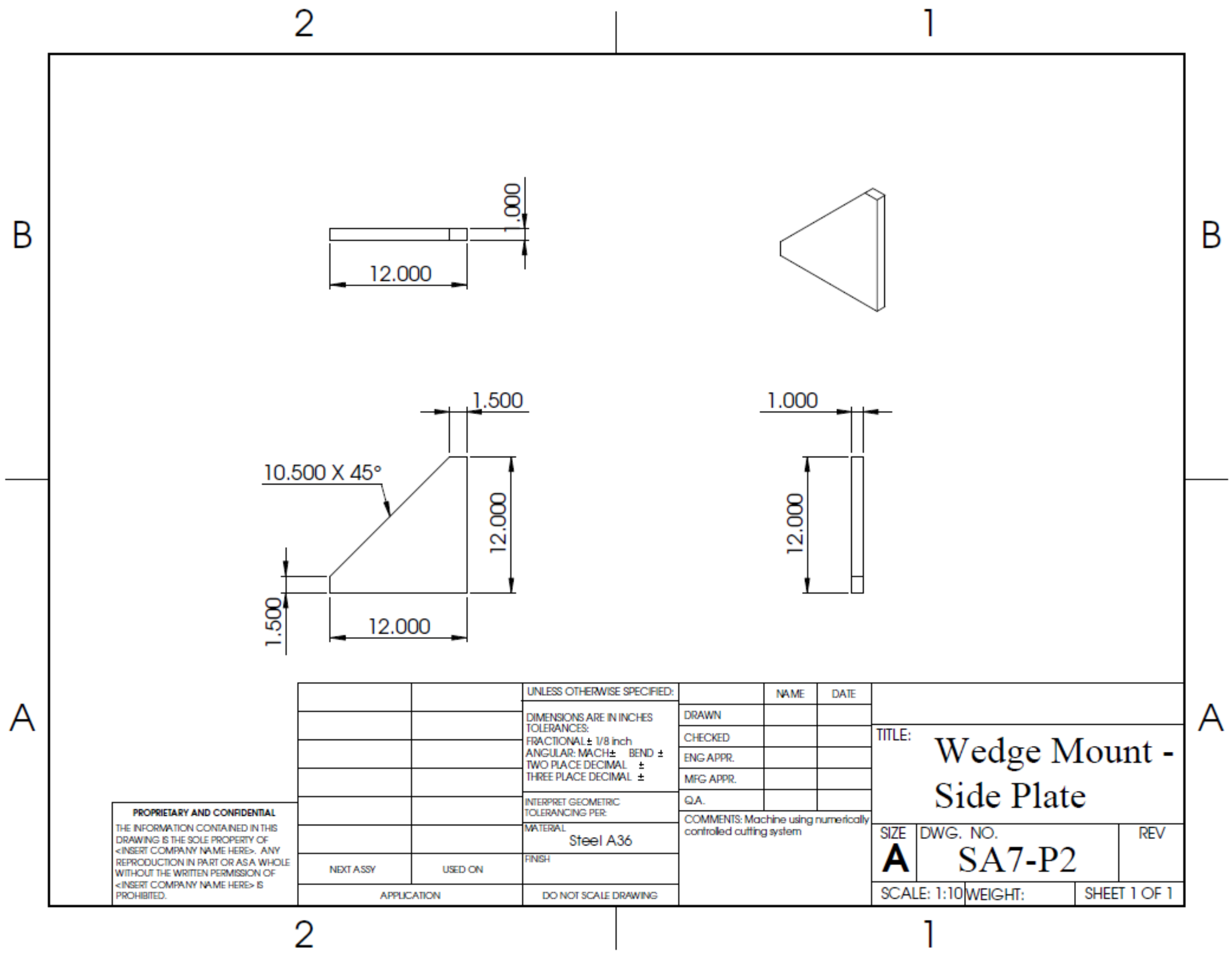

Figure A-41. Drawing of the wedge mount—side plates (SA7-P2)

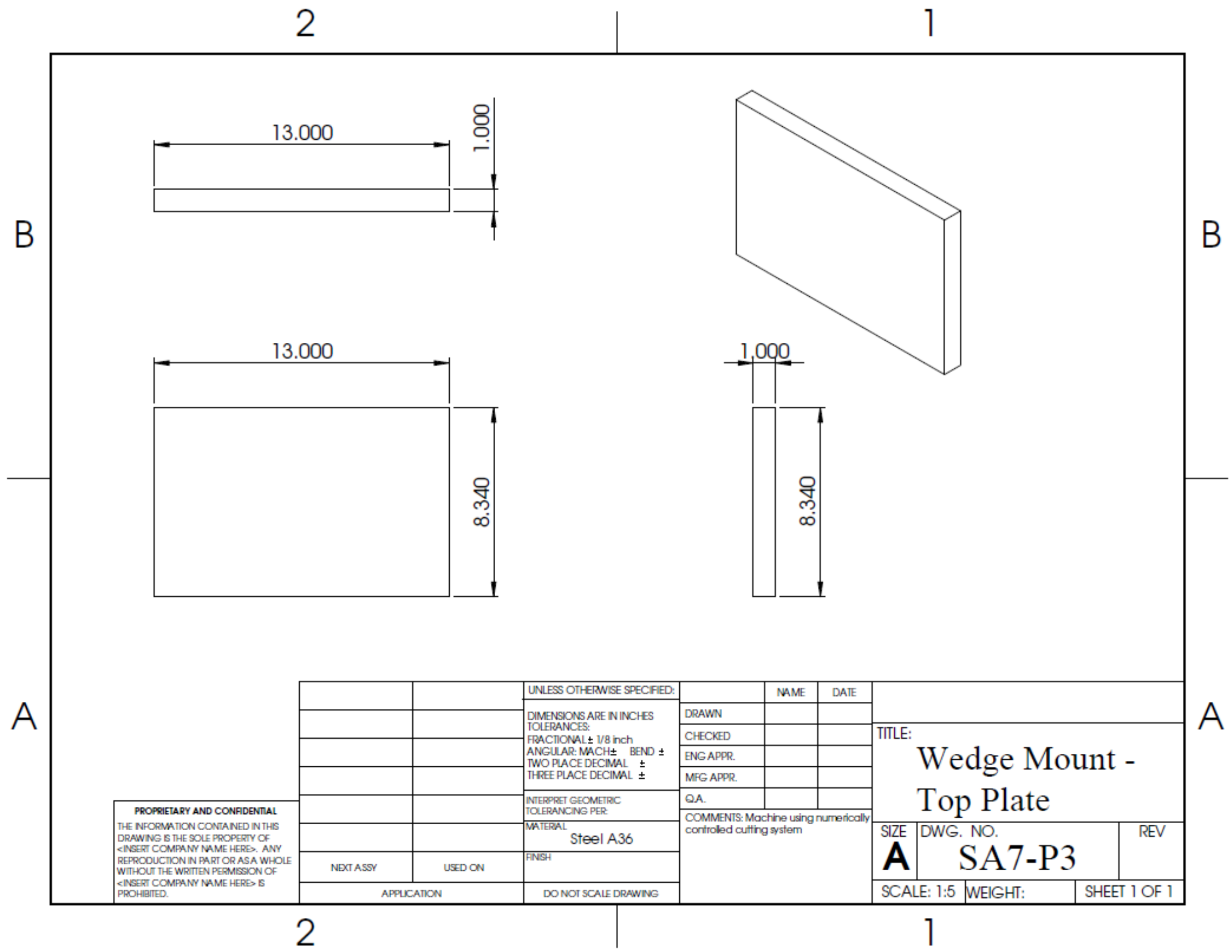

Figure A-42. Drawing of the wedge mount—top plate (SA7-P3)

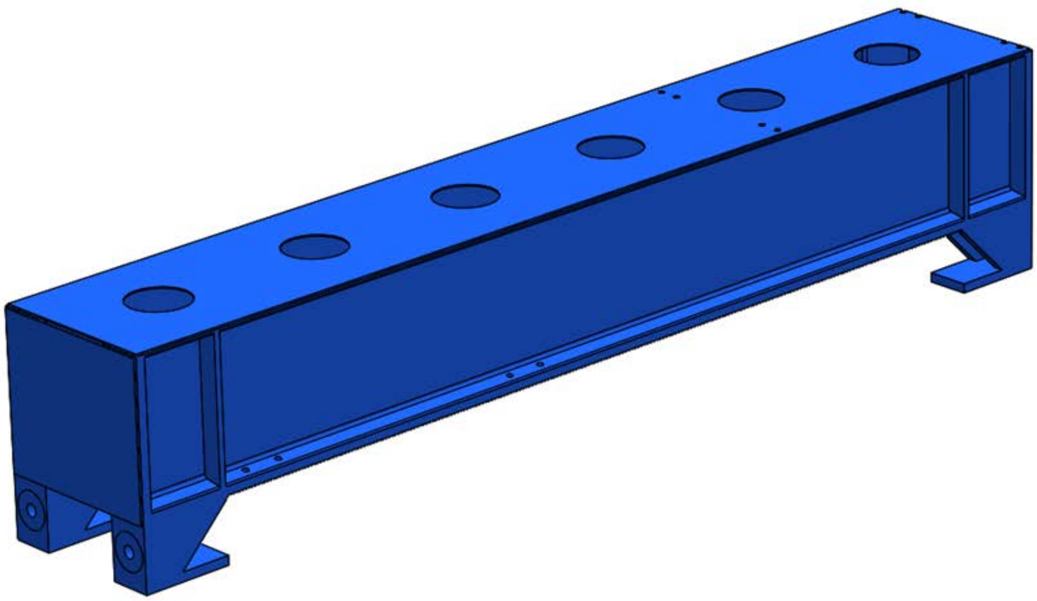

Figure A-43. 3-D model of the base assembly (SA8)

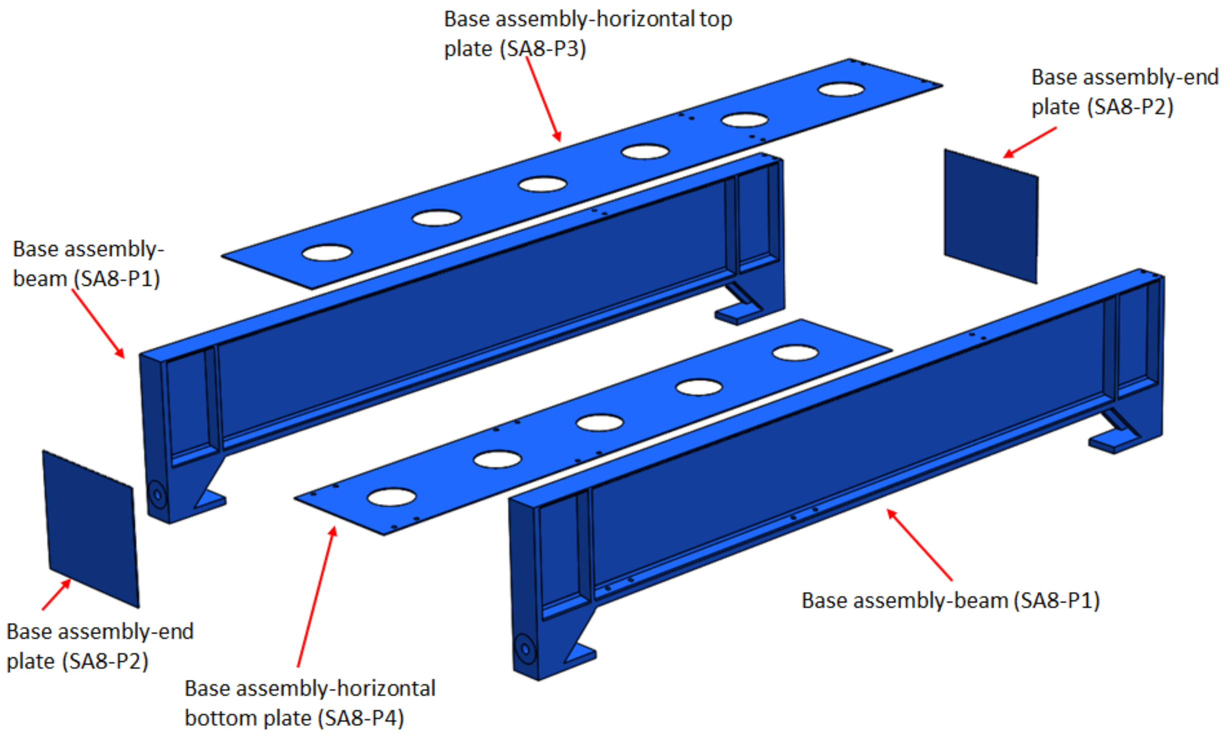

Figure A-44. Exploded view of the base assembly (SA8)

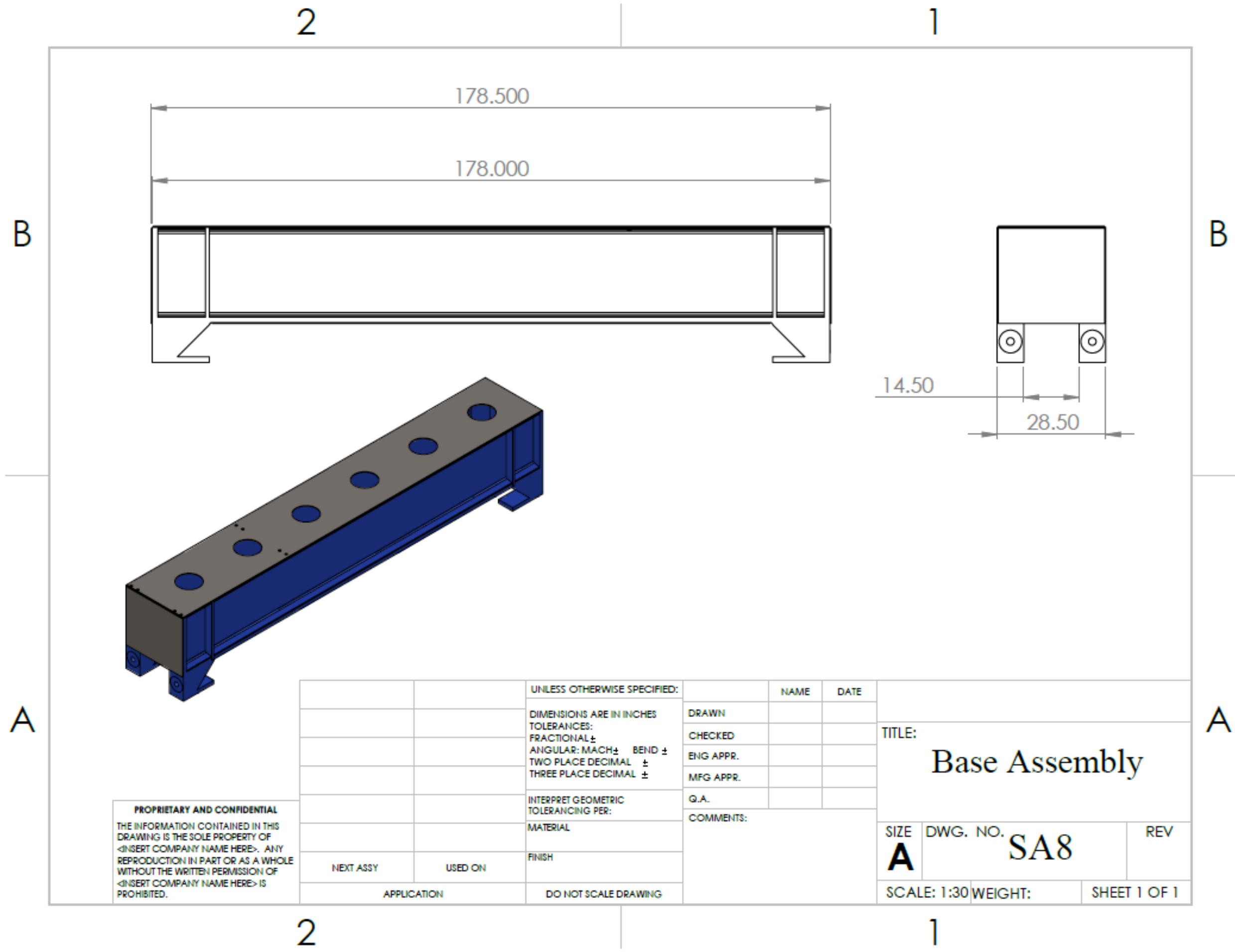

Figure A-45. Drawing of the base assembly (SA8)

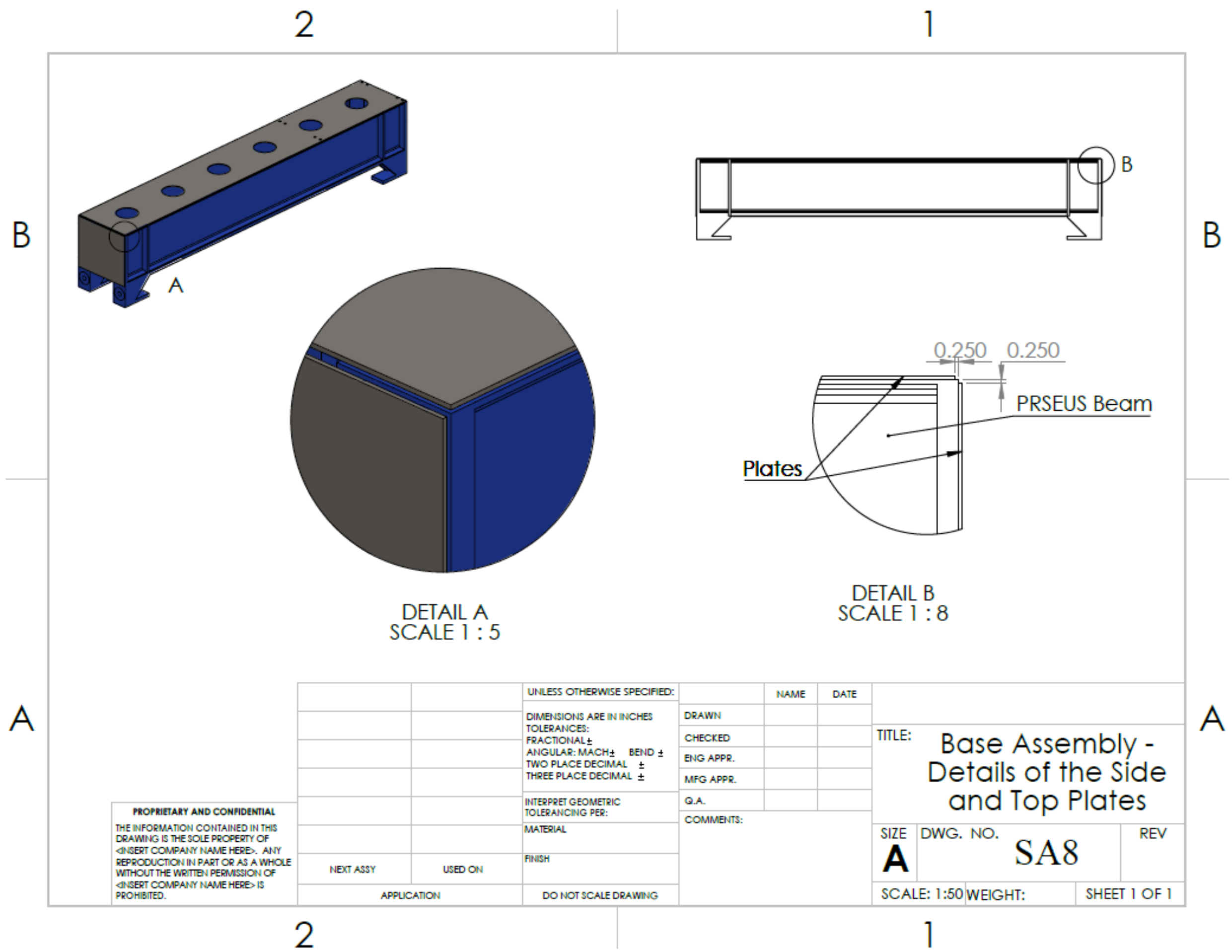

Figure A-46. Drawing of the base assembly—details of the side and top plates (SA8)

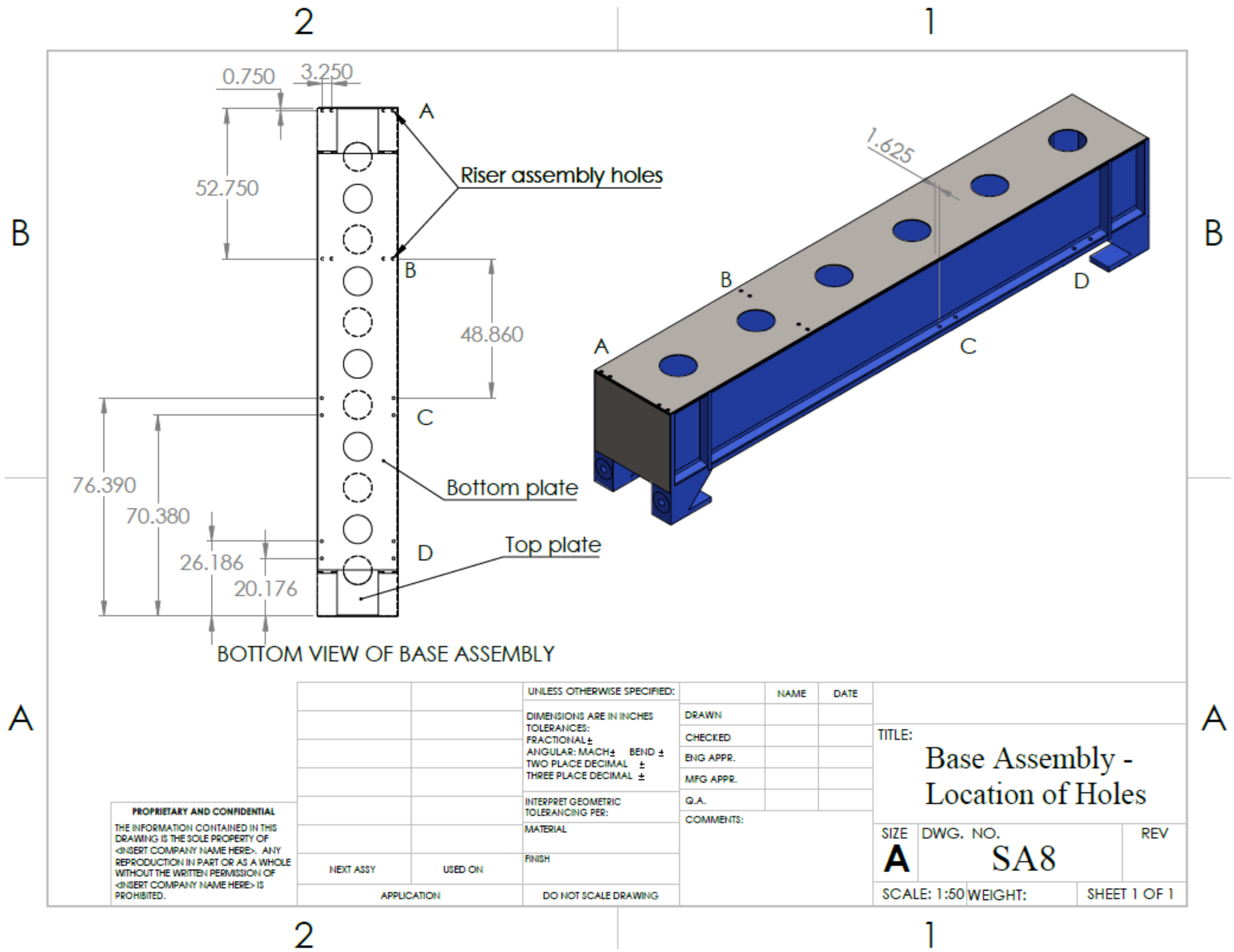

Figure A-47. Drawing of the base assembly—location of holes (SA8)

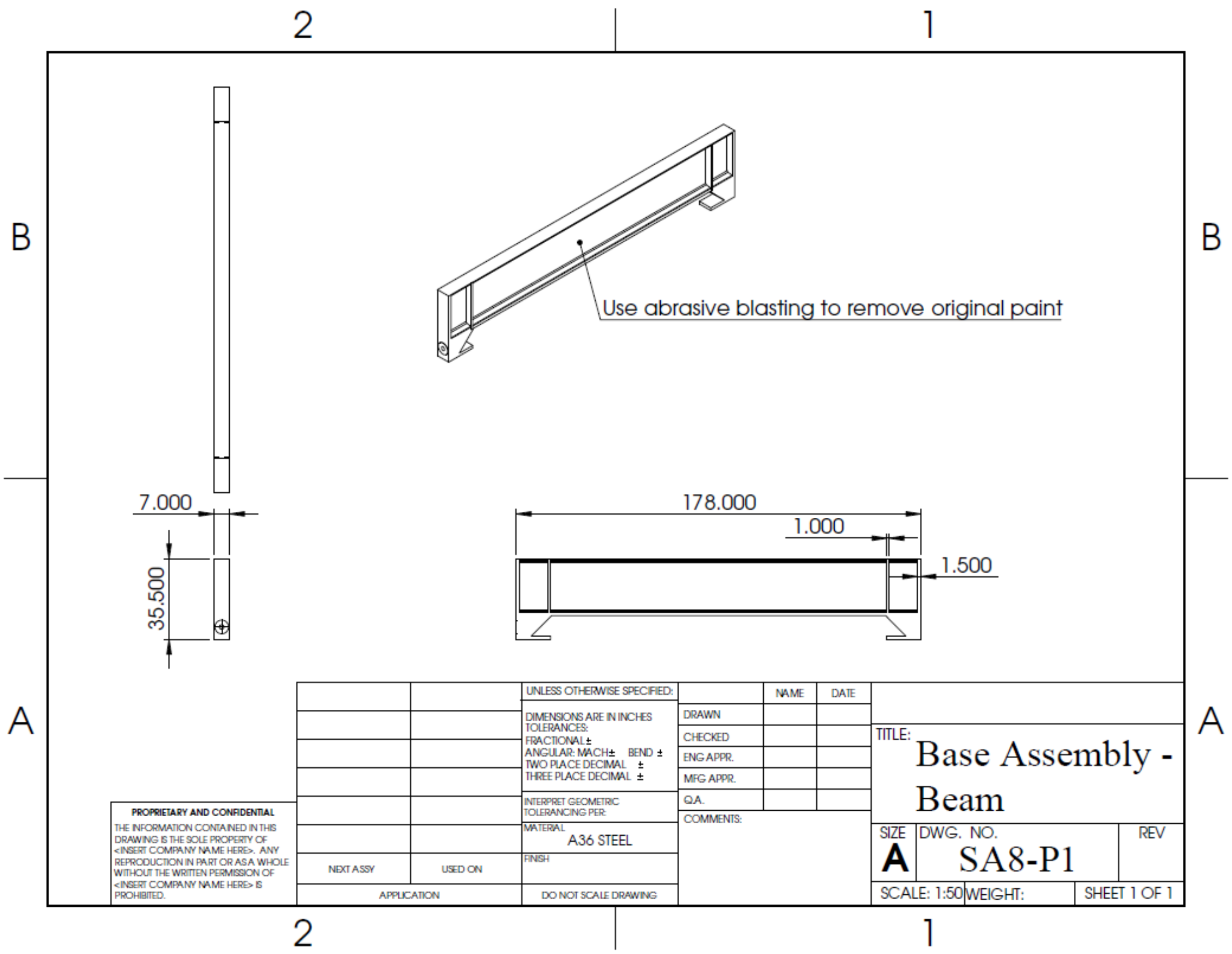

Figure A-48. Drawing of the base assembly—beam (SA8-P1)

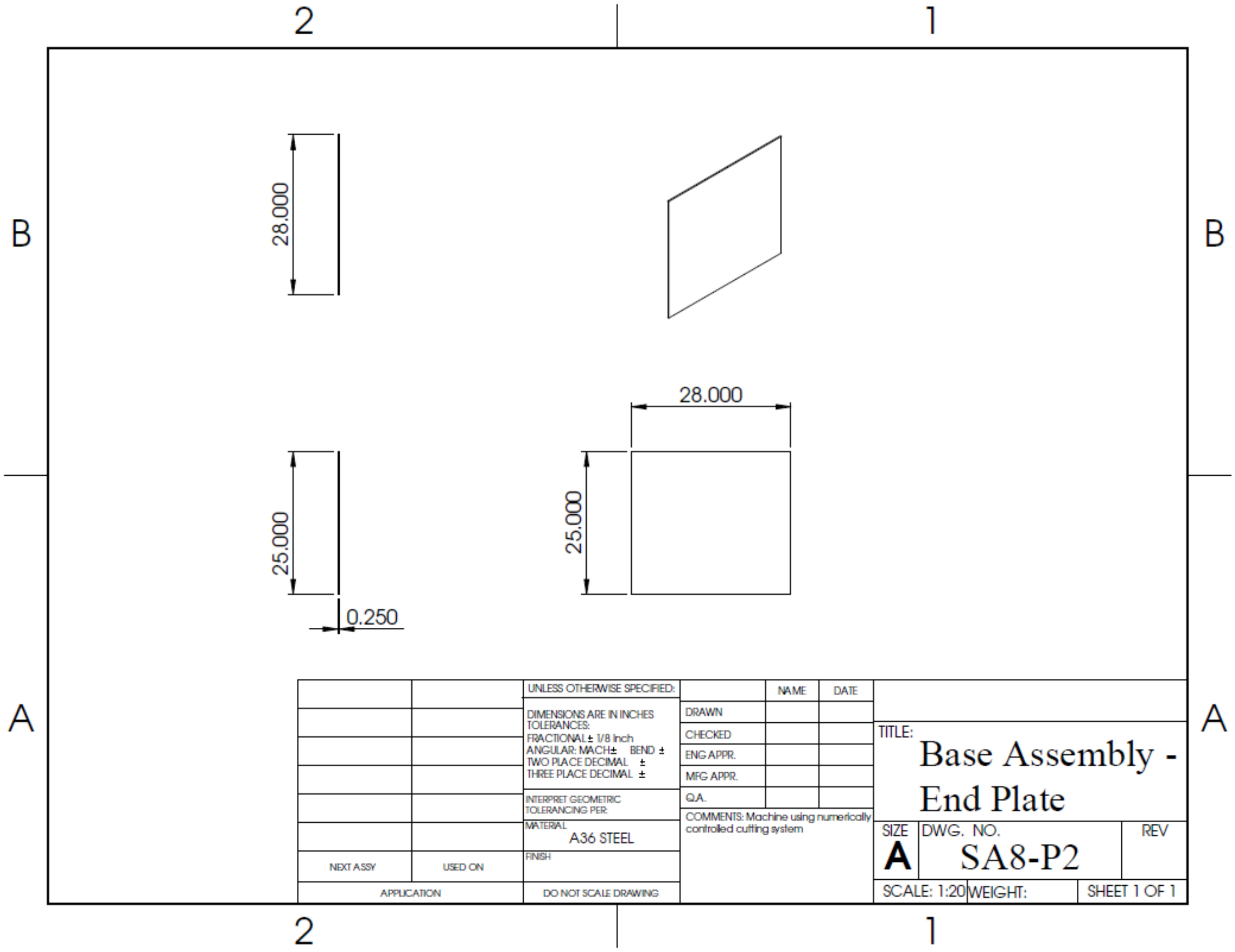

Figure A-49. Drawing of the base assembly—end plate (SA8-P2)

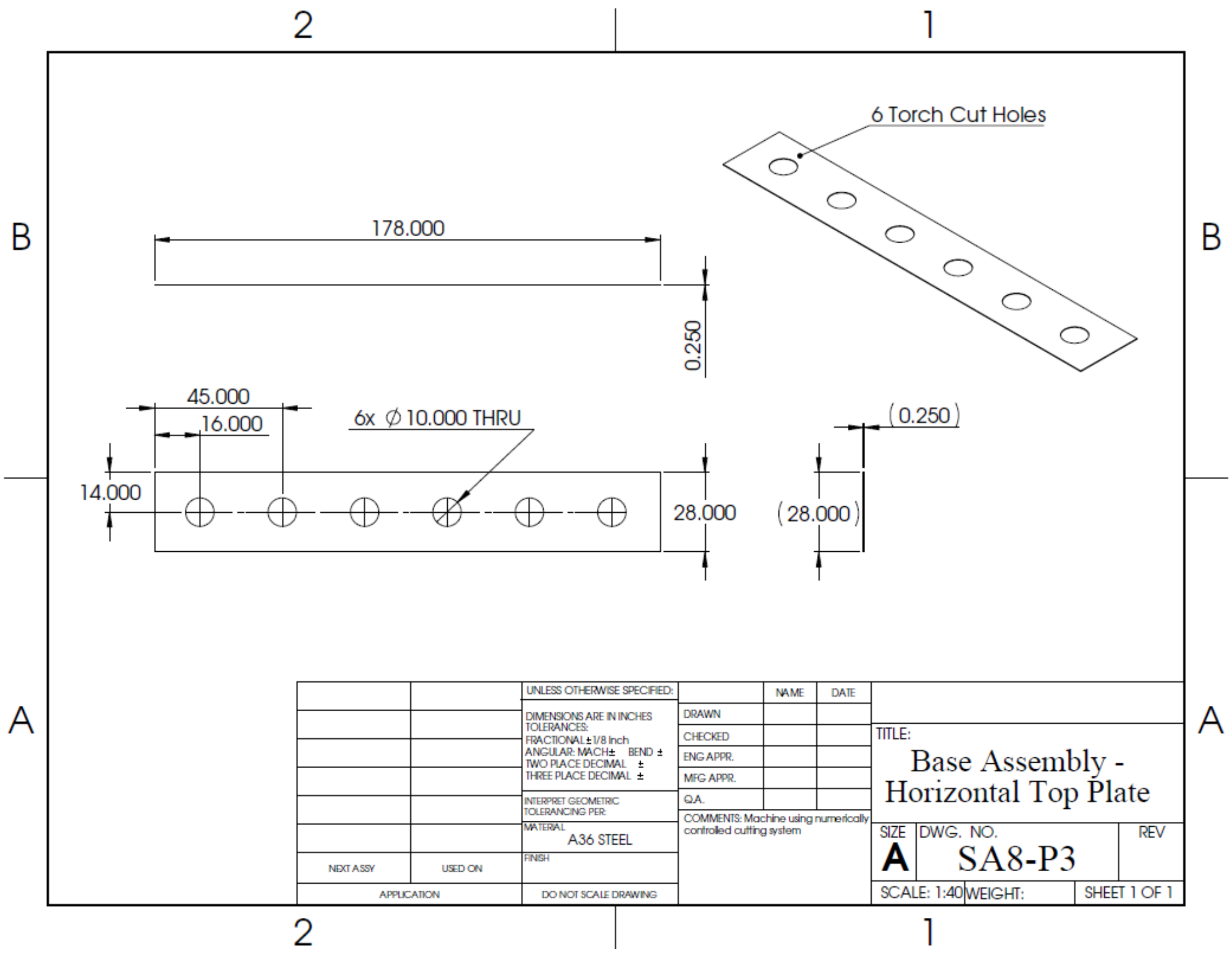

Figure A-50. Drawing of the base assembly—horizontal top plate (SA8-P3)

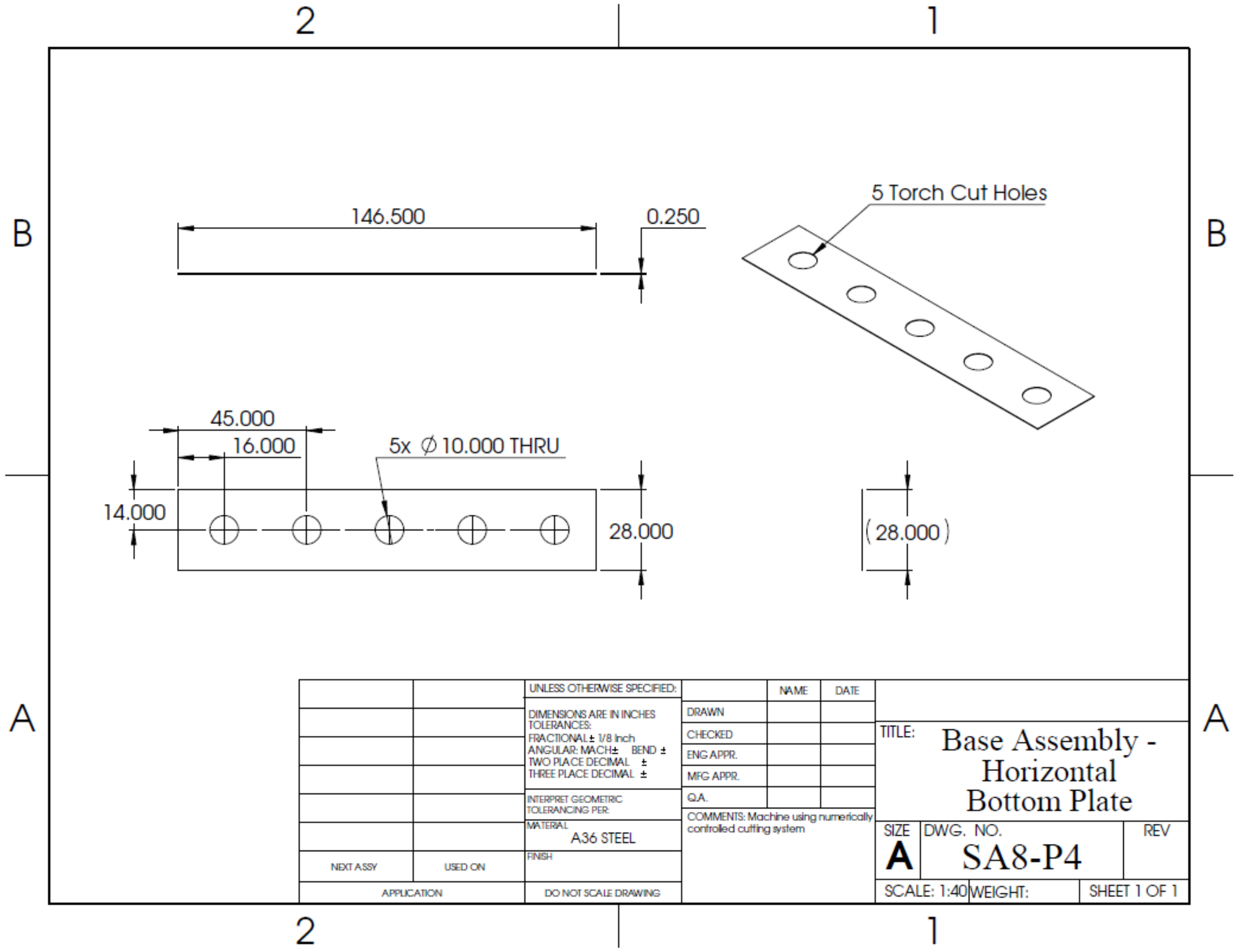

Figure A-51. Drawing of the base assembly—horizontal bottom plate (SA8-P4)